STRUCTURAL CHEMISTRY OF PENTA- AND HEXANITRATO THORIUM(IV) COMPLEXES ISOLATED USING N-H DONORS

*Madeline C. Shore,[1] Aaron D. Nicholas,[2] Monica Vasiliu,[3] Kyle C. Edwards,[3] Gabriel F. de Melo,[3] Jeffery A. Bertke,[1] David A. Dixon,[3] and Karah E. Knope[1,]**

[1] Department of Chemistry, Georgetown University, Washington, D.C. 20057, United States of America
[2] Pacific Northwest National Laboratory, 902 Battelle Boulevard, Richland, WA, 99354, United States of America
[3] Department of Chemistry and Biochemistry, The University of Alabama, Tuscaloosa, Alabama 35487, United States of America

*kek44@georgetown.edu

ELECTRONIC SUPPLEMENTAL INFORMATION

Table of Contents

1. SYNTHETIC DETAILS. **2**
2. CRYSTALLOGRAPHIC REFINEMENT DETAILS OF COMPOUNDS 1–15. .... **5**
3. ORTEP DIAGRAMS OF COMPOUNDS 1–15. .... **8**
4. SUPRAMOLECULAR PACKING DIAGRAMS. **23**
5. POWDER X-RAY DIFFRACTION PLOTS OF COMPOUNDS 1–15. .... **38**
6. RAMAN AND INFRARED PLOTS OF COMPOUNDS 1–15. .... **46**
7. SUPRAMOLECULAR INTERACTIONS OBSERVED IN COMPOUNDS 1–15. .... **64**
8. COMPUTATIONAL METHODS. **69**
9. REFERENCES. **96**

1. SYNTHETIC DETAILS.

Synthesis of PiperH$_2$[Th(NO$_3$)$_5$(H$_2$O)$_2$]$_2$•[PiperH$_2$(NO$_3$)$_2$] (1)

$Th(NO_3)_4$ (0.048 g, 0.1 mmol) was dissolved in nitric acid ($HNO_{3(aq)}$, 500 μL, 1M) to form an acidic Th^{IV} solution (0.25 M). The 3mL glass vial was then charged with piperazine (0.0086 g, 0.1 mmol) layered with 500 μL of 1-hexanol yielding a clear solution, which was left to evaporate under a nitrogen atmosphere. After approximately 4 days, clear block crystals formed at the bottom of the vial. Single crystal X-ray diffraction determined the crystals to be PiperH$_2$[Th(NO$_3$)$_5$(H$_2$O)$_2$]$_2$•[PiperH$_2$(NO$_3$)$_2$] (1). The bulk phase was found to be impure from powder X-ray diffraction, therefore elemental analysis is not reported. Yield: 42.5%.

Synthesis of (TerpyH$_2$)[Th(NO$_3$)$_5$(H$_2$O)$_2$]$_2$•[(TerpyH$_2$)$_3$(NO$_3$)$_6$]•4(H$_2$O) (2)

$Th(NO_3)_4$ (0.048 g, 0.1 mmol) was dissolved in nitric acid ($HNO_{3(aq)}$, 500 μL, 1M) to form an acidic Th^{IV} solution (0.25 M). The 3mL glass vial was then charged with terpyridine (0.0233 g, 0.1 mmol) layered with 500 μL of 1-hexanol yielding a clear solution, which was left to evaporate under a nitrogen atmosphere. After approximately 4 days, clear block crystals formed at the bottom of the vial. Single crystal X-ray diffraction determined the crystals to be (TerpyH$_2$)[Th(NO$_3$)$_5$(H$_2$O)$_2$]•[TerpyH$_2$(NO$_3$)$_3$] (**2**). The bulk phase was found to be impure from powder X-ray diffraction, therefore elemental analysis is not reported. Yield: 25.2%.

Synthesis of (PyH)$_2$[Th(NO$_3$)$_6$]•(PyH•NO$_3$) (3)

$Th(NO_3)_4$ (0.048 g, 0.1 mmol) was dissolved in nitric acid ($HNO_{3(aq)}$, 500 μL, 1M) to form an acidic Th^{IV} solution (0.25 M). The 3mL glass vial was then charged with Pyridine (8.08 μL, 0.1 mmol) layered with 500 μL of 1-hexanol yielding a clear solution, which was left to evaporate under a nitrogen atmosphere. After approximately 4 days, clear block crystals formed at the bottom of the vial. Single crystal X-ray diffraction determined the crystals to be (HPy)$_2$[Th(NO$_3$)$_6$]•(HPy)(NO$_3$) (3). The bulk phase was found to be impure from powder X-ray diffraction, therefore elemental analysis is not reported. Yield: 32.3%. Raman and IR spectroscopies are also reported for this compound.

Synthesis of (PyH)$_2$[Th(NO$_3$)$_6$]•2(PyH•NO$_3$) (4)

$Th(NO_3)_4$ (0.048 g, 0.1 mmol) was dissolved in nitric acid ($HNO_{3(aq)}$, 500 μL, 3M) to form an acidic Th^{IV} solution (0.25 M). The 3mL glass vial was then charged with Pyridine (8.08 μL, 0.1 mmol yielding a clear solution, which was left to evaporate under a nitrogen atmosphere. After approximately 4 days, clear block crystals formed at the bottom of the vial. Single crystal X-ray diffraction determined the crystals to be (HPy)$_2$[Th(NO$_3$)$_6$]•(HPy)$_2$(NO$_3$)$_2$ (4). The bulk phase was found to be impure from powder X-ray diffraction, therefore elemental analysis is not reported. Yield: 27.7%. Raman and IR spectroscopies are also reported for this compound.

Synthesis of (3,5-DiMePyH)$_2$[Th(NO$_3$)$_6$]•[(3,5-DiMePyH)(NO$_3$)] (5)

$Th(NO_3)_4$ (0.048 g, 0.1 mmol) was dissolved in nitric acid ($HNO_{3(aq)}$, 500 μL, 3M) to form an acidic Th^{IV} solution (0.25 M). The 3mL glass vial was then charged with 3,5-dimethylpyridine (11.35 μL, 0.1 mmol yielding a clear solution, which was left to evaporate under a nitrogen atmosphere. After approximately 4 days, clear block crystals formed at the bottom of the vial. Single crystal X-ray diffraction determined the crystals to be (3,5-DiMePy)$_2$[Th(NO$_3$)$_6$]•[(3,5-DiMePyH)(NO$_3$)] (5). The bulk phase was found to be impure from powder X-ray diffraction, therefore elemental analysis is not reported. Yield: 25.3%. Raman and IR spectroscopies are also reported for this compound.

Synthesis of $(3,5\text{-DiMePyH})_2[Th(NO_3)_6]$ (6)

$Th(NO_3)_4$ (0.048 g, 0.1 mmol) was dissolved in nitric acid ($HNO_{3(aq)}$, 500 μL, 1M) to form an acidic Th^{IV} solution (0.25 M). The 3mL glass vial was then charged with 3,5-dimethylpyridine (11.35 μL, 0.1 mmol) yielding a clear solution, which was left to evaporate under a nitrogen atmosphere. After approximately 4 days, clear block crystals formed at the bottom of the vial. Single crystal X-ray diffraction determined the crystals to be $(3,5\text{-DiMePyH})_2[Th(NO_3)_6]$. The bulk phase was found to be impure from powder X-ray diffraction, therefore elemental analysis is not reported. Yield: 22.6%. Raman and IR spectroscopies are also reported for this compound.

Synthesis of $(TerpyH_2)[Th(NO_3)_6]\bullet(TerpyH_2)(NO_3)_2$ (7). $Th(NO_3)_4$ (0.048 g, 0.1 mmol) was dissolved in nitric acid ($HNO_{3(aq)}$, 500 μL, 3M) to form an acidic Th^{IV} solution (0.25 M). The 3mL glass vial was then charged with Terpyridine (0.0233 g, 0.1 mmol) yielding a clear solution, which was left to evaporate under a nitrogen atmosphere. After approximately 4 days, clear block crystals formed at the bottom of the vial. Single crystal X-ray diffraction determined the crystals to be $(TerpyH_2)[Th(NO_3)_6]\bullet(TerpyH_2)(NO_3)_2$ (7). The bulk phase was found to be impure from powder X-ray diffraction, therefore elemental analysis is not reported. Yield: 45.54%. Raman and IR spectroscopies are also reported for this compound.

Synthesis of $(4\text{-MePyH})_2[Th(NO_3)_6]$ (8). $Th(NO_3)_4$ (0.048 g, 0.1 mmol) was dissolved in nitric acid ($HNO_{3(aq)}$, 500 μL, 1M) to form an acidic Th^{IV} solution (0.25 M). The 3mL glass vial was then charged with 4-methylpyridine (9.87 μL, 0.1 mmol) yielding a clear solution, which was left to evaporate under a nitrogen atmosphere. After approximately 4 days, clear block crystals formed at the bottom of the vial. Single crystal X-ray diffraction determined the crystals to be $(4\text{-MePyH})_2[Th(NO_3)_6]$ (8). The bulk phase was found to be impure from powder X-ray diffraction, therefore elemental analysis is not reported. Yield: 13.6%. Raman and IR spectroscopies are also reported for this compound.

Synthesis of $[4,4\text{-BipyH}_2]_2[Th(NO_3)_6]_2\bullet[4,4\text{-BipyH}_2\bullet 2NO_3]$ (9). $Th(NO_3)_4$ (0.048 g, 0.1 mmol) was dissolved in nitric acid ($HNO_{3(aq)}$, 500 μL, 1M) to form an acidic Th^{IV} solution (0.25 M). The 3mL glass vial was then charged with Bipyridine (0.0156 g, 0.1 mmol) layered with 500 μL of 1-hexanol yielding a clear solution, which was left to evaporate under a nitrogen atmosphere. After approximately 4 days, clear block crystals formed at the bottom of the vial. Single crystal X-ray diffraction determined the crystals to be $(4,4\text{-BipyH}_2)[Th(NO_3)_6]\bullet[(4,4\text{-BipyH}_2)(NO_3)_2]$ (10). The bulk phase was found to be impure from powder X-ray diffraction, therefore elemental analysis is not reported. Yield: 11.5%. Raman and IR spectroscopies are also reported for this compound.

Synthesis of $(PhthalH)_2[Th(NO_3)_6]$ (10). $Th(NO_3)_4$ (0.048 g, 0.1 mmol) was dissolved in nitric acid ($HNO_{3(aq)}$, 500 μL, 1M) to form an acidic Th^{IV} solution (0.25 M). The 3mL glass vial was then charged with Phthalazine (0.0130 g, 0.1 mmol) layered with 500 μL of 1-hexanol yielding a clear solution, which was left to evaporate under a nitrogen atmosphere. After approximately 4 days, clear block crystals formed at the bottom of the vial. Single crystal X-ray diffraction determined the crystals to be $(PhthalH)_2[Th(NO_3)_6]$ (11). The bulk phase was found to be impure from powder X-ray diffraction, therefore elemental analysis is not reported. Yield: 15.8%. Raman and IR spectroscopies are also reported for this compound.

Synthesis of [TerpyH$_2$][Th(NO$_3$)$_6$]•H$_2$O (11) Th(NO$_3$)$_4$ (0.048 g, 0.1 mmol) was dissolved in nitric acid (HNO$_{3(aq)}$, 500 µL, 3M) to form an acidic Th^{IV} solution (0.25 M). The 3mL glass vial was then charged with Terpyridine (0.0233 g, 0.1 mmol) yielding a clear solution, which was left to evaporate under a nitrogen atmosphere. After approximately 4 days, clear block crystals formed at the bottom of the vial. Single crystal X-ray diffraction determined the crystals to be [TerpyH$_2$][Th(NO$_3$)$_6$][H$_2$O] (12). The bulk phase was found to be impure from powder X-ray diffraction, therefore elemental analysis is not reported. Yield: 32.5%. Raman and IR spectroscopies are also reported for this compound.

Synthesis of (2-MePyH)$_2$[Th(NO$_3$)$_6$]•2H$_2$O (12). Th(NO$_3$)$_4$ (0.048 g, 0.1 mmol) was dissolved in nitric acid (HNO$_{3(aq)}$, 500 µL, 3M) to form an acidic Th^{IV} solution (0.25 M). The 3mL glass vial was then charged with 2-methylpyridine (9.875 µL, 0.1 mmol) a clear solution, which was left to evaporate under a nitrogen atmosphere. After approximately 4 days, clear block crystals formed at the bottom of the vial. Single crystal X-ray diffraction determined the crystals to be (2-MePyH)$_2$[Th(NO$_3$)$_6$]•2H$_2$O (13). The bulk phase was found to be impure from powder X-ray diffraction, therefore elemental analysis is not reported. Yield: 15.7%. Raman and IR spectroscopies are also reported for this compound.

Synthesis of (3-MePyH)$_2$[Th(NO$_3$)$_6$] (13). Th(NO$_3$)$_4$ (0.048 g, 0.1 mmol) was dissolved in nitric acid (HNO$_{3(aq)}$, 500 µL, 1M) to form an acidic Th^{IV} solution (0.25 M). The 3mL glass vial was then charged with 3-methylpyridine (9.875 µL, 0.1 mmol yielding a clear solution, which was left to evaporate under a nitrogen atmosphere. After approximately 4 days, clear block crystals formed at the bottom of the vial. Single crystal X-ray diffraction determined the crystals to be (3-MePyH)$_2$[Th(NO$_3$)$_6$] (14). The bulk phase was found to be impure from powder X-ray diffraction, therefore elemental analysis is not reported. Yield: 31.6%. Raman and IR spectroscopies are also reported for this compound.

Synthesis of (3-ClPyH)$_2$[Th(NO$_3$)$_6$] (14). Th(NO$_3$)$_4$ (0.048 g, 0.1 mmol) was dissolved in nitric acid (HNO$_{3(aq)}$, 500 µL, 3M) to form an acidic Th^{IV} solution (0.25 M). The 3mL glass vial was then charged with 3-chloropyridine (9.5 µL, 0.1 mmol) yielding a clear solution, which was left to evaporate under a nitrogen atmosphere. After approximately 4 days, clear block crystals formed at the bottom of the vial. Single crystal X-ray diffraction determined the crystals to be (3-ClPyH)$_2$[Th(NO$_3$)$_6$] (9). The bulk phase was found to be impure from powder X-ray diffraction, therefore elemental analysis is not reported. Yield: 31.5%. Raman and IR spectroscopies are also reported for this compound.

Synthesis of (PhenH)$_2$[Th(NO$_3$)$_6$]•2[H$_2$O] (15). Th(NO$_3$)$_4$ (0.048 g, 0.1 mmol) was dissolved in nitric acid (HNO$_{3(aq)}$, 500 µL, 1M) to form an acidic Th^{IV} solution (0.25 M). The 3mL glass vial was then charged with Phenanthroline (0.0180 g, 0.1 mmol) layered with 500 µL of 1-hexanol yielding a clear solution, which was left to evaporate under a nitrogen atmosphere. After approximately 4 days, clear block crystals formed at the bottom of the vial. Single crystal X-ray diffraction determined the crystals to be (PhenH)$_2$[Th(NO$_3$)$_6$][H$_2$O]$_2$ (15). The bulk phase was found to be impure from powder X-ray diffraction, therefore elemental analysis is not reported. Yield: 19.9%. Raman and IR spectroscopies are also reported for this compound.

2. CRYSTALLOGRAPHIC REFINEMENT DETAILS OF COMPOUNDS **1**–**15**.

Note: Crystallographic refinement details can be found in the "experimental refinement section" of the crystallographic information files (CIFs). Details are also provided below for ease of the reader.

For **1-15**, non-hydrogen atoms were found in the Fourier difference map and refined anisotropically. Hydrogen atoms bound to carbons of heterocyclic rings were placed in calculated positions and their Ueq values were assigned values 1.2 times that of their parent atom. The protonated nitrogen heterocycle H atom was located in the difference map and its position was allowed to freely refine. Remaining H atoms were included as riding idealized contributors. The protonated nitrogen heterocycles H atom U's were assigned as 1.5 times U_{eq} of the carrier atom; remaining H atom U's were assigned as 1.2 times carrier U_{eq}. If the X–H distance (X=N, O) was not within reasonable limits, the distance was fixed; for water molecules, O–H distances were fixed at 0.88(0.02) Å. For the protonated nitrogen atoms contained within heterocyclic counterions, N–H distances were fixed to 0.86(0.02) Å. All esds (except the esd in the dihedral angle between two l.s. planes) are estimated using the full covariance matrix. The cell esds are considered individually in the estimation of esds in distances, angles, and torsion angles; correlations between esds in cell parameters are only used when they are defined by crystal symmetry. An approximate (isotropic) treatment of cell esds is used for estimating esds involving l.s. planes. Details for each compound are provided below.

Compound 1

The asymmetric unit of **1** consists of the anionic $[Th(NO_3)_5(H_2O)_2]^{1-}$ moiety, one NO_3^{1-}, and two half $[PiperH_2]^{2+}$ moieties that lie on inversion centers. The H atoms for the coordinated water molecule were located in the difference map and their positions were allowed to freely refine. Remaining H atoms were included as riding idealized contributors. Water H atom U's were assigned as 1.5 times U_{eq} of the carrier atom; remaining H atom U's were assigned as 1.2 times carrier U_{eq}.

Compound 2

All structural components of **2** sit on general positions within the asymmetric unit. The $[TerpyH_2]^{2+}$ N-H and water H atoms were located in the difference map. The N-H distances were restrained to be 0.88 (esd 0.01Å) and the O-H distances were restrained to be 0.84 (esd 0.01Å). Remaining H atoms were included as riding idealized contributors. Water and amine H atom U's were assigned as 1.5 times U_{eq} of the carrier atom; remaining H atom U's were assigned as 1.2 times carrier U_{eq}.

Compound 3

The asymmetric unit of **3** consists of one half of the anionic $[Th(NO_3)_6]^{2-}$ moiety, with Th1 lying on an inversion center. Additionally, there is one $[PyH]^{1+}$ cation, and one half $(NO_3)^{1-}$ and one half $[PyH]^{1+}$ moieties that lie about two-fold axes. The pyridinium N-H hydrogen atoms were located in the difference map and the distances were restrained to be 0.88 (esd 0.02 Å). Remaining H atoms were included as riding idealized contributors. Heteroatom H U's were assigned as 1.5 times U_{eq} of the carrier atom; remaining H atom U's were assigned as 1.2 times carrier U_{eq}.

Compound 4

The asymmetric unit of **4** consists of one half of the anionic $[Th(NO_3)_6]^{2-}$ moiety in which Th1 lies on an inversion center, one $(NO_3)^{1-}$ and two $[PyH]^{1+}$ moieties at general positions. All of the coordinated $(NO_3)^{1-}$ anions are disordered over two orientations. The like N-O distances were restrained to be similar (esd 0.01Å). Similar displacement amplitudes (esd 0.01) were imposed on disordered sites overlapping by less than the sum of van der Waals radii. The pyridinium N-H hydrogen atoms were located in the difference map and the positions were allowed to freely refine. Remaining H atoms were included as riding idealized contributors. Pyridinium N-H atom U's were assigned as 1.5 times U_{eq} of the carrier atom; remaining H atom U's were assigned as 1.2 times carrier U_{eq}.

Compound 5

All components of **5** sit on general positions within the asymmetric unit. The $[3,5\text{-DiMePyH}]^{1+}$ N-H hydrogren atoms were located in the difference map. The N-H distances were restrained to be 0.84 (esd 0.02Å). Remaining H atoms were included as riding idealized contributors. The pyridinium heteroatom H U's were assigned as 1.5 times U_{eq} of the carrier atom; remaining H atom U's were assigned as 1.2 times carrier U_{eq}.

Compound 6

A structural model consisting of one half of the $[Th(NO_3)_6]^{2-}$ anion and one $(3,5\text{-DiMePyH})^{1+}$ cation per asymmetric unit was developed. The $(3,5\text{-DiMePyH})^{1+}$ N-H hydrogen was located in the difference map and the position was allowed to freely refine. Methyl H atom positions, R-CH_3, were optimized by rotation about R-C bonds with idealized C-H, R--H and H--H distances. Remaining H atoms were included as riding idealized contributors. $(3,5\text{-DiMePyH})^{1+}$ heteroatom H U's were assigned as 1.5 times U_{eq} of the carrier atom; remaining H atom U's were assigned as 1.2 times carrier U_{eq}.

Compound 7

The asymmetric unit of **7** consists of one half of the anionic $[Th(NO_3)_6]^{2-}$ moiety in which Th1 lies about a two-fold axis, one $(NO_3)^{1-}$ and one $[TerpyH_2]^{2+}$ moieties are at general positions. The $[TerpyH_2]^{2+}$ N-H H atoms were located in the difference map and the positions were allowed to freely refine. Remaining H atoms were included as riding idealized contributors. The $[TerpyH_2]^{2+}$ heteroatom H U's were assigned as 1.5 times U_{eq} of the carrier atom; remaining H atom U's were assigned as 1.2 times carrier U_{eq}.

Compound 8

The asymmetric unit of **8** consists of one half of the anionic $[Th(NO_3)_6]^{2-}$ moiety in which Th1 lies on an inversion center, and one $[4\text{-MePyH}]^{1+}$ moiety at a general position. The $[4\text{-MePyH}]^{1+}$ N-H H atom was located in the difference map and the position was allowed to freely refine. Remaining H atoms were included as riding idealized contributors. The $[4\text{-MePyH}]^{1+}$ heteroatom H U's were assigned as 1.5 times U_{eq} of the carrier atom; remaining H atom U's were assigned as 1.2 times carrier U_{eq}.

Compound 9

The asymmetric unit of **9** consists of the $[Th(NO_3)_6]^{2-}$ moiety, one $(NO_3)^{1-}$, and one $[4,4'\text{-BipyH}_2]^{2+}$ in general positions as well as one half $[4,4'\text{-BipyH}_2]^{2+}$ lying on an inversion center. The $[4,4'\text{-BipyH}_2]^{2+}$ N-H H atoms were located in the difference map and their positions were allowed to freely refine. Remaining H atoms were included as riding idealized contributors. $[4,4\text{-BipyH}_2]^{2+}$ N-H H atom U's were assigned as 1.5 times U_{eq} of the carrier atom; remaining H atom U's were assigned as 1.2 times carrier U_{eq}.

Compound 10

The asymmetric unit of **10** consists of one half of the anionic $[Th(NO_3)_6]^{2-}$ moiety in which Th1 lies on a two-fold axis, and one $[\text{PhthalH}]^{1+}$ moiety at a general position. The $[\text{PhthalH}]^{1+}$ N-H H atom could not be located in the difference map and thus was placed in a calculated position. Remaining H atoms were also included as riding idealized contributors. H atom U's were assigned as 1.2 times carrier U_{eq}.

Compound 11

All components of **11** sit on general positions within the asymmetric unit. The $[\text{TerpyH}_2]^{2+}$ N-H and water H atoms were located in the difference map and their positions were allowed to freely refine. Remaining H atoms were included as riding idealized contributors. Water and $[\text{TerpyH}_2]^{2+}$ N-H H atom U's were assigned as 1.5 times U_{eq} of the carrier atom; remaining H atom U's were assigned as 1.2 times carrier U_{eq}.

Compound 12

The asymmetric unit of **12** consists of one half of the anionic $[Th(NO_3)_6]^{2-}$ moiety in which Th1 lies on a two-fold axis, and one $[2\text{-MePyH}]^{1+}$ moiety and one water molecule at general positions. The $[2\text{-MePyH}]^{1+}$ N-H and water H atoms were located in the difference map and their positions were allowed to freely refine. Remaining H atoms were included as riding idealized contributors. Water and $[2\text{-MePyH}]^{1+}$ heteroatom hydrogen U's were assigned as 1.5 times U_{eq} of the carrier atom; remaining H atom U's were assigned as 1.2 times carrier U_{eq}.

Compound 13

The asymmetric unit of **13** consists of one half of the anionic $[Th(NO_3)_6]^{2-}$ moiety in which Th1 lies on a two-fold axis, and one $[3\text{-MePyH}]^{1+}$ moiety at a general position. The $[3\text{-MePyH}]^{1+}$ N-H H atom was located in the difference map and its position was allowed to freely refine. Remaining H atoms were included as riding idealized contributors. The $[3\text{-MePyH}]^{1+}$ N-H H atom U's were assigned as 1.5 times U_{eq} of the carrier atom; remaining H atom U's were assigned as 1.2 times carrier U_{eq}.

Compound 14

The asymmetric unit of **14** consists of one half of the anionic $[Th(NO_3)_6]^{2-}$ moiety in which Th1 lies on a two-fold axis, and one $[3\text{-ClPyH}]^{1+}$ moiety at a general position. The $[3\text{-ClPyH}]^{1+}$ N-H H atom was located in the difference map and its position was allowed to freely refine. Remaining H atoms were included as riding idealized contributors. $[3\text{-ClPyH}]^{1+}$ heteroatom H U's were assigned as 1.5 times U_{eq} of the carrier atom; remaining H atom U's were assigned as 1.2 times carrier U_{eq}.

Compound 15

The asymmetric unit of **15** consists of one half of the anionic $[Th(NO_3)_6]^{2-}$ moiety in which Th1 lies on an inversion center, and one $[\text{PhenH}]^{1+}$ moiety and one water molecule at general positions. The $[\text{PhenH}]^{1+}$ N-H and water H atoms were located in the difference map and their positions were allowed to freely refine. Remaining H atoms were included as riding idealized contributors. Water and two of the $[\text{PhenH}]^{1+}$ N-H H atom U's were assigned as 1.5 times U_{eq} of the carrier atom; remaining H atom U's were assigned as 1.2 times carrier U_{eq}

3. ORTEP DIAGRAMS OF COMPOUNDS **1**–**15**.

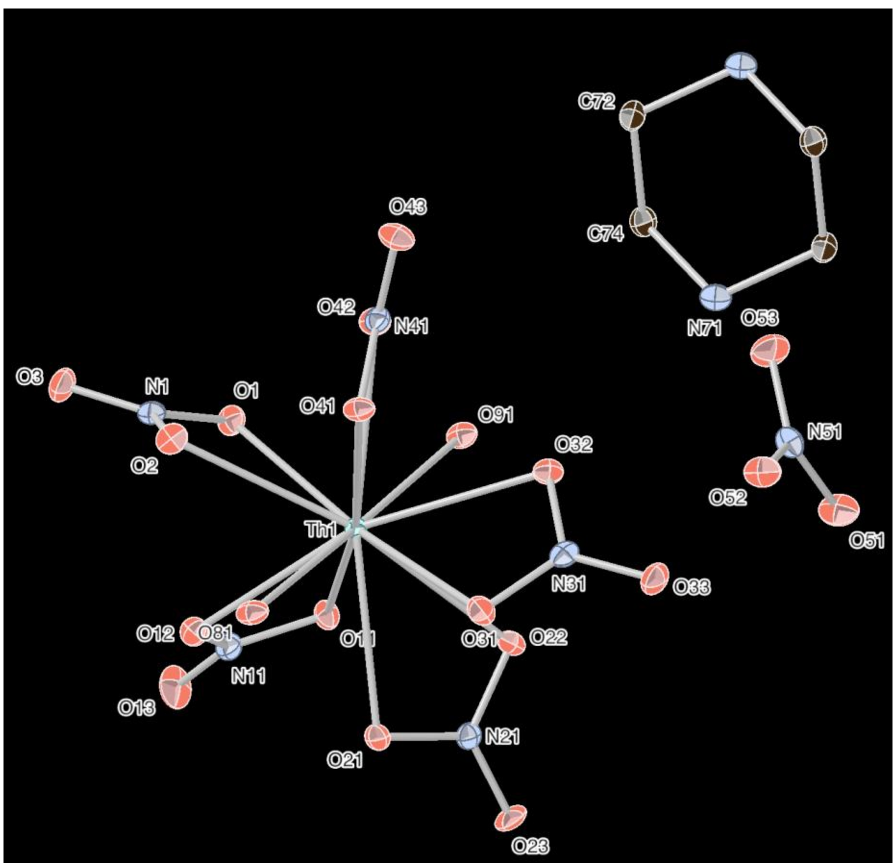

Figure S1. Thermal ellipsoid plot (50% probability level) of compound **1**, $\text{PiperH}_2[Th(NO_3)_5(H_2O)_2]_2\bullet[\text{PiperH}_2(NO_3)_2]$at 100 K. Symmetry equivalent atoms were generated through their respective symmetry elements (i = 1 – x ,1 – y , 1 – z).

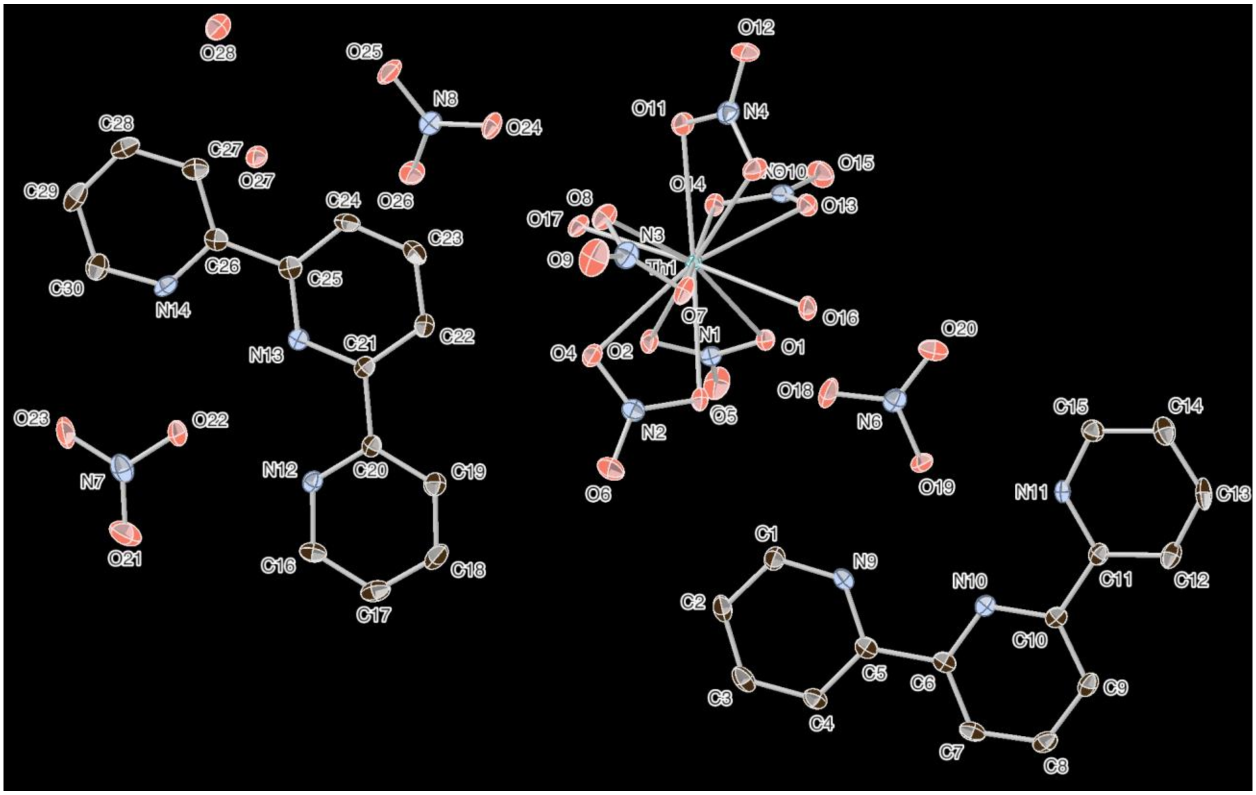

Figure S2. Thermal ellipsoid plot (50% probability level) of compound **2**, $(TerpyH_2)[Th(NO_3)_5(H_2O)_2]2\bullet[(TerpyH_2)_3(NO_3)_6]\bullet4(H_2O)$, at 100 K.

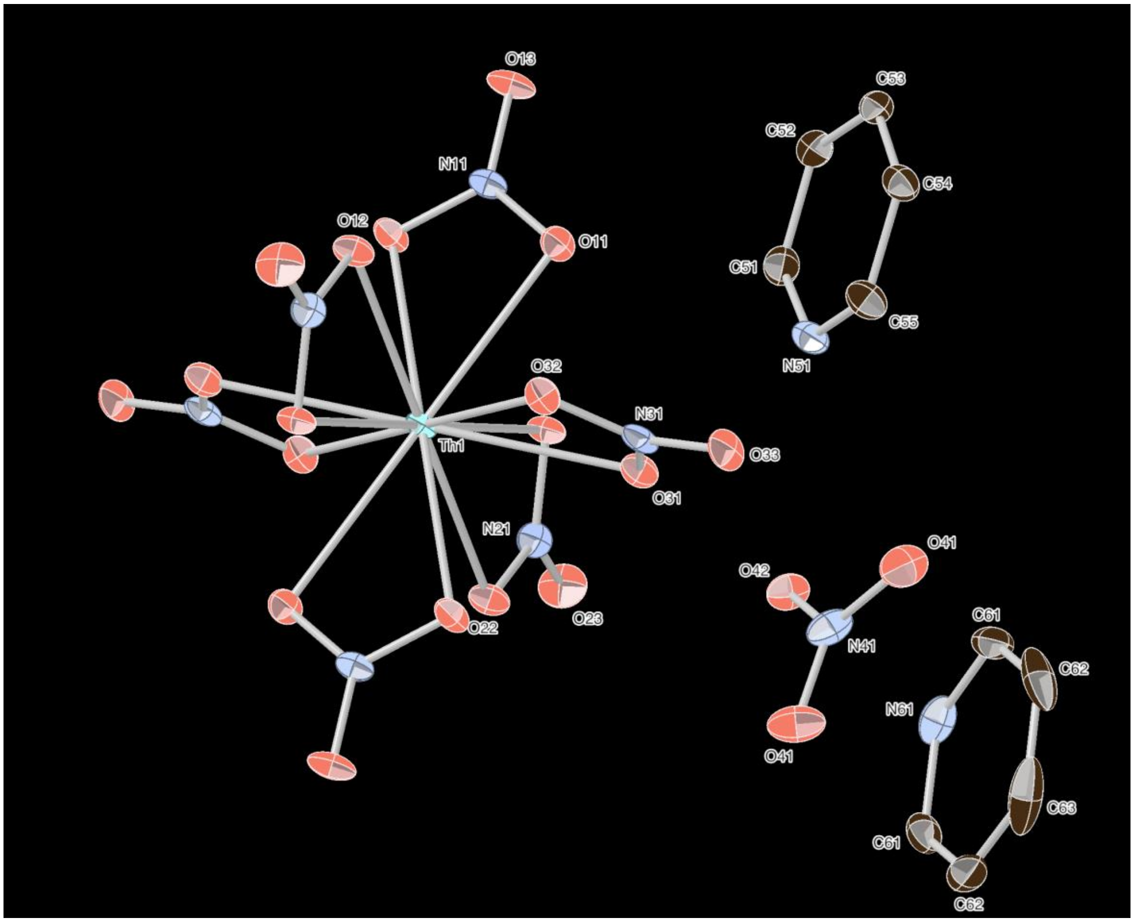

Figure S3. Thermal ellipsoid plot (50% probability level) of compound **3**, $(PyH)_2[Th(NO_3)_6]$•$(PyH$•$NO_3)$, at 100 K. Symmetry equivalent atoms were generated through their respective symmetry elements (i = 1 – x ,1 – y , 1 – z).

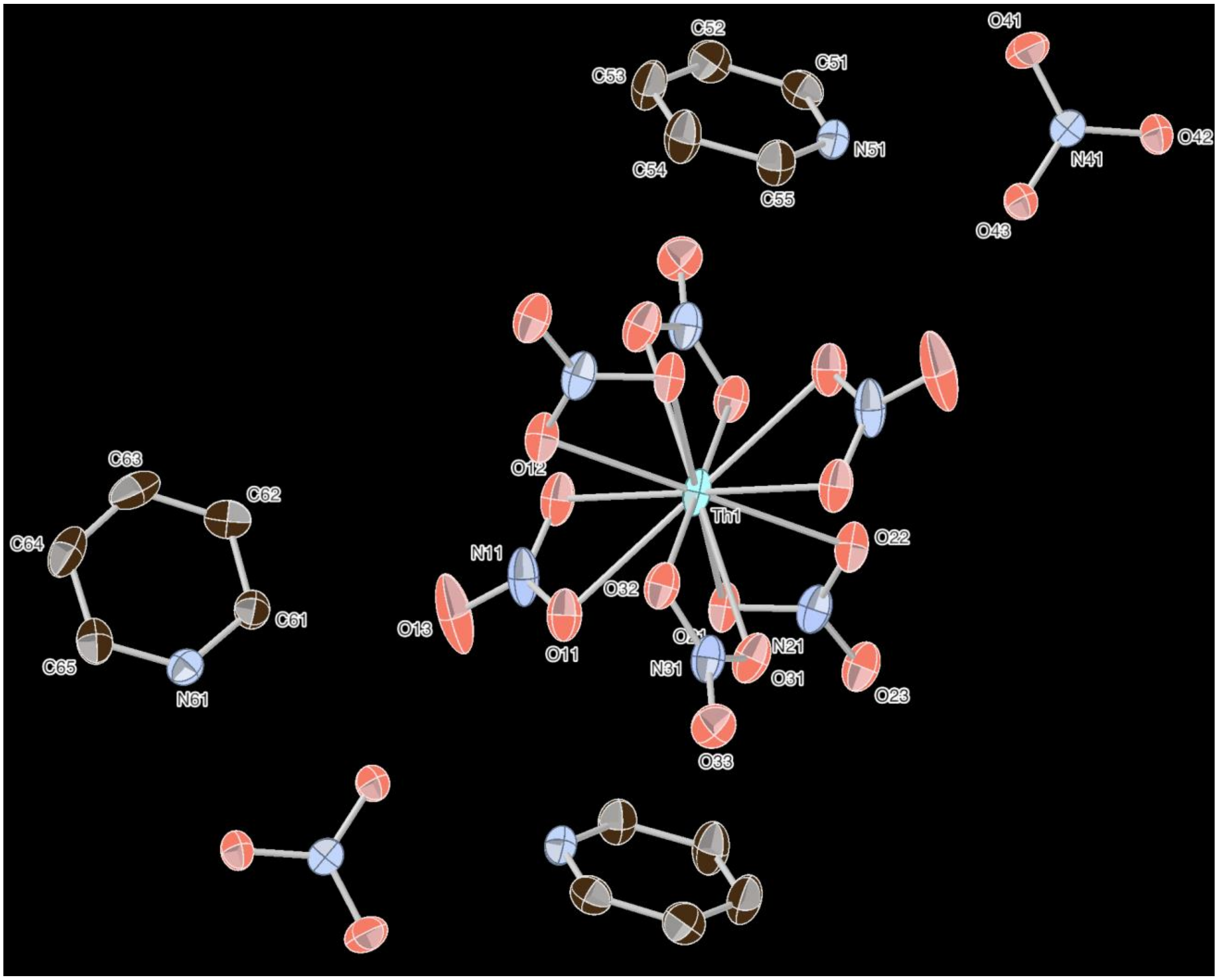

Figure S4. Thermal ellipsoid plot (50% probability level) of compound **4**, $(PyH)_2[Th(NO_3)_6]•2(PyH•NO_3)$, at 100 K. Symmetry equivalent atoms were generated through their respective symmetry elements (i = 1 – x ,1 – y , 1 – z).

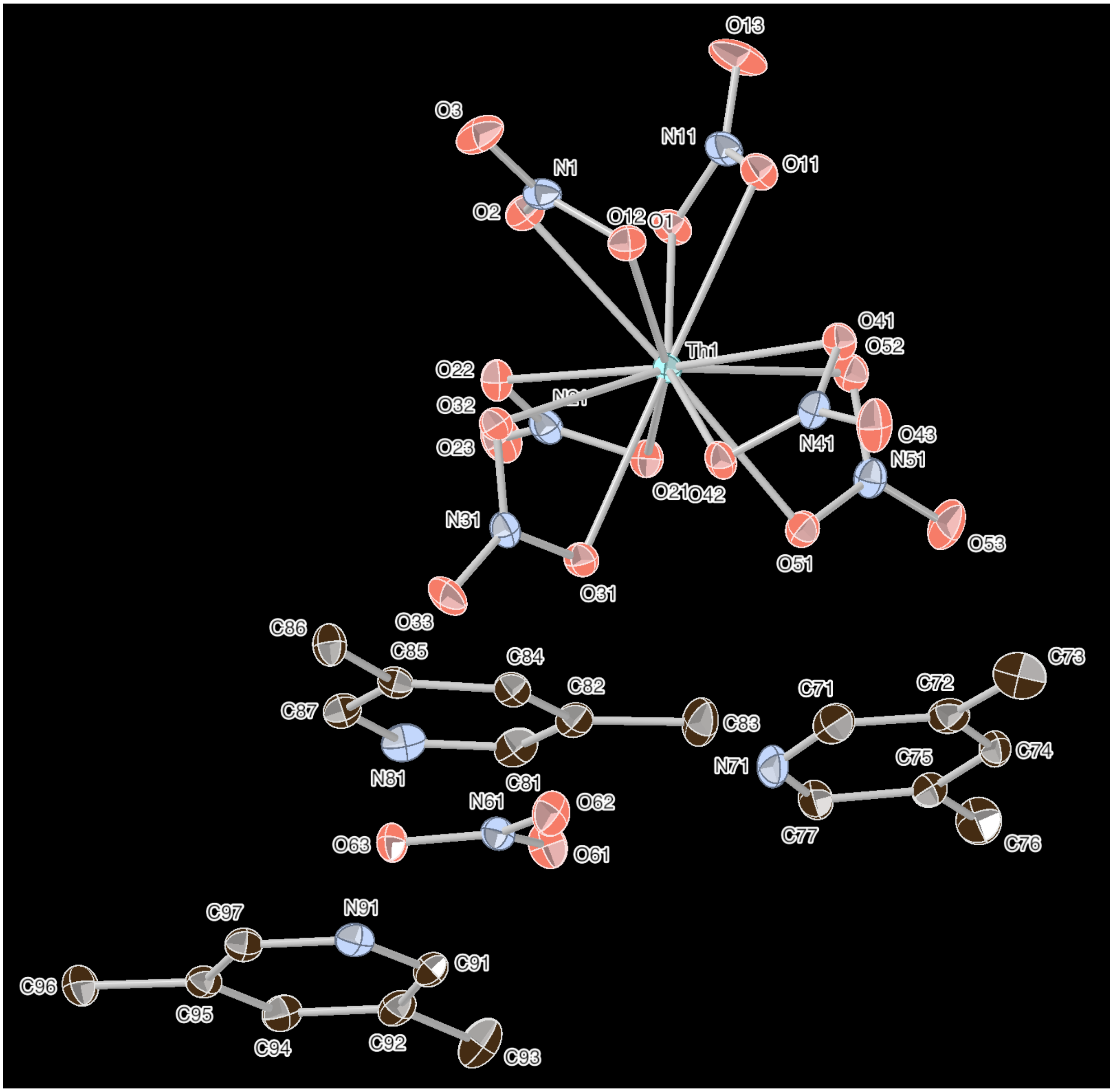

Figure S5. Thermal ellipsoid plot (50% probability level) of compound **5**, (3,5-DiMePyH)$_2$[Th(NO$_3$)$_6$]•[(3,5-DiMePyH)(NO$_3$)], at 100 K.

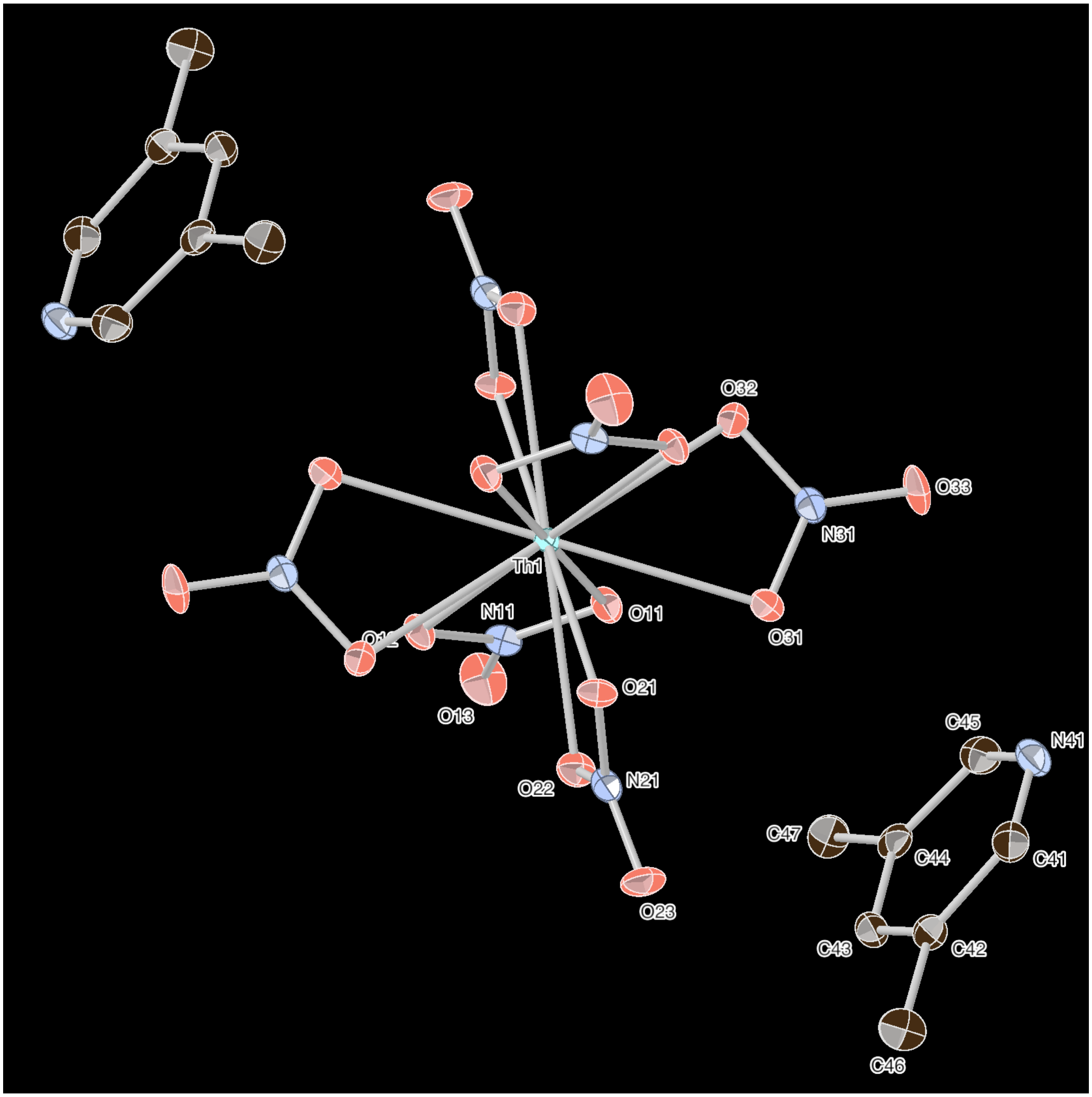

Figure S6. Thermal ellipsoid plot (50% probability level) of compound **6**, (3,5-DiMePyH)$_2$[Th(NO$_3$)$_6$], at 100 K. Symmetry equivalent atoms were generated through their respective symmetry elements (i = 1 – x ,1 – y , 1 – z).

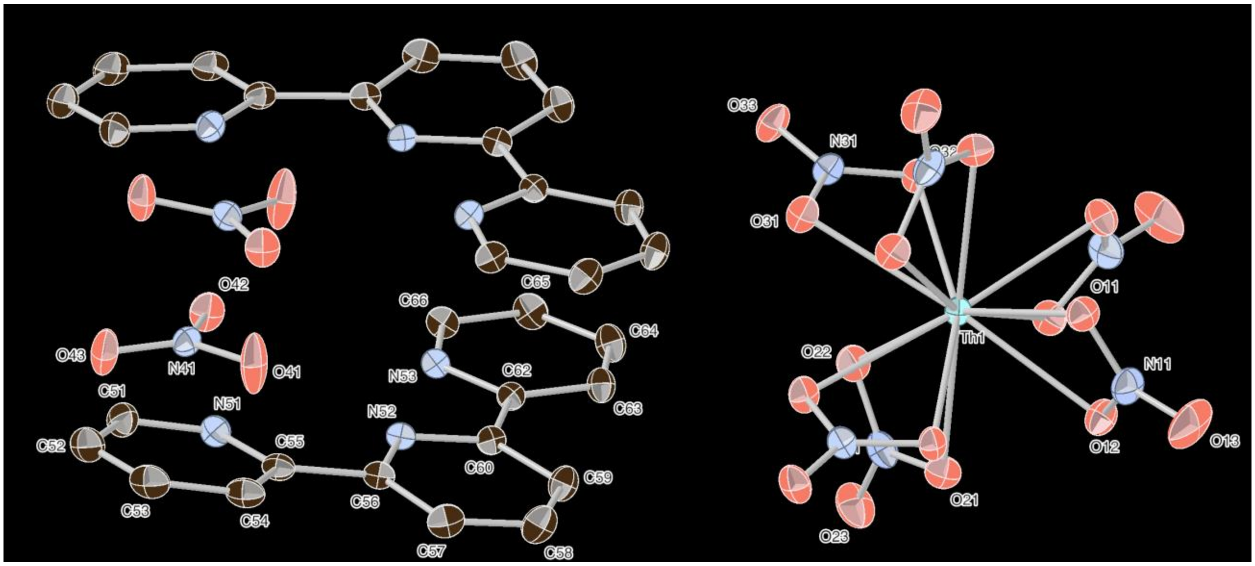

Figure S7. Thermal ellipsoid plot (50% probability level) of compound **7**, $(TerpyH_2)[Th(NO_3)_6]$•$(TerpyH_2)(NO_3)_2$, at 100 K. Symmetry equivalent atoms were generated through the following symmetry operations: i = 1 – x , y , ½ – z; ii = 1 – x , y , 3/2 – z.

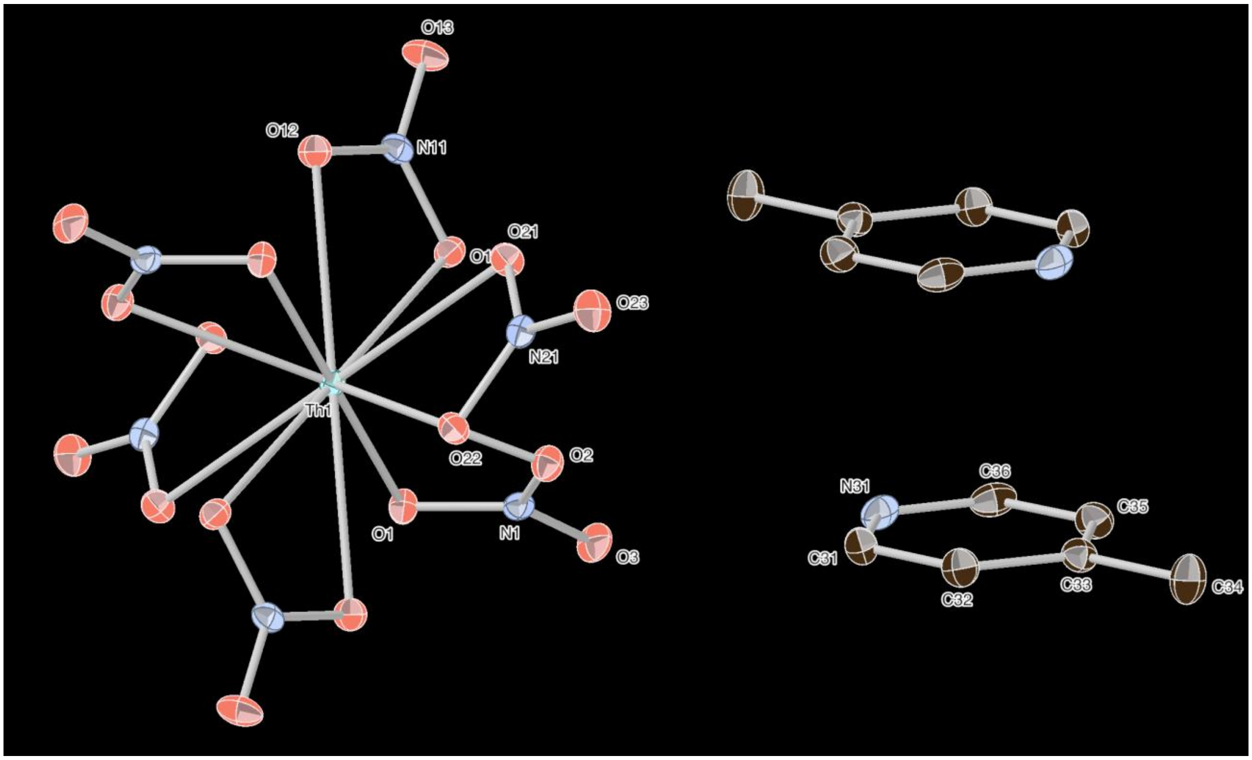

Figure S8. Thermal ellipsoid plot (50% probability level) of compound **8**, $(4\text{-MePyH})_2[Th(NO_3)_6]$, at 100 K. Symmetry equivalent atoms were generated through the following symmetry operations: i = ½– x , ½ + y , ½ – z; ii = 2– x , 1 – y , 1 – z.

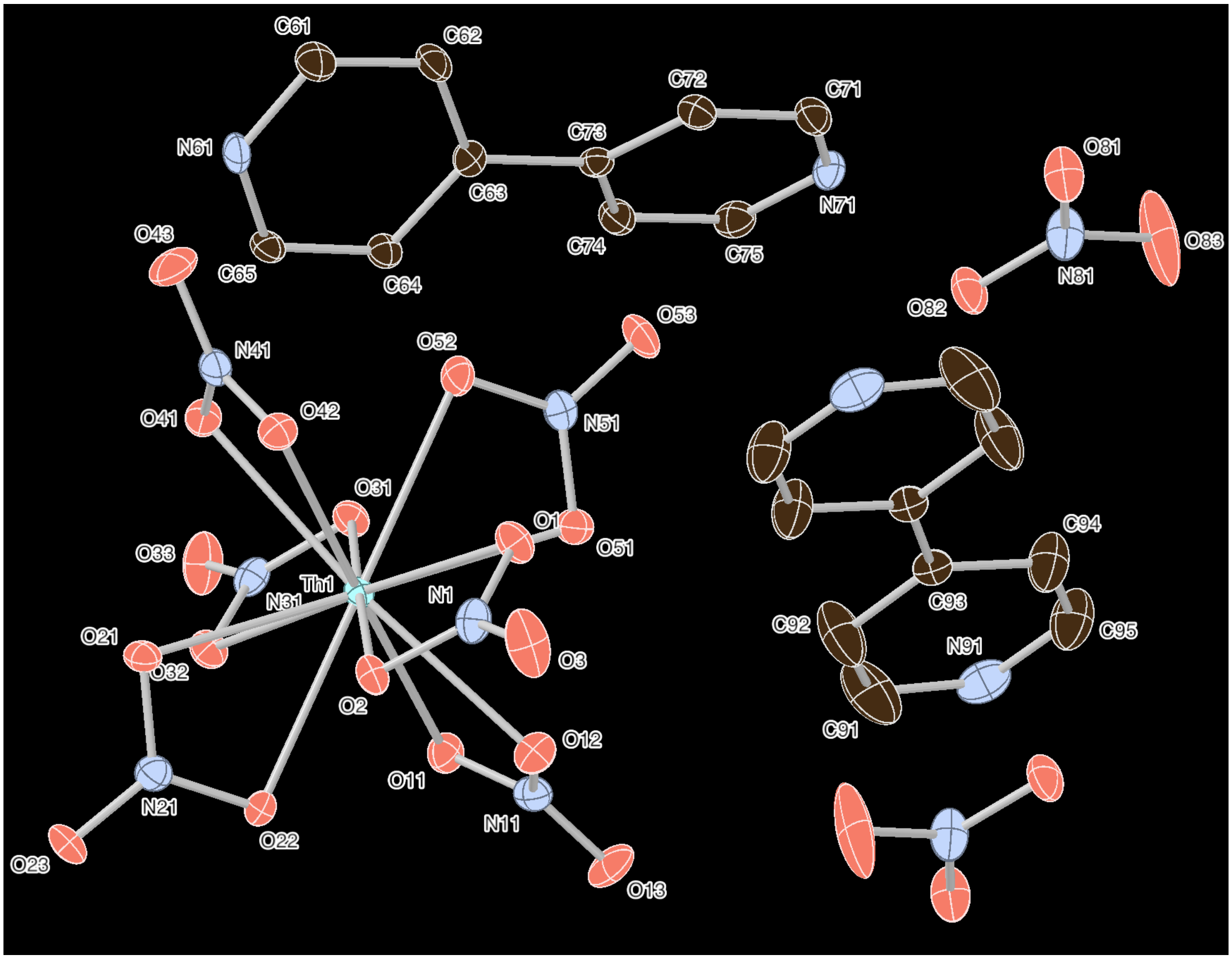

Figure S9. Thermal ellipsoid plot (50% probability level) of compound **9**, $[4,4'\text{-}BipyH_2]_2[Th(NO_3)_6]_2 \cdot [4,4'\text{-}BipyH_2 \cdot 2NO_3]$, at 100 K. Symmetry equivalent atoms were generated through the following operation: i = 1 – x , 1 - y , 1 – z.

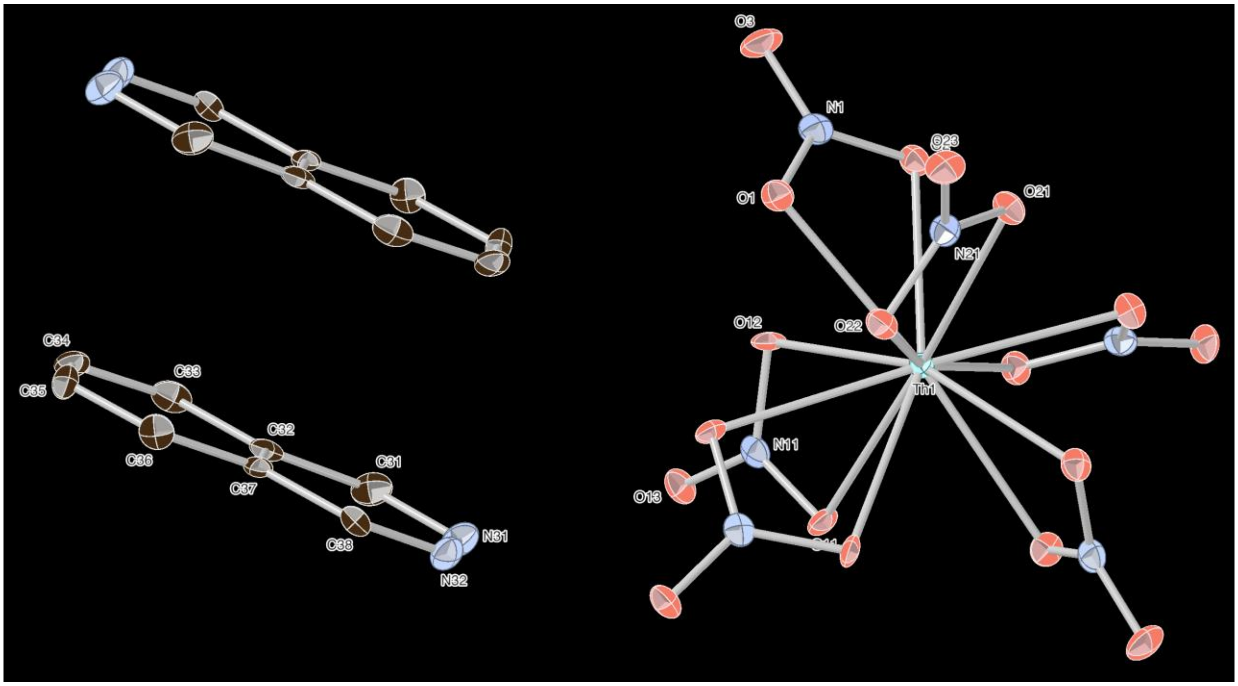

Figure S10. Thermal ellipsoid plot (50% probability level) of compound **10**, $(PhthalH)_2[Th(NO_3)_6]$, at 100 K. Symmetry equivalent atoms were generated through the following operations: i = 1– x , y , ½ – z; ii = 1– x , y , 3/2 – z.

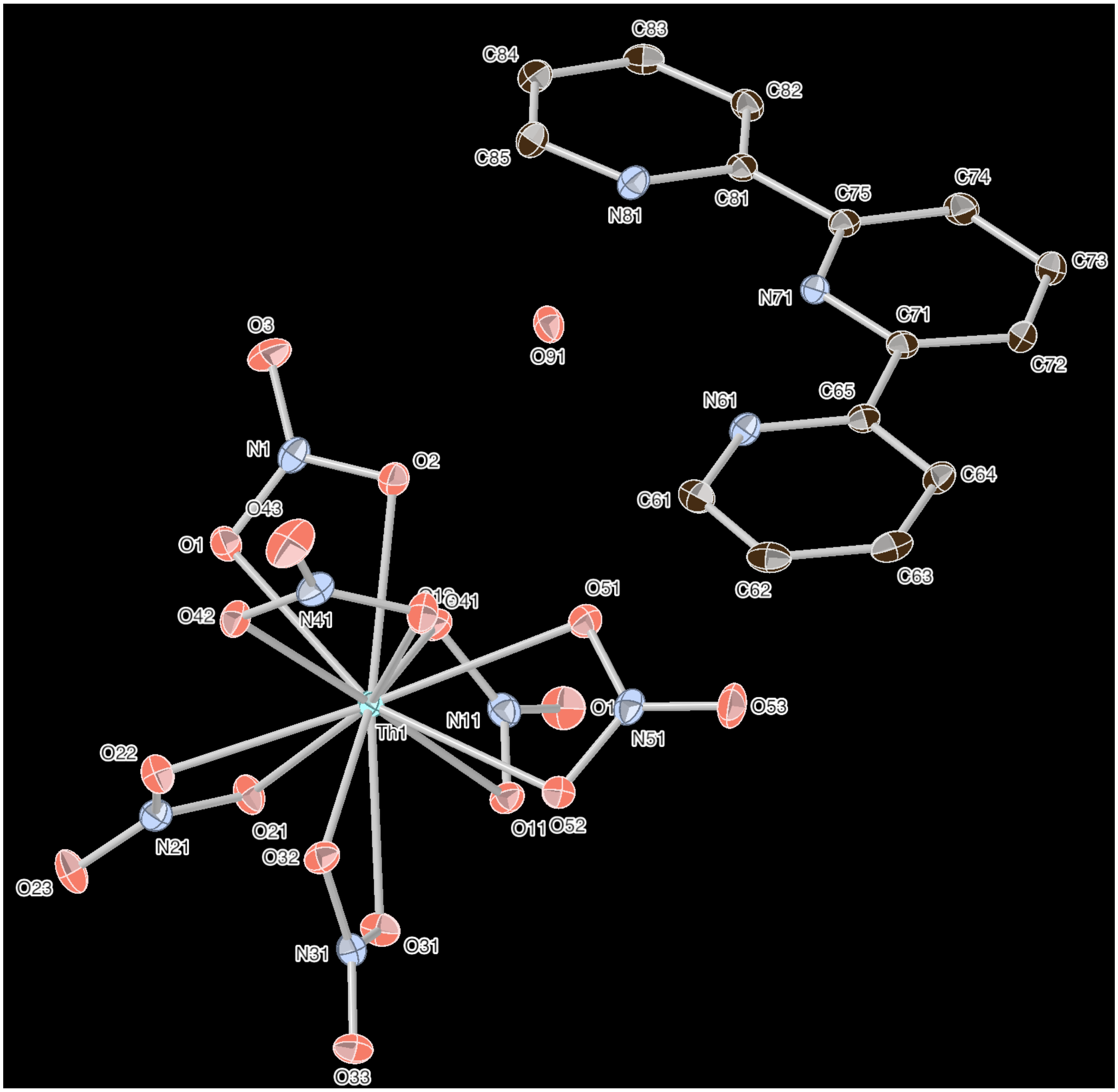

Figure S11. Thermal ellipsoid plot (50% probability level) of compound **11**, $[TerpyH_2][Th(NO_3)_6]{\bullet}H_2O$, at 100 K.

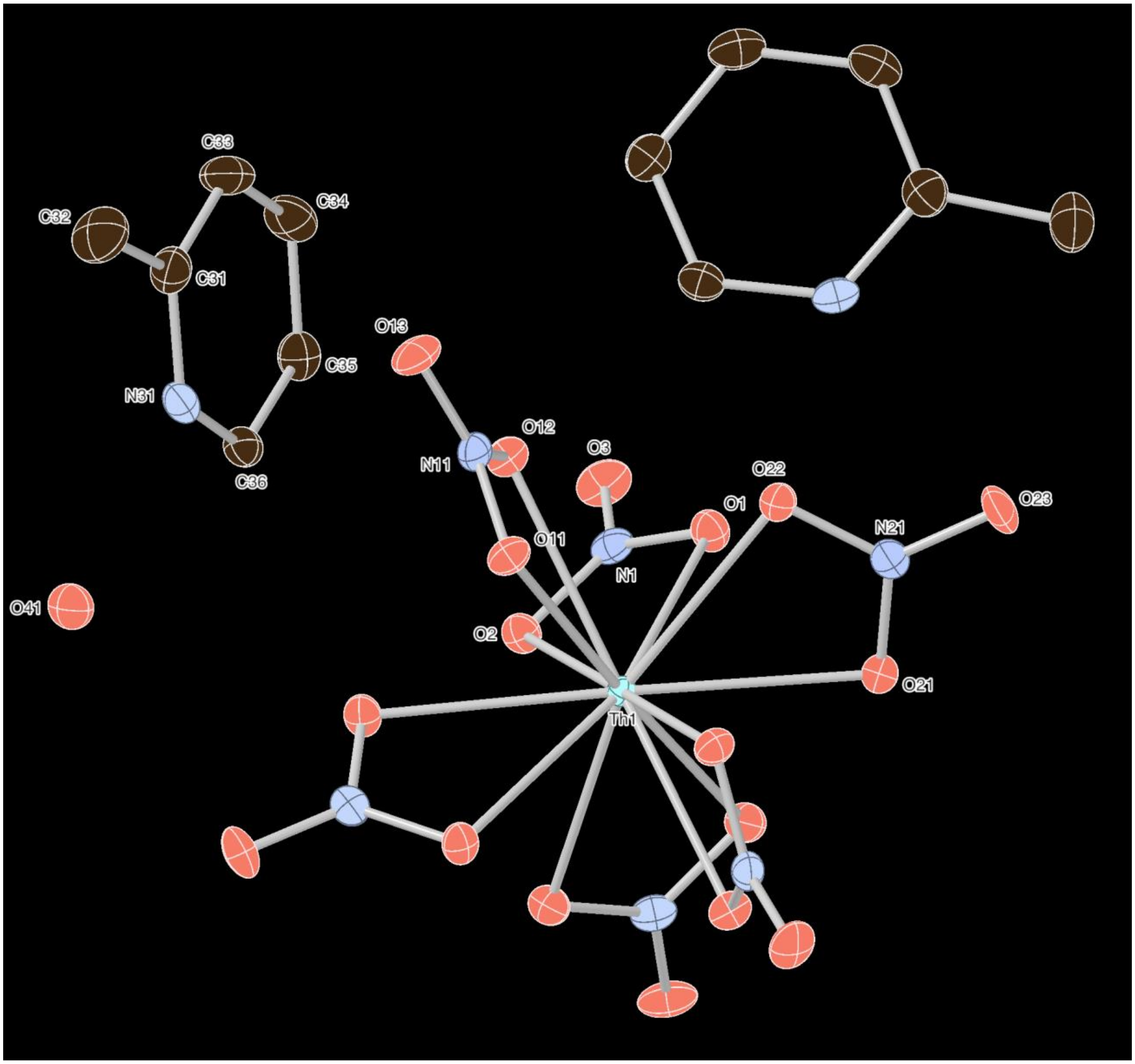

Figure S12. Thermal ellipsoid plot (50% probability level) of compound **12**, $(2MePyH)_2[Th(NO_3)_6]\cdot 2H_2O$, at 100 K. Symmetry equivalent atoms were generated through the following symmetry operation: i = 1–x, y, ½ – z.

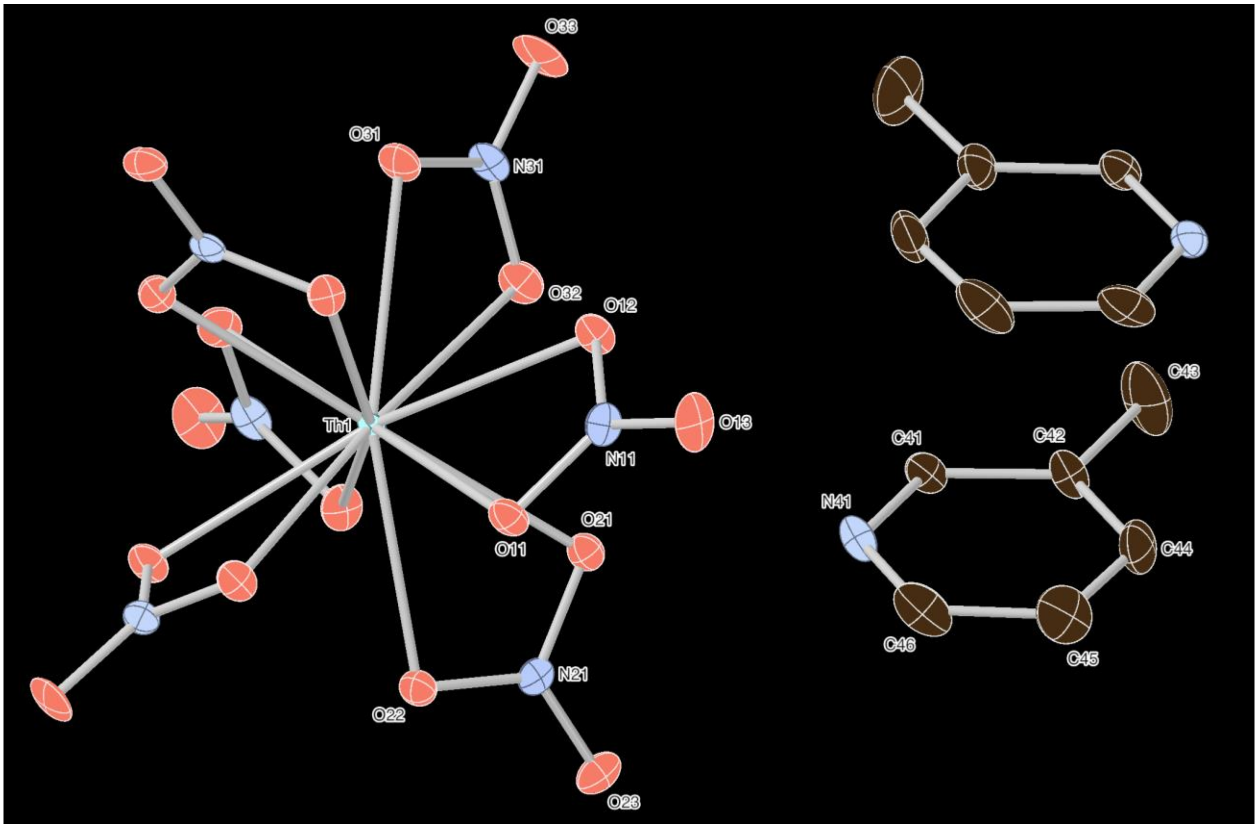

Figure S13. Thermal ellipsoid plot (50% probability level) of compound **13**, **(**3-MePyH)$_2$[Th(NO$_3$)$_6$], at 100 K. Symmetry equivalent atoms were generated through the following symmetry operations: i = 1– x , y , 1 – z; ii= 1– x , y , 3/2 – z.

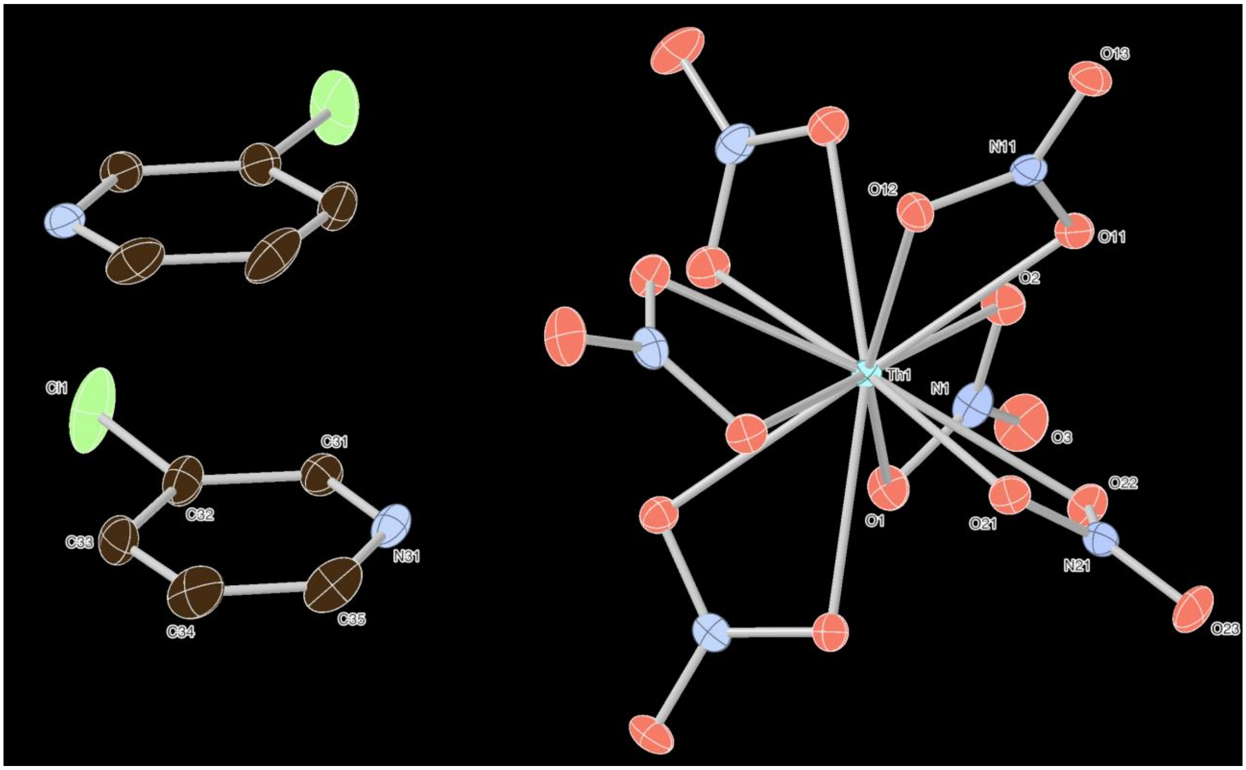

Figure S14. Thermal ellipsoid plot (50% probability level) of compound **14**, $(3\text{-}ClPyH)_2[Th(NO_3)_6]$, at 100 K. Symmetry equivalent atoms were generated the following operations: i = 1 – x, y , 3/2 – z.

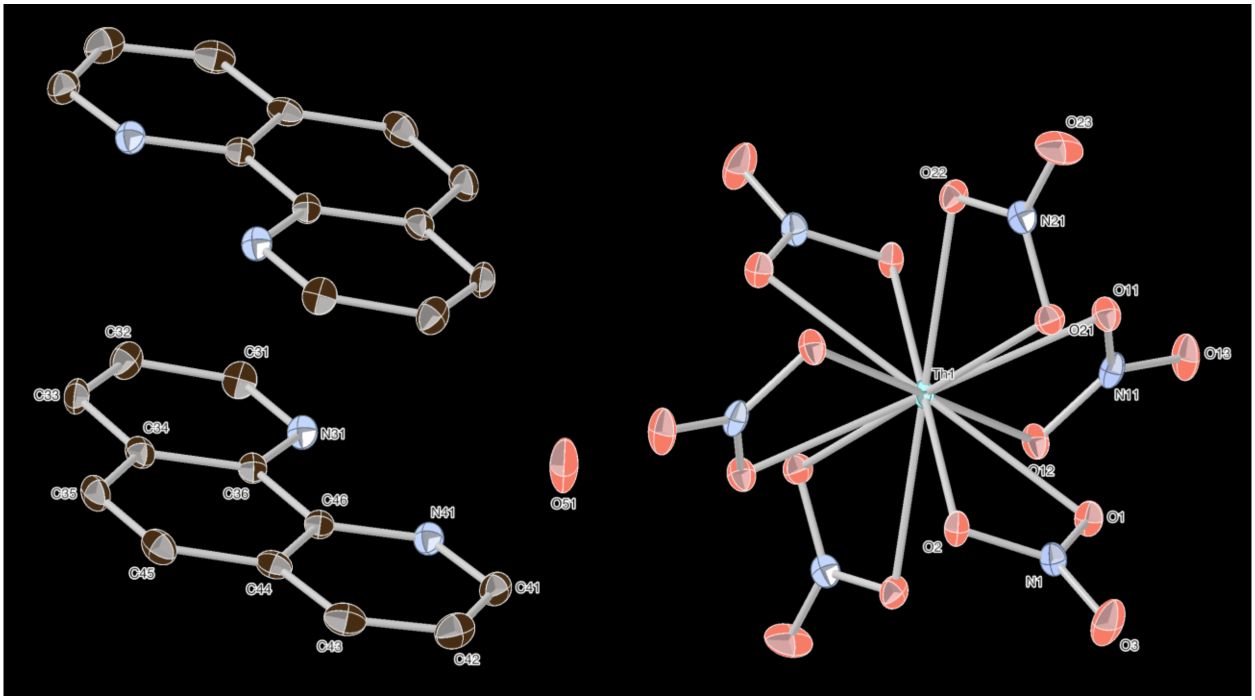

Figure S15. Thermal ellipsoid plot (50% probability level) of compound **15**, $(PhenH)_2[Th(NO_3)_6]•2[H_2O]$, at 100 K. Symmetry equivalent atoms were generated the following symmetry operations: i = 1 – x, 1 – y , 1 – z.

4. SUPRAMOLECULAR PACKING DIAGRAMS.

The structures of the compounds reported herein adopt supramolecular extended networks that result from noncovalent interactions including hydrogen bonding, and π-π stacking interactions.

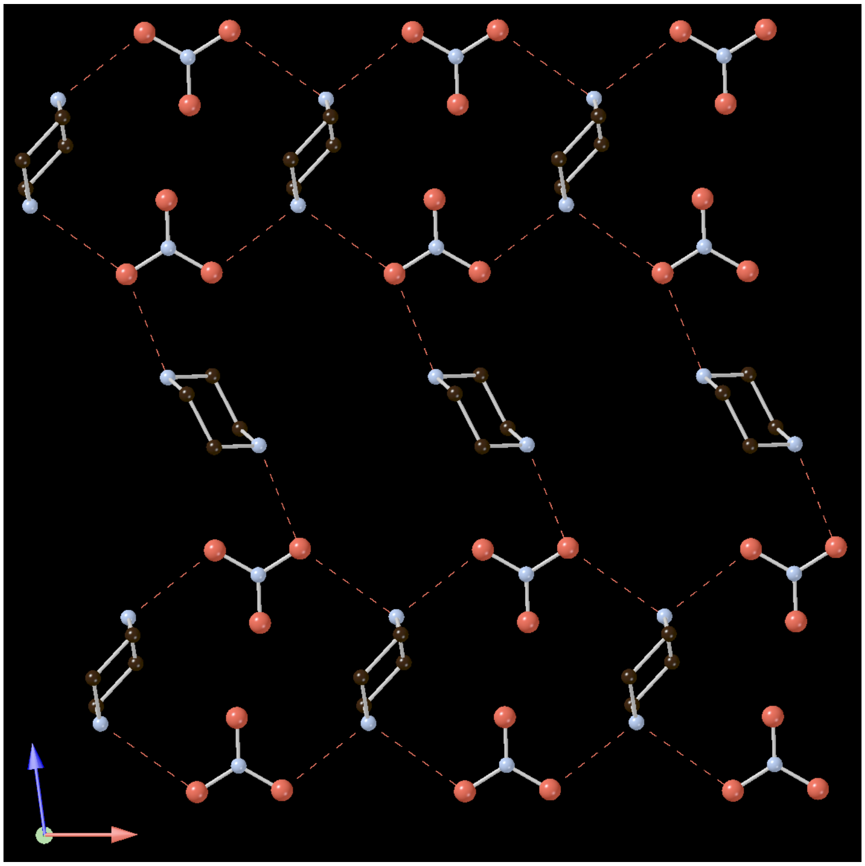

Figure S16. Packing diagram of (1) $PiperH_2[Th(NO_3)_5(H_2O)_2]_2$•$[PiperH_2(NO_3)_2]$ Looking down the y-axis. The H-bonding network along x and z axes further propagates into a 2D supramolecular network.

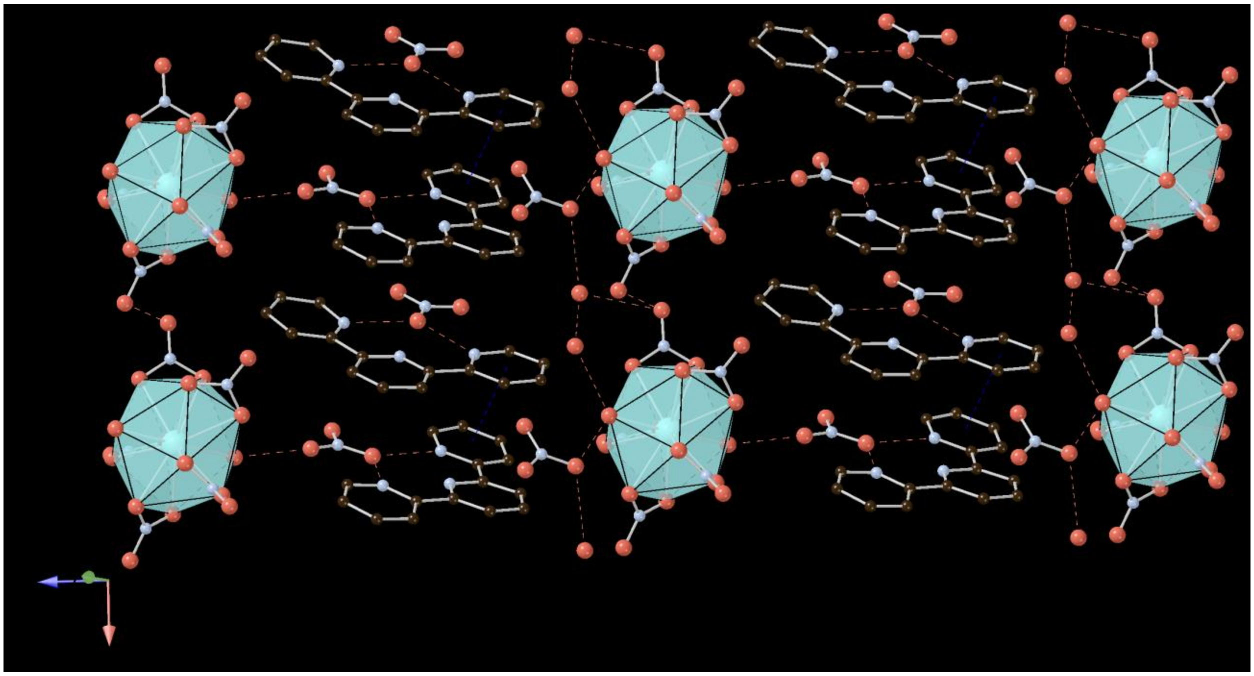

Figure S17. Packing diagram of (2) $[TerpyH_2]_2[Th(NO_3)_5][NO_3]_3[H_2O]_2$
From the pentanitrato structural unit H-bonding and pi-pi stacking along the x-axis further propagate this compound into a 3D supramolecular framework.

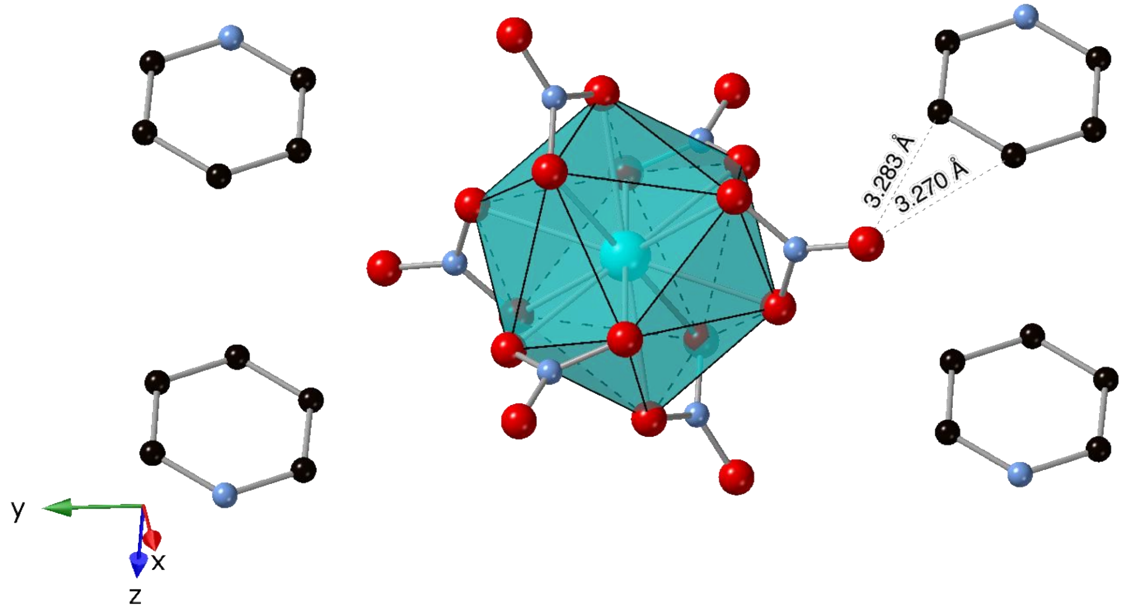

Figure S18. Packing diagram of (3), $(PyH)_2[Th(NO_3)_6]$•$(PyH$•$NO_3)$
In this 0D supramolecular network, there are no non-covalent interactions along the y-axis, however, in this figure C-H---O interaction distances are shown for clarity.

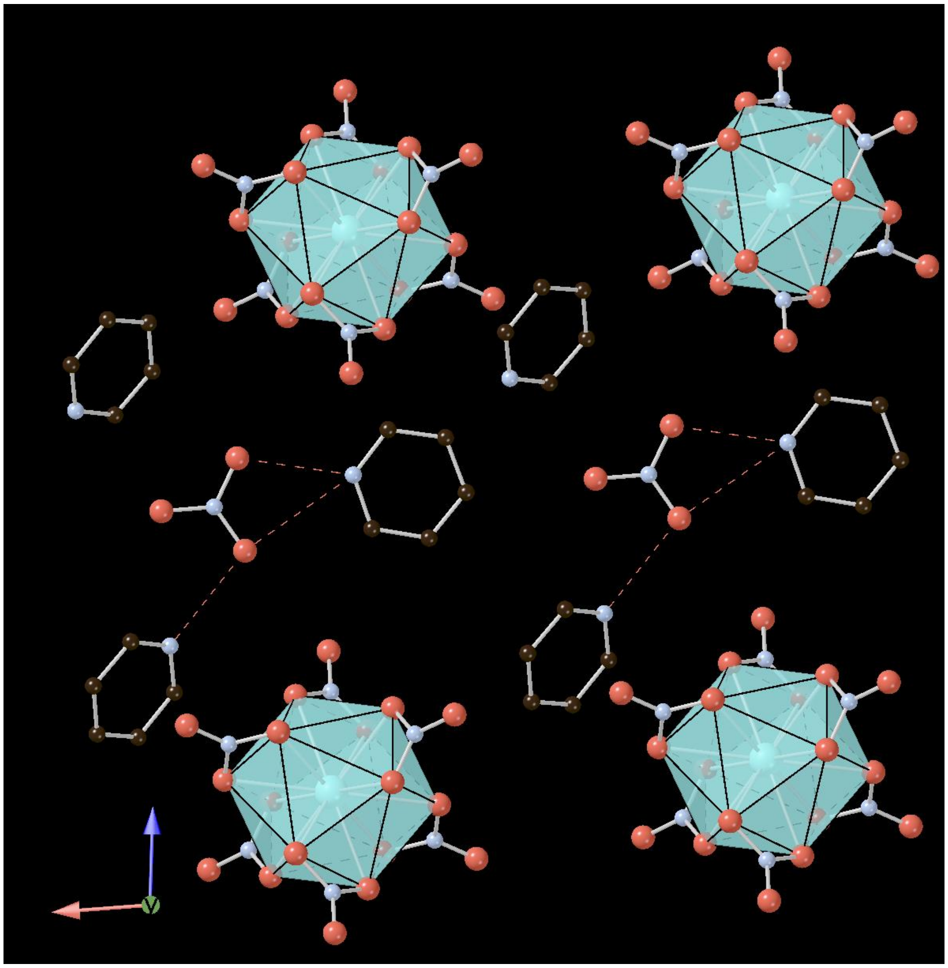

Figure S19. Packing diagram of (4), $(PyH)_2[Th(NO_3)_6]$•2(PyH•NO_3)
Carbon atoms have been omitted for clarity. Viewed down the y-axis there are no non-covalent interactions between the thorium structural units which further indicates the 0D network for this compound.

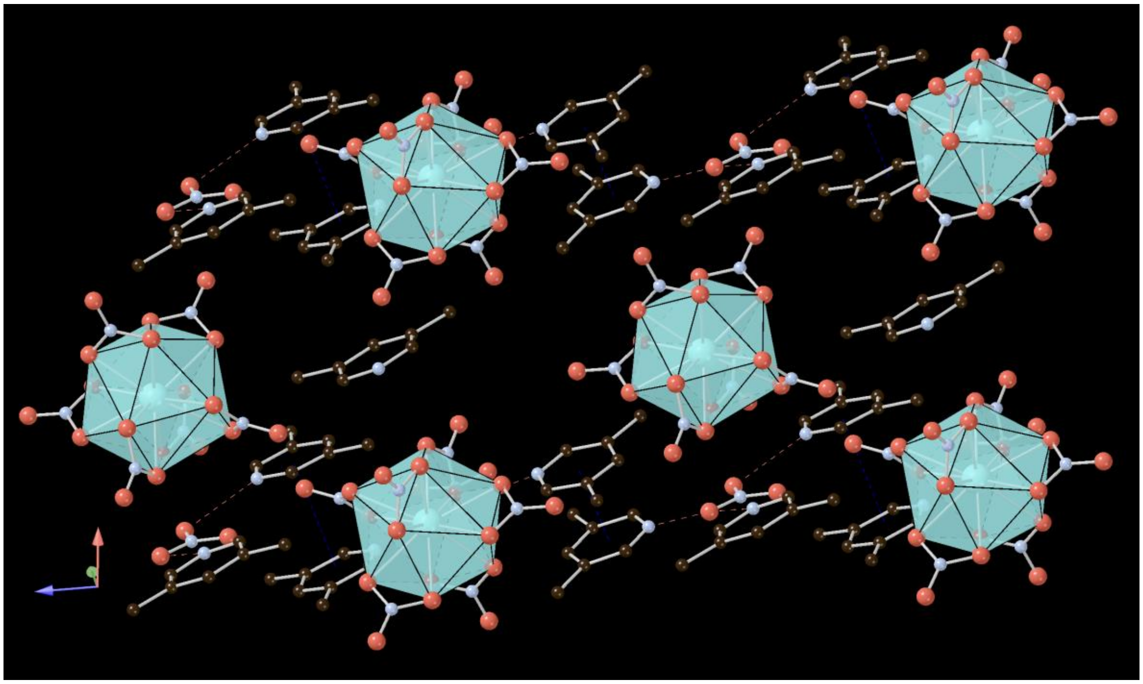

Figure S20. Packing diagram of (5) $(3,5\text{-DiMePyH})_2[Th(NO_3)_6]$•$[(3,5\text{-DiMePyH})(NO_3)]$ There is no propagation along the z-axis further indicating the 0D nature of this unit.

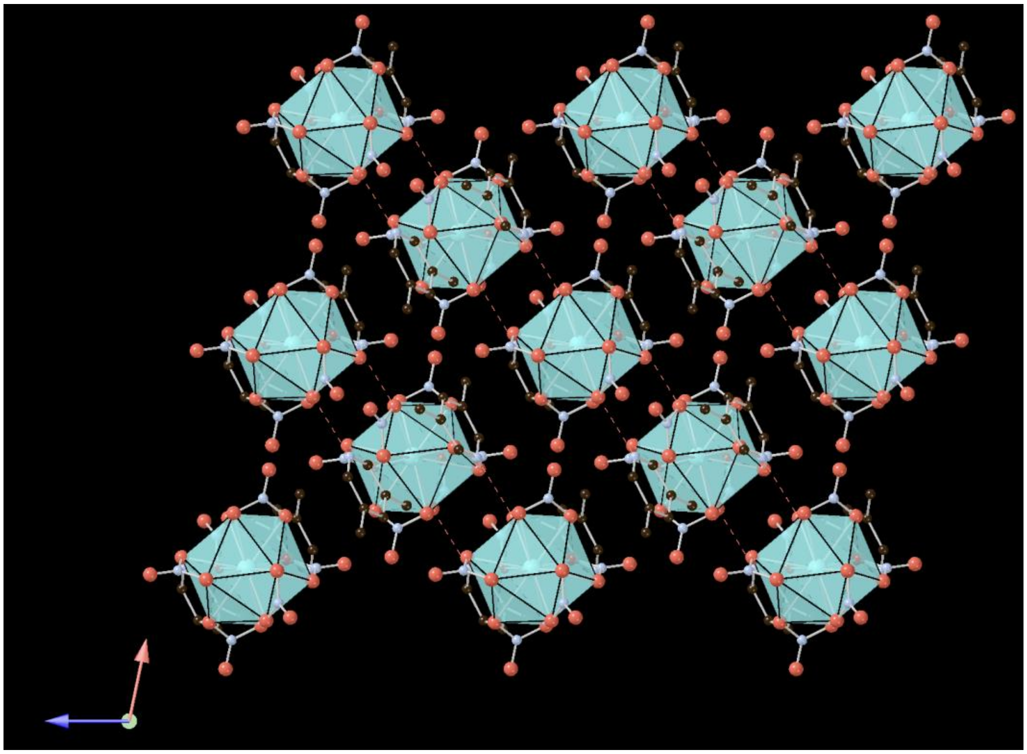

Figure S21. Packing diagram of (6) $[3,5\text{-DiMePy}]_2[Th(NO_3)_6]$.

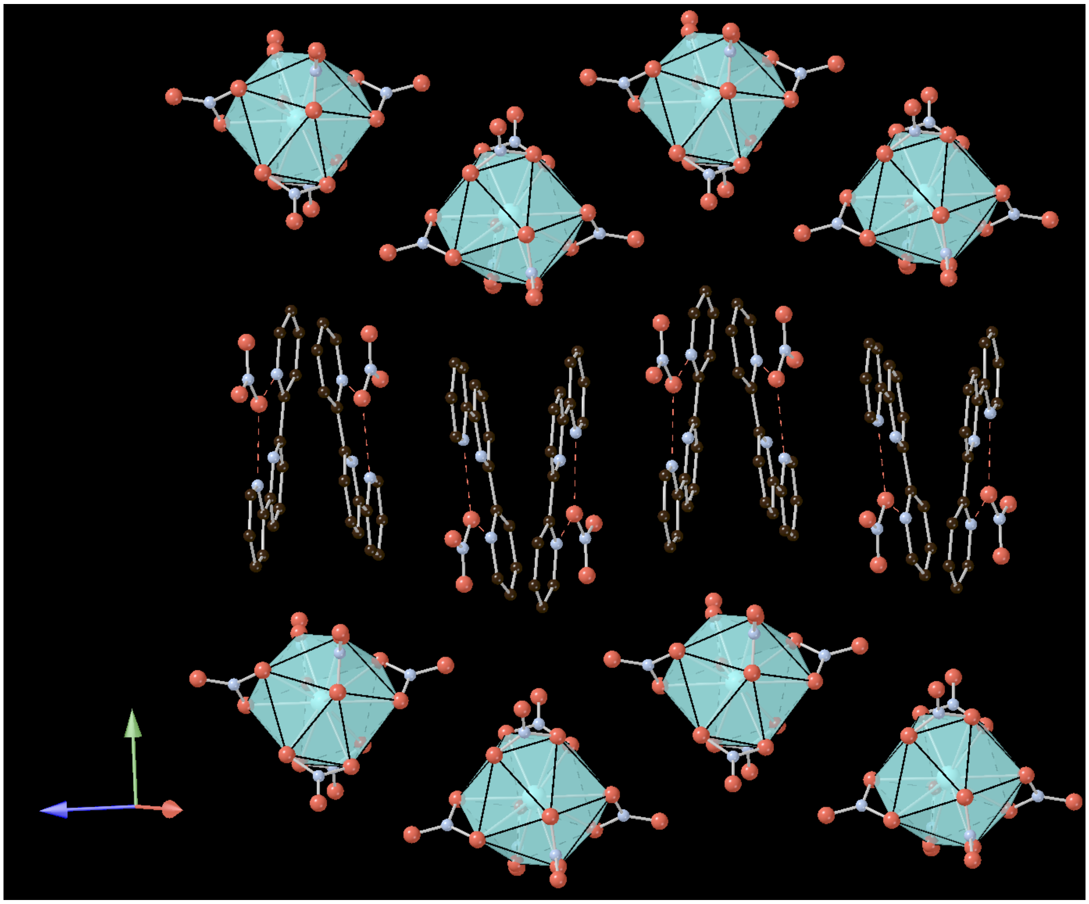

Figure S22. Packing diagram of (7) $(TerpyH_2)[Th(NO_3)_6]\bullet(TerpyH_2)(NO_3)_2$
There are no non-covalent interactions between the thorium structural units further indicating the 0D supramolecular framework.

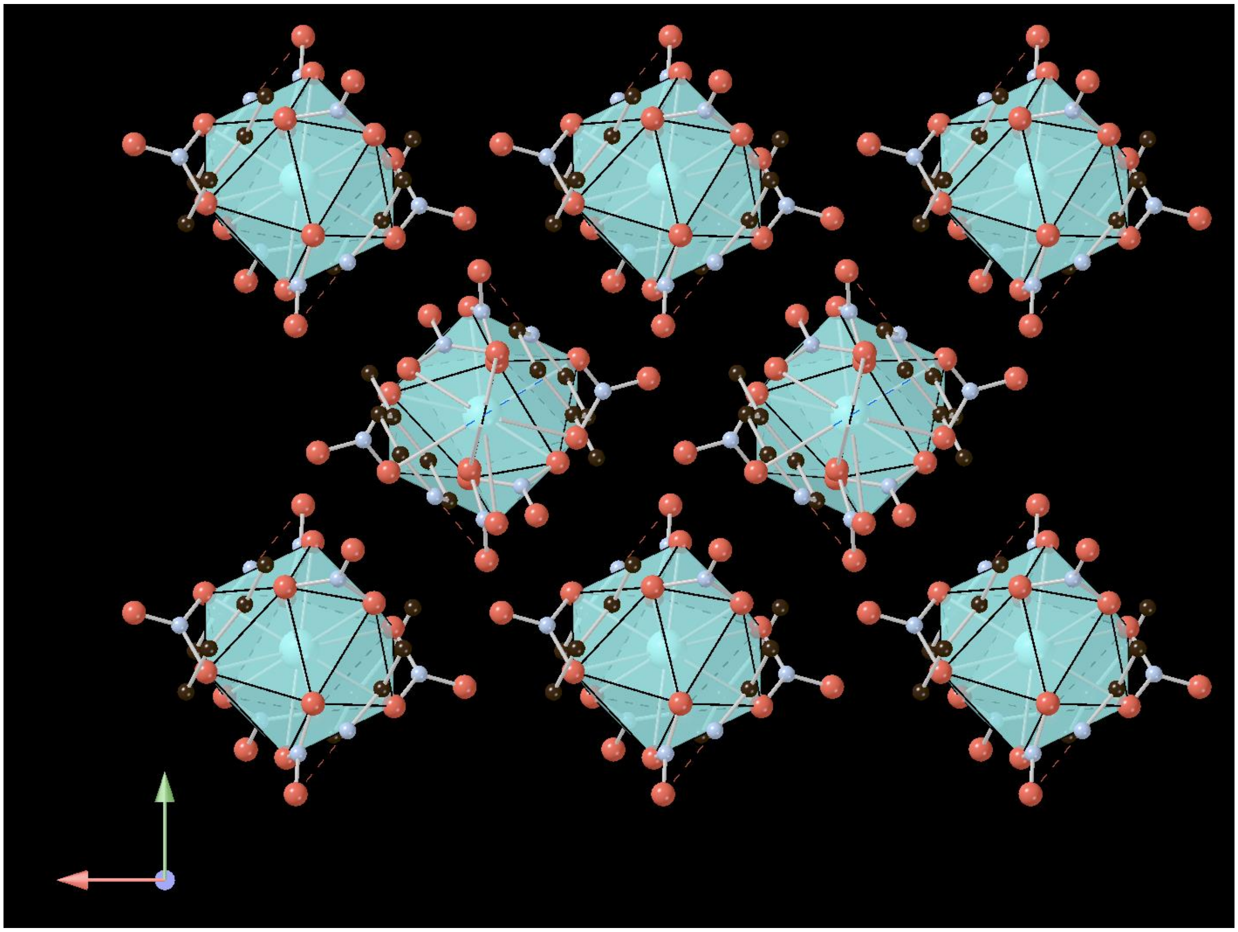

Figure S23. Packing diagram of (8) $[4\text{-MePyH}]_2[Th(NO_3)_6]$

There is no propagation along the y or x axes further indicating the 1D connectivity along the z axis of this supramolecular network.

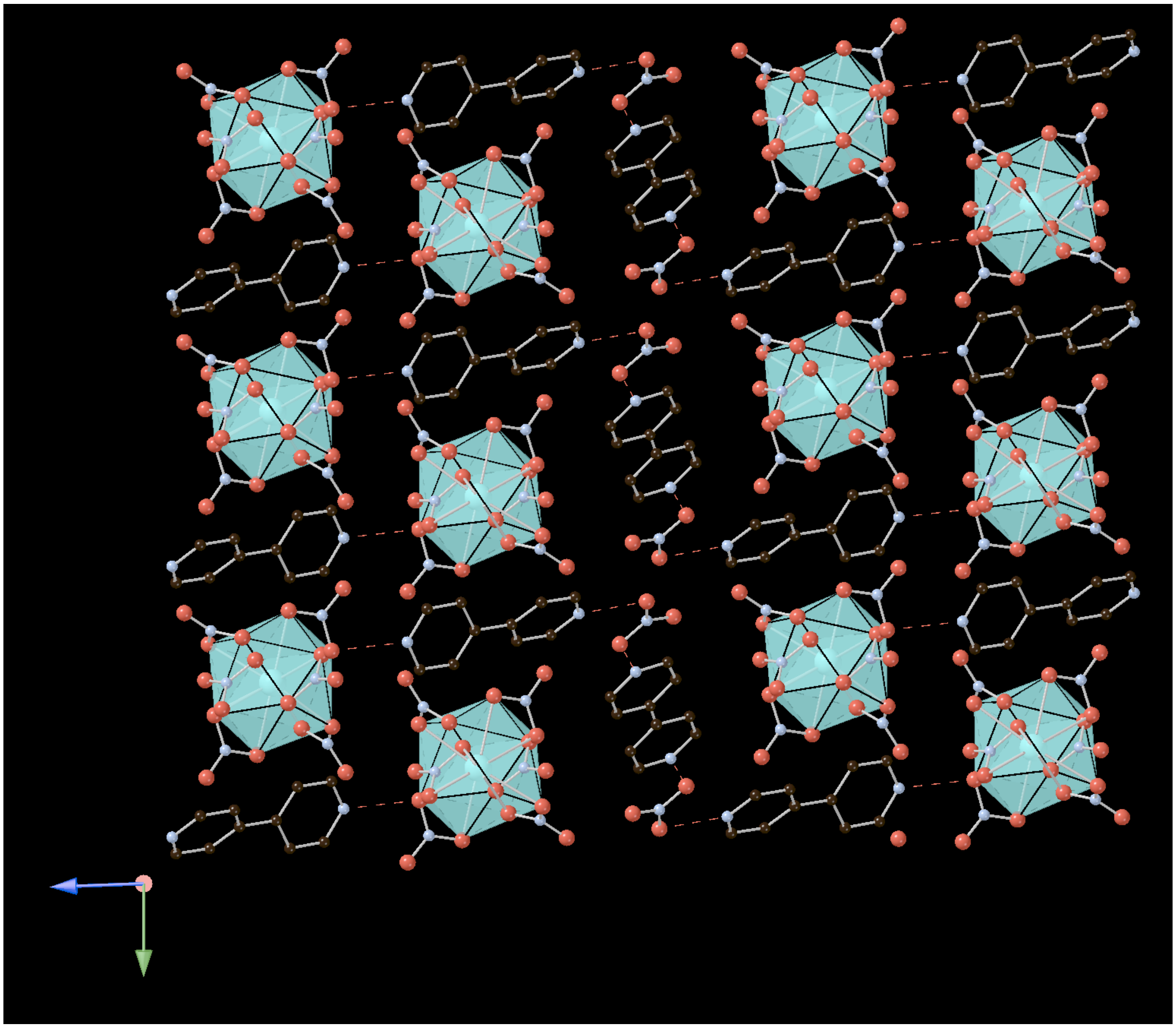

Figure S24. Packing diagram of (9) $[4,4\text{-BipyH}_2]_2[Th(NO_3)_6]_2$•$[4,4\text{-BipyH}_2$•$2NO_3]$ Propagating along z axis from the thorium metal center, H-bonding interactions connect between the outer coordination sphere bipyridinium's as well as the nitrates to form 1D chains.

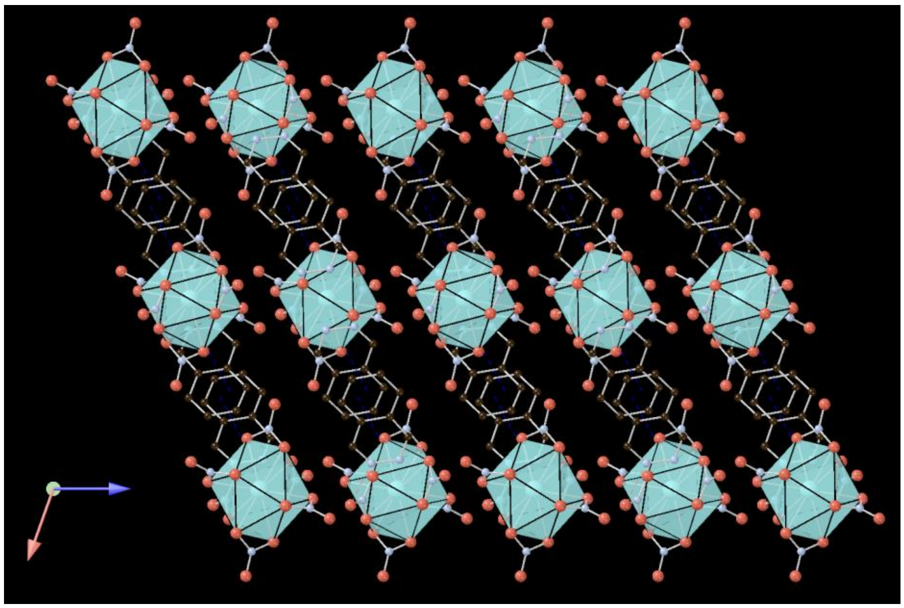

Figure S25. Packing diagram of (10) $(PhthalH)_2[Th(NO_3)_6]$
While the 1D chains propagate along the z-axis, here one can see there is no propagation along the x axis, further indicating the 1D supramolecular network.

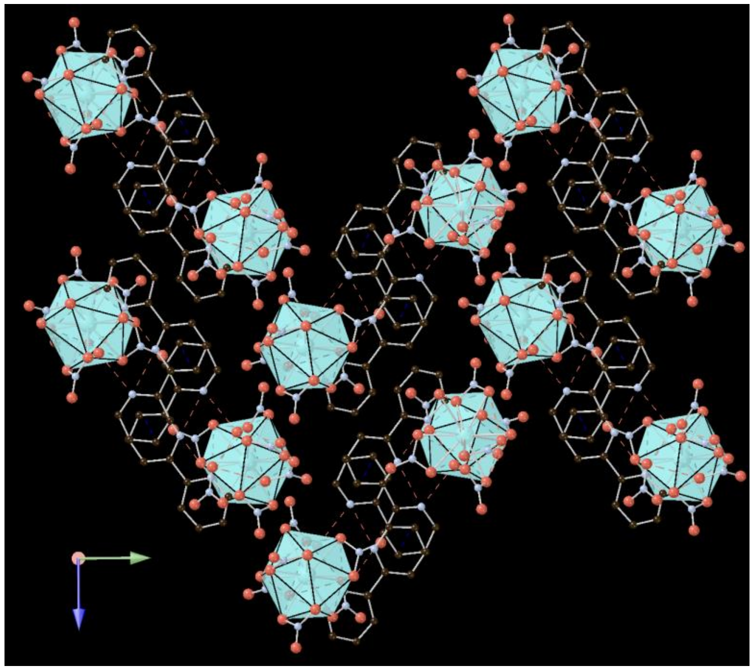

Figure S26. Packing diagram of (11) [TerpyH_2][Th$(NO_3)_6$]•H_2O
Viewed down the x-axis showing the non-covalent interactions that propagate this system into a 1D supramolecular network.

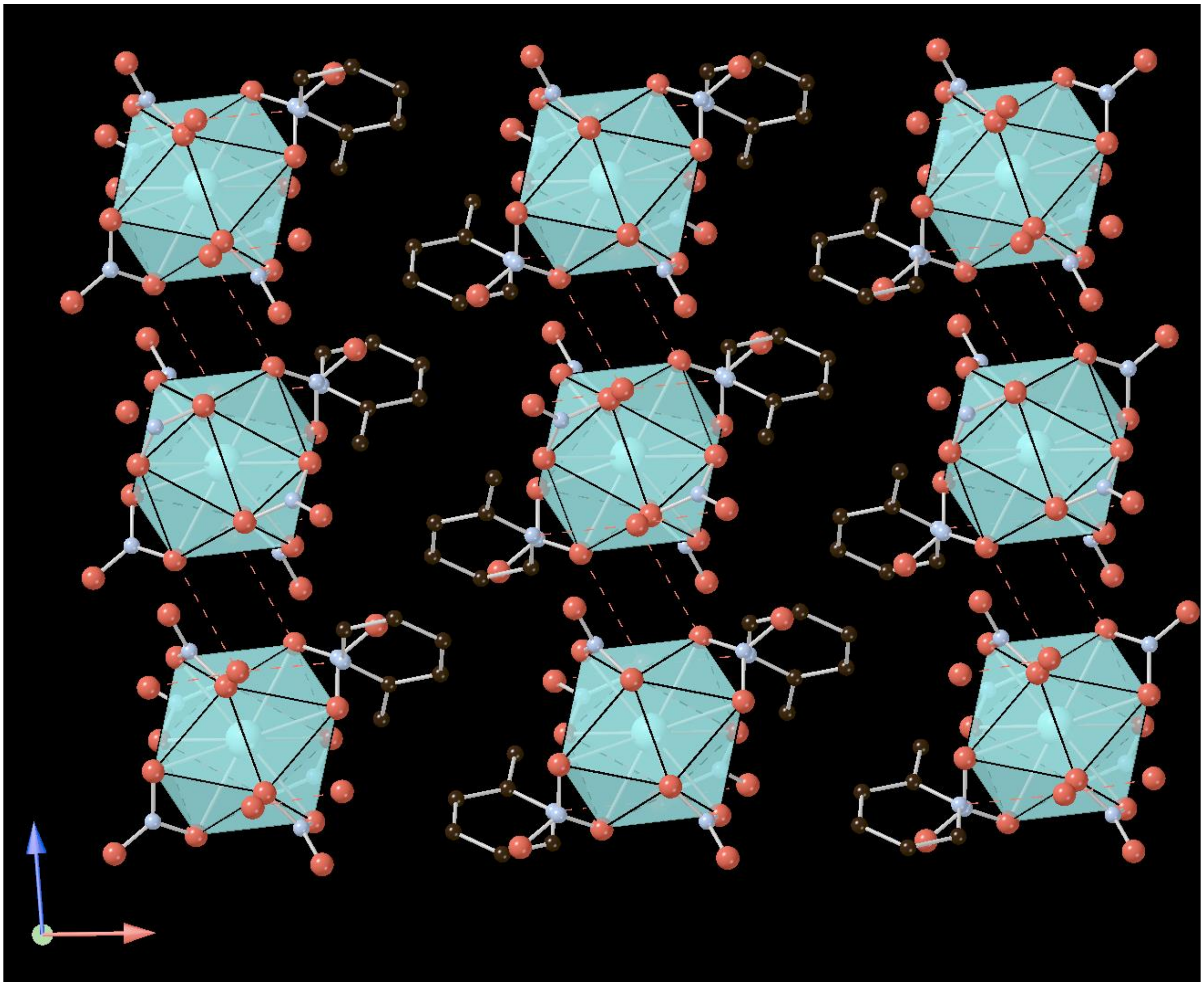

Figure S27. Packing diagram of (12) $(2MePyH)_2[Th(NO_3)_6]•2H_2O$
Viewed down the y-axis showing the non-covalent interactions along the z-axis that propagate this system into a 2D supramolecular network.

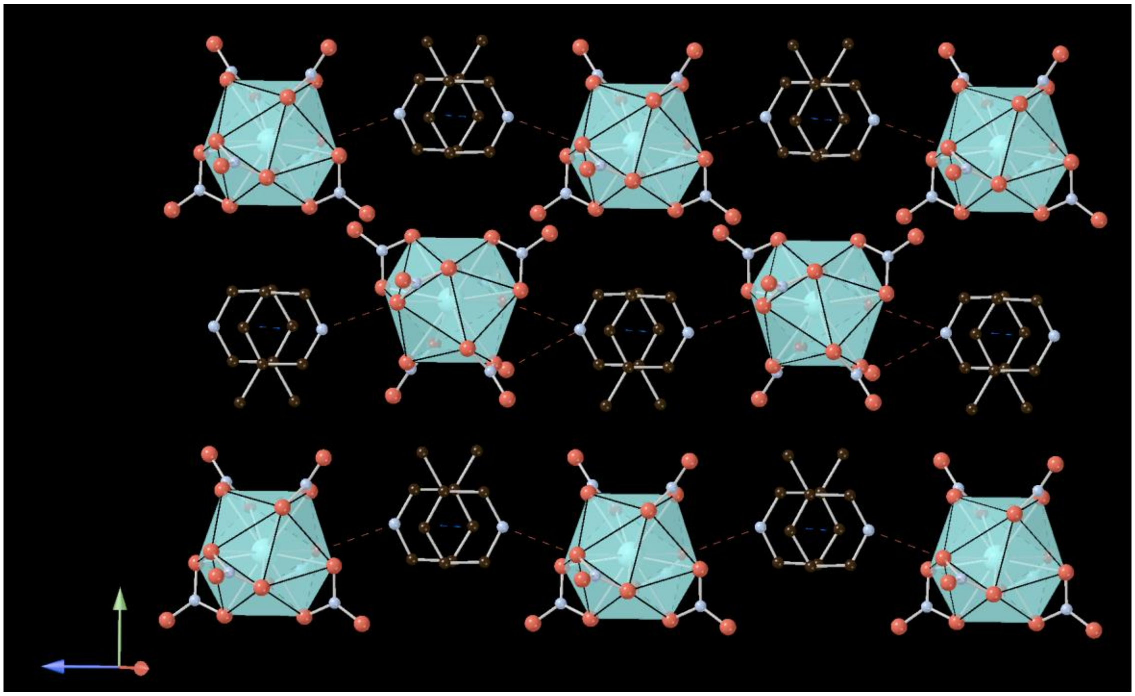

Figure S28. Packing diagram of (13) **(**3-MePyH)$_2$[Th(NO$_3$)$_6$]
Shows the non-covalent interactions along the z-axis that propagate this system into a 2D supramolecular network.

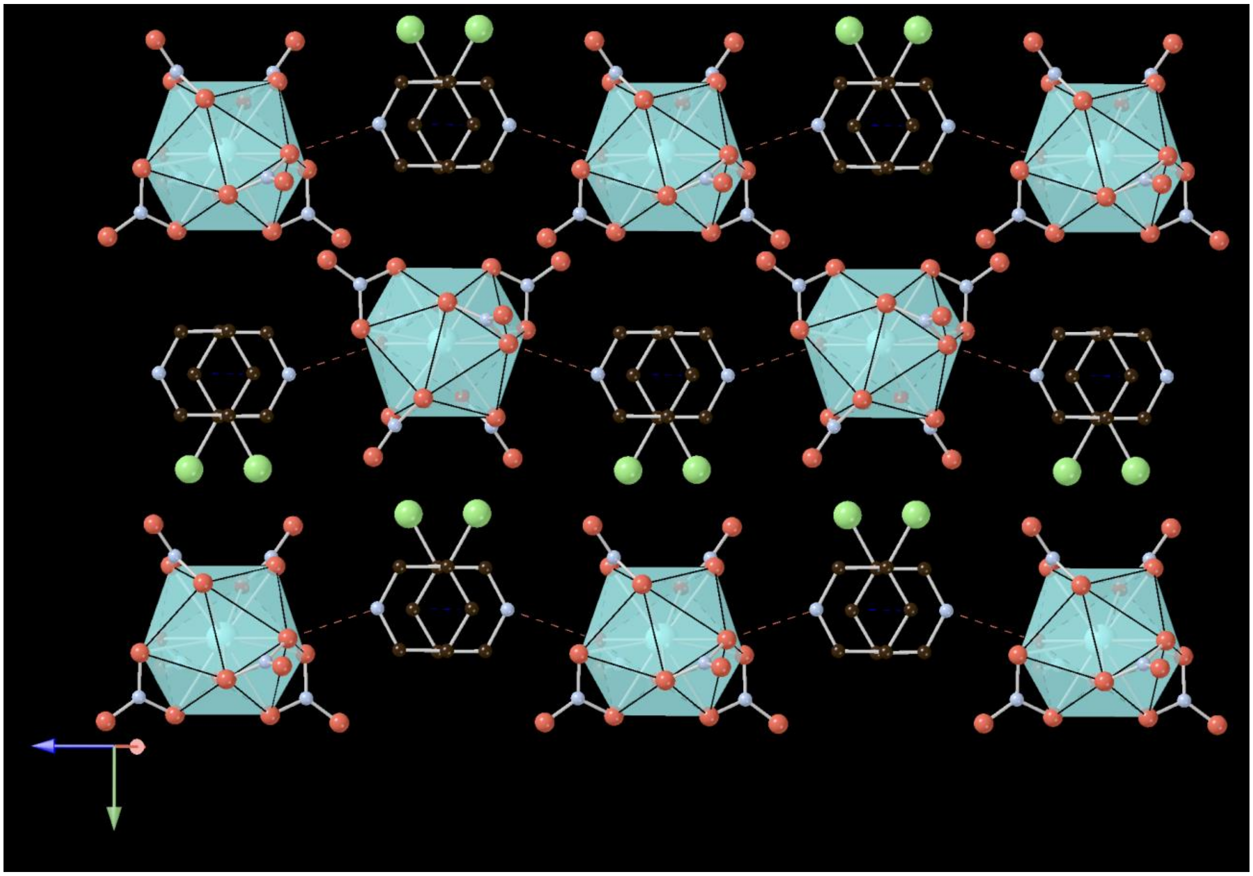

Figure S29. Packing diagram of (14) $[3\text{-ClPyH}]_2[Th(NO_3)_6]$
Viewed down the x-axis showing the non-covalent interactions along the z axis that propagates this system into a 2D supramolecular network.

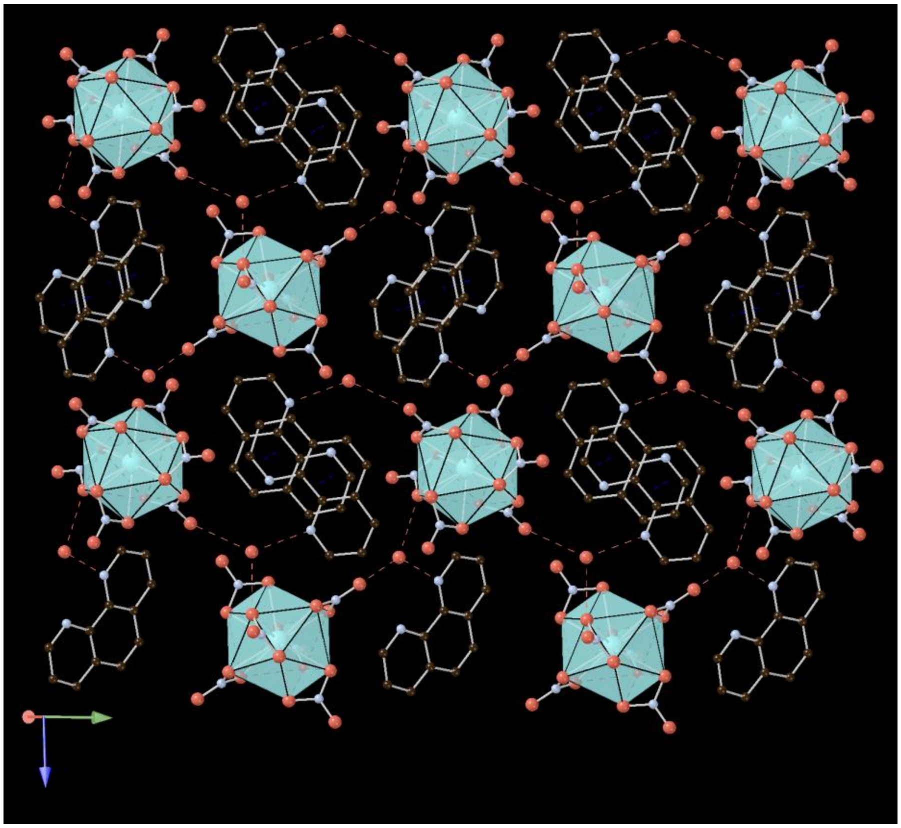

Figure S30. Packing diagram of (15) $(PhenH)_2[Th(NO_3)_6]$•$2[H_2O]$
Shows the non-covalent interactions down the x-axis, which further propagate this system into a 2D supramolecular network.

5. POWDER X-RAY DIFFRACTION PLOTS OF COMPOUNDS **1**–**15**.

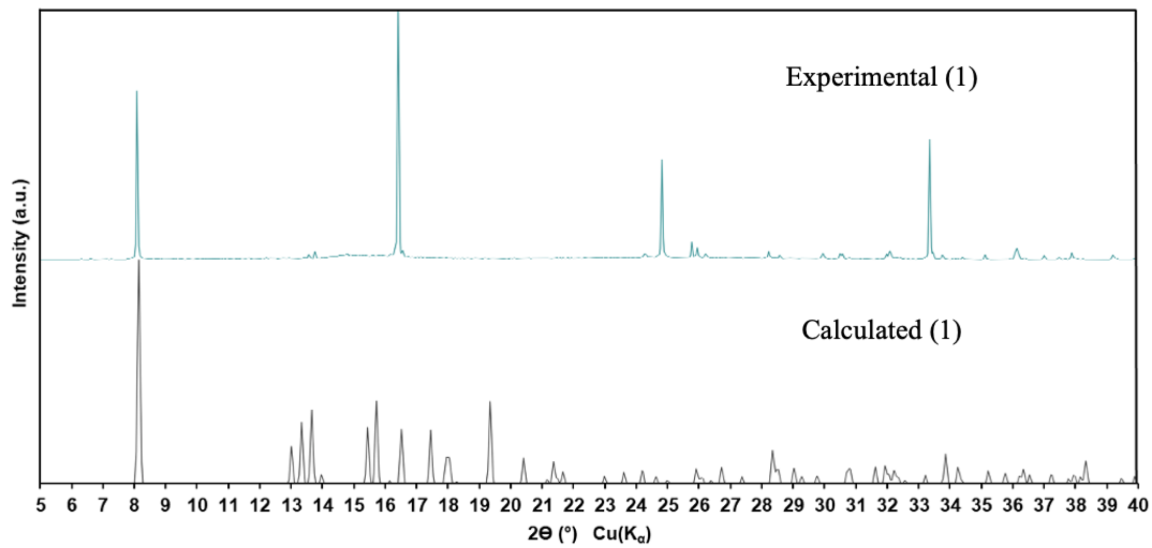

Figure S31. Powder X-ray diffraction pattern (collected with Cu Kα radiation) observed for 1 (teal) overlaid with the pattern calculated from the single crystal structure of 1 at 100 K (black).

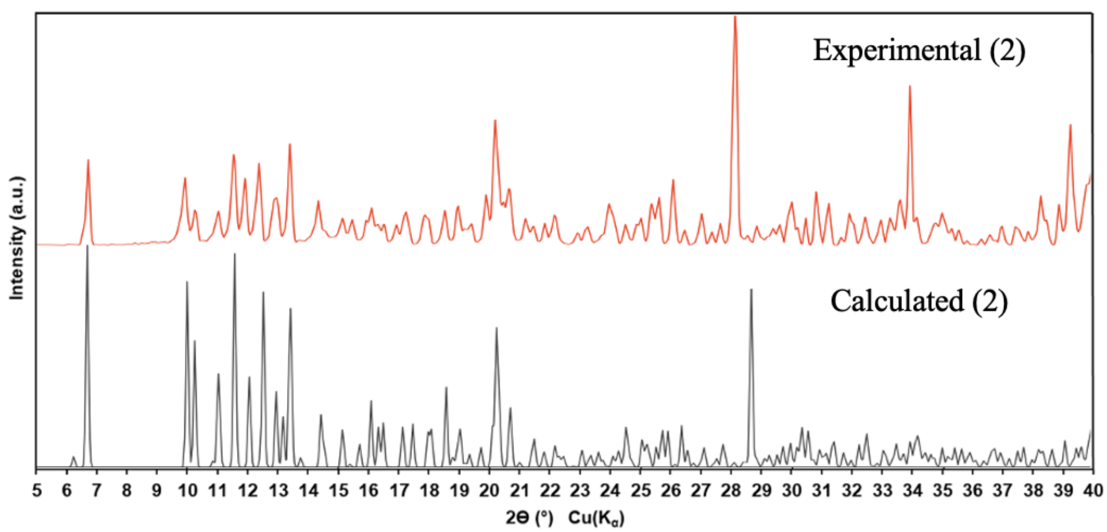

Figure S32. Powder X-ray diffraction pattern (collected with Cu Kα radiation) observed for 2 (orange) overlaid with the pattern calculated from the single crystal structure of 2 at 100 K (black)

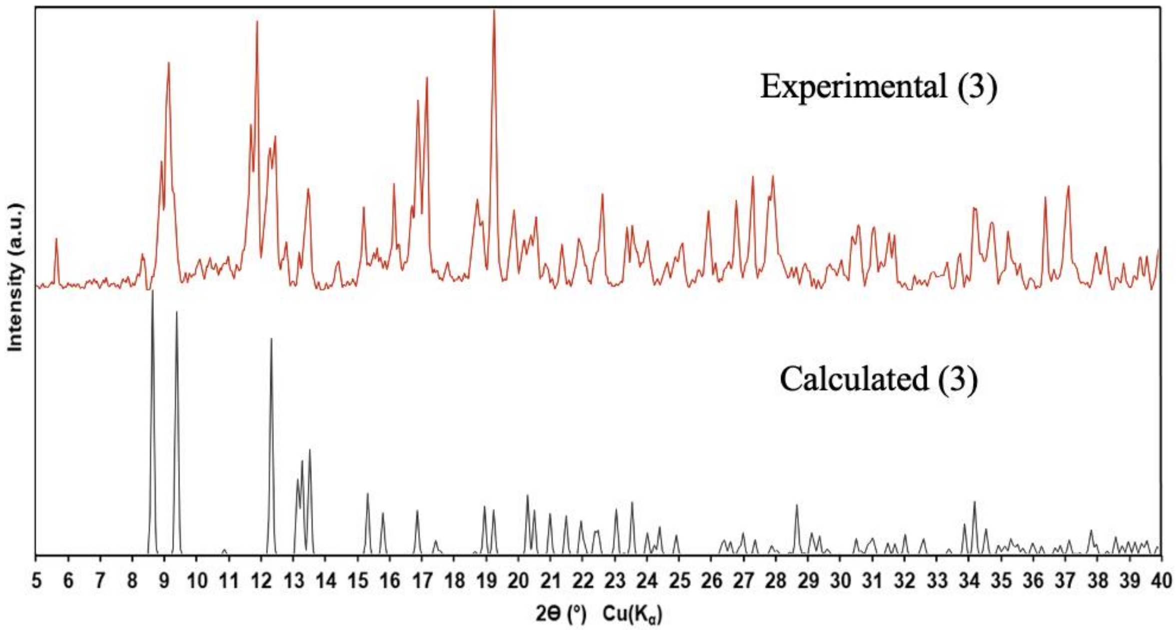

Figure S33. Powder X-ray diffraction pattern (collected with Cu Kα radiation) observed for 3 (red) overlaid with the pattern calculated from the single crystal structure of 3 at 100 K (black)

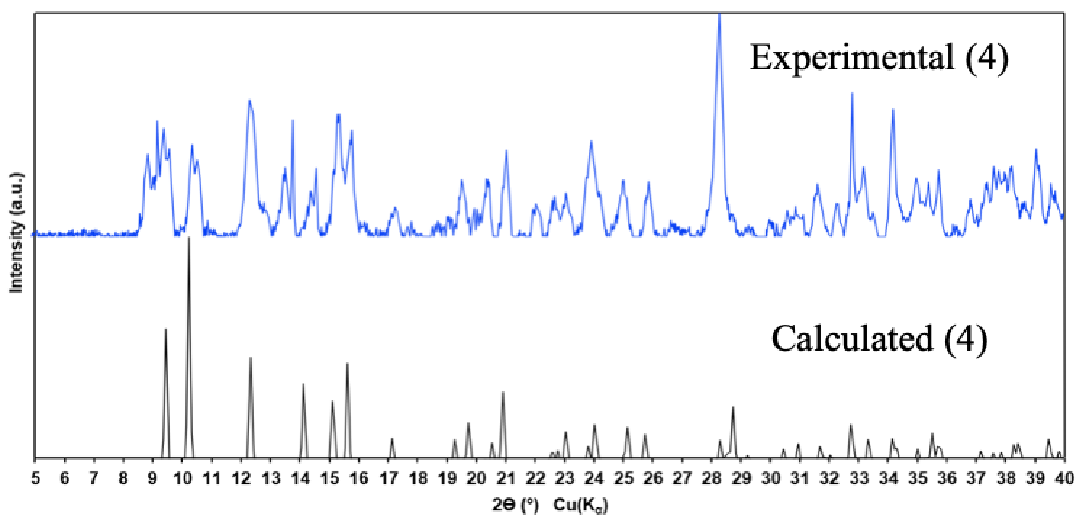

Figure S34. Powder X-ray diffraction pattern (collected with Cu Kα radiation) observed for 4 (blue) overlaid with the pattern calculated from the single crystal structure of 4 at 100 K (black)

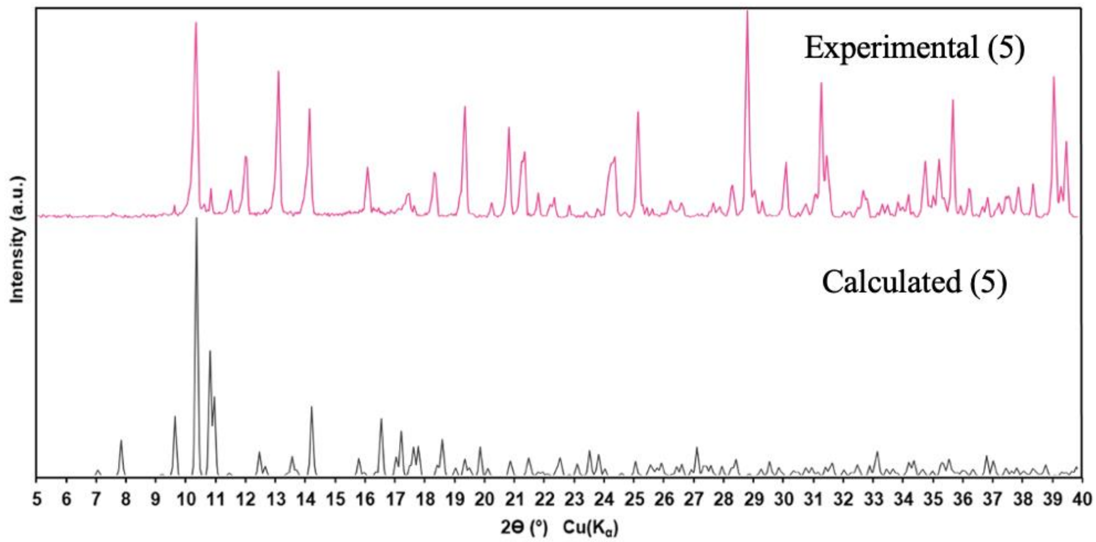

Figure S35. Powder X-ray diffraction pattern (collected with Cu Kα radiation) observed for 5 (pink) overlaid with the pattern calculated from the single crystal structure of 5 at 100 K (black).

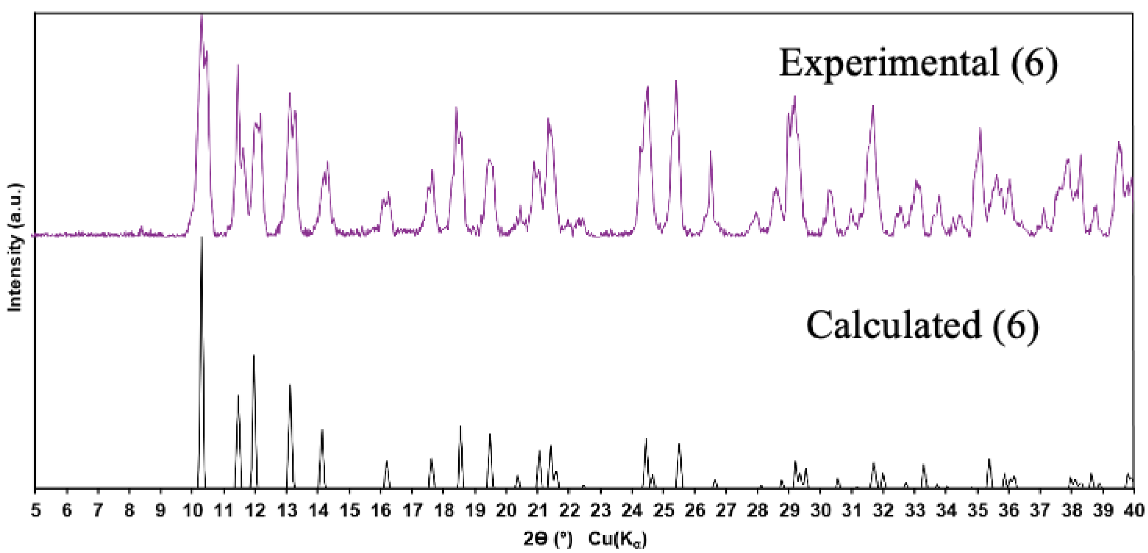

Figure S36. Powder X-ray diffraction pattern (collected with Cu Kα radiation) observed for 6 (purple) overlaid with the pattern calculated from the single crystal structure of 6 at 100 K (black).

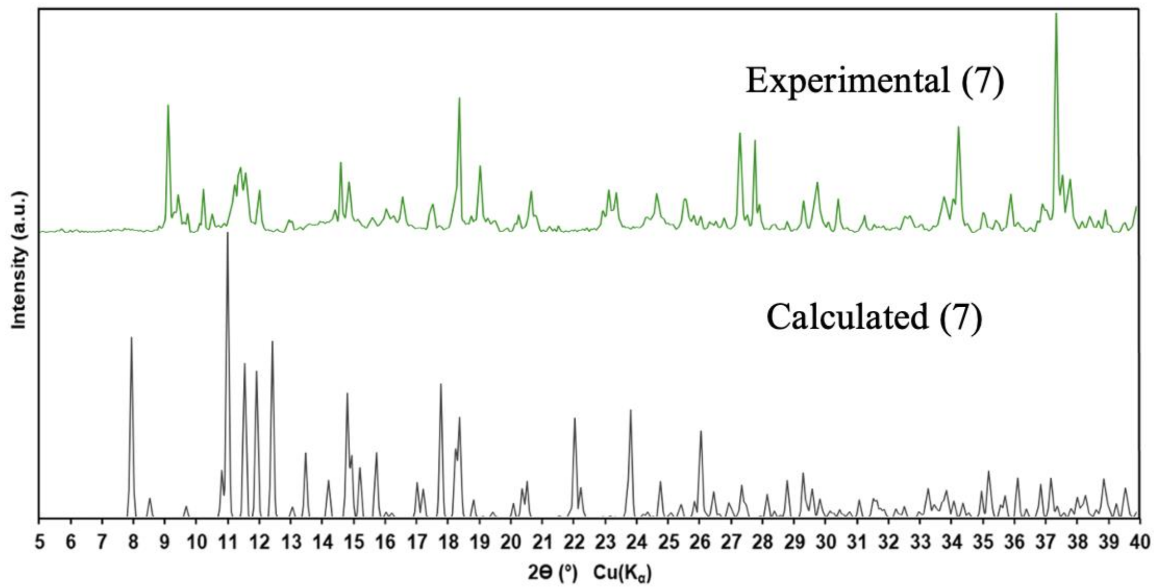

Figure S37. Powder X-ray diffraction pattern (collected with Cu Kα radiation) observed for 7 (green) overlaid with the pattern calculated from the single crystal structure of 7 at 100 K (black).

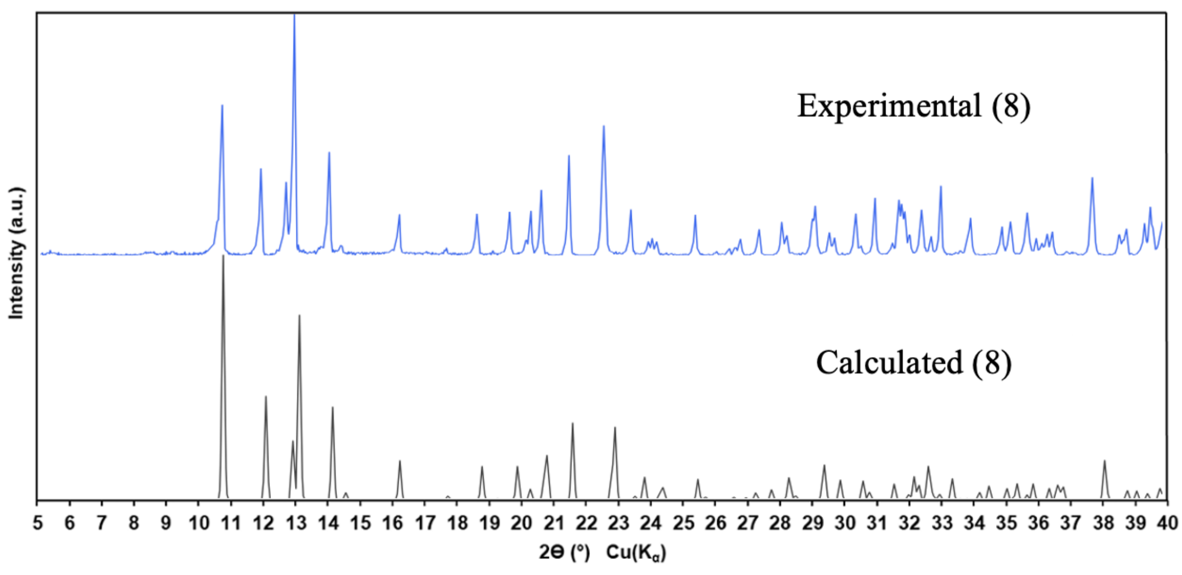

Figure S38. Powder X-ray diffraction pattern (collected with Cu Kα radiation) observed for 8 (blue) overlaid with the pattern calculated from the single crystal structure of 8 at 100 K (black).

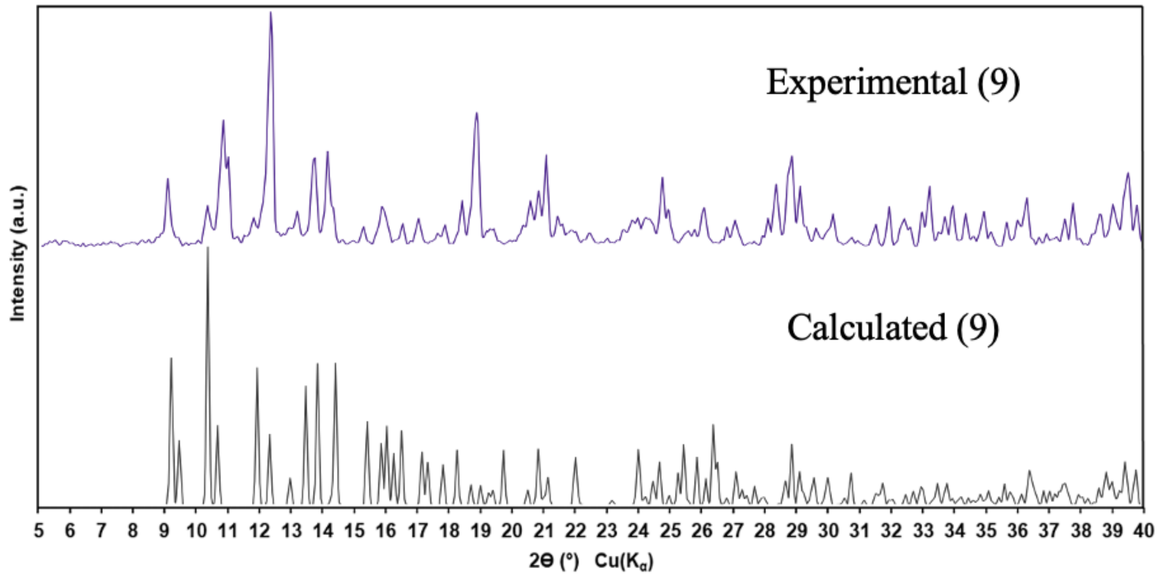

Figure S39. Powder X-ray diffraction pattern (collected with Cu Kα radiation) observed for 9 (purple) overlaid with the pattern calculated from the single crystal structure of 9 at 100 K (black)

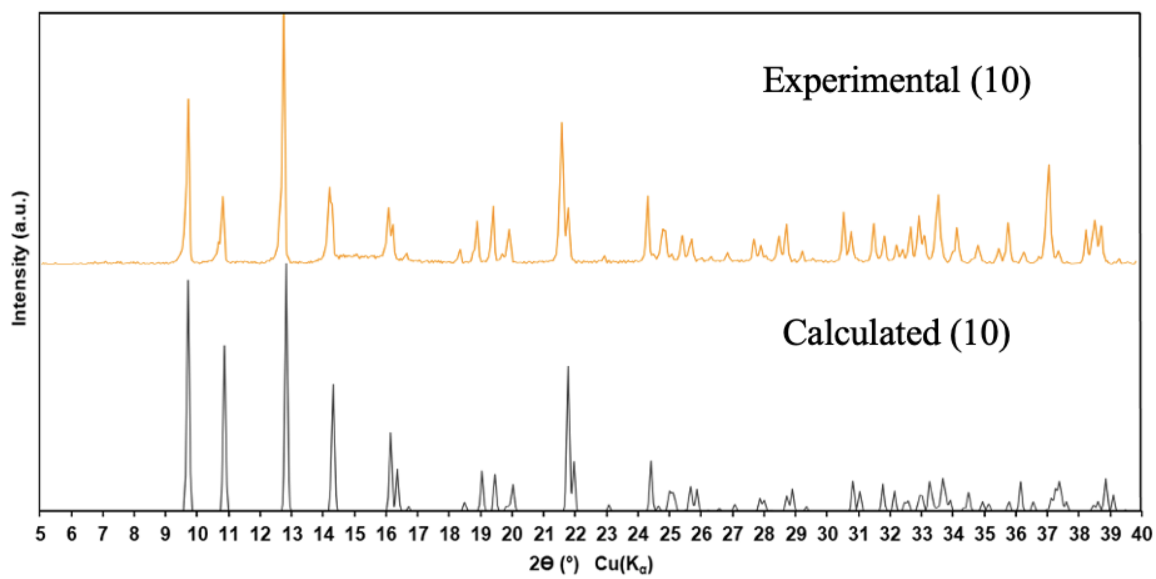

Figure S40. Powder X-ray diffraction pattern (collected with Cu Kα radiation) observed for 10 (orange) overlaid with the pattern calculated from the single crystal structure of 10 at 100 K (black)

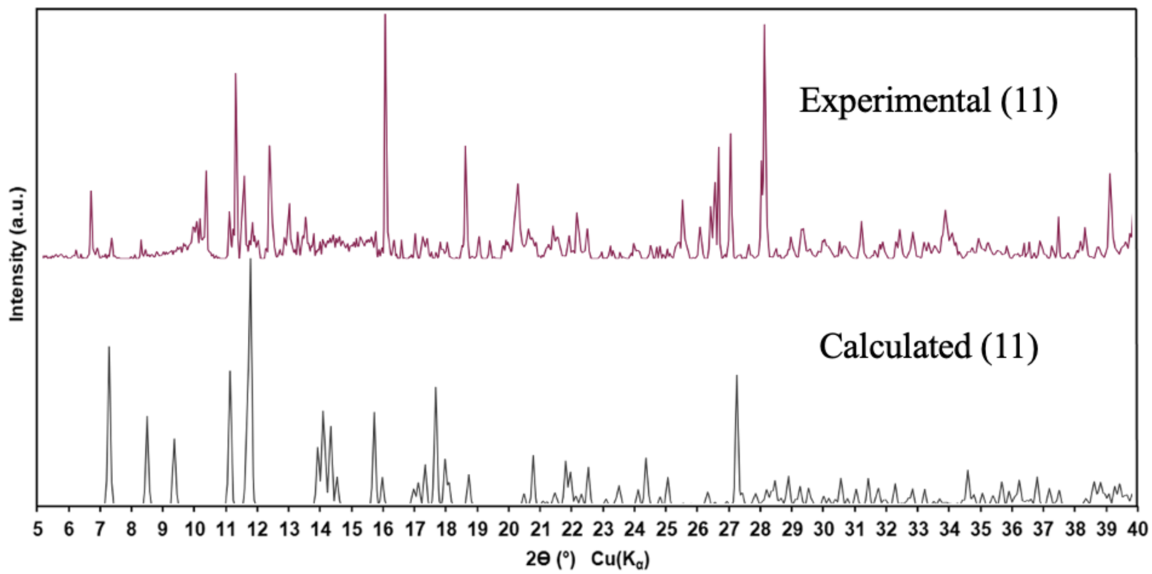

Figure S41. Powder X-ray diffraction pattern (collected with Cu Kα radiation) observed for 11 (maroon) overlaid with the pattern calculated from the single crystal structure of 11 at 100 K (black).

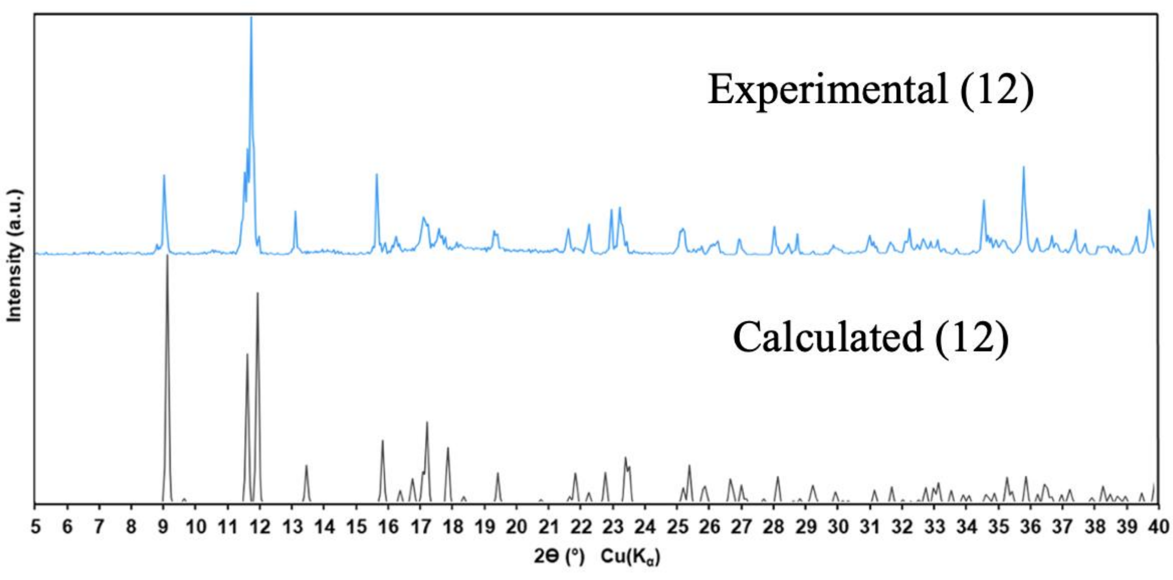

Figure S42. Powder X-ray diffraction pattern (collected with Cu Kα radiation) observed for 12 (blue) overlaid with the pattern calculated from the single crystal structure of 12 at 100 K (black).

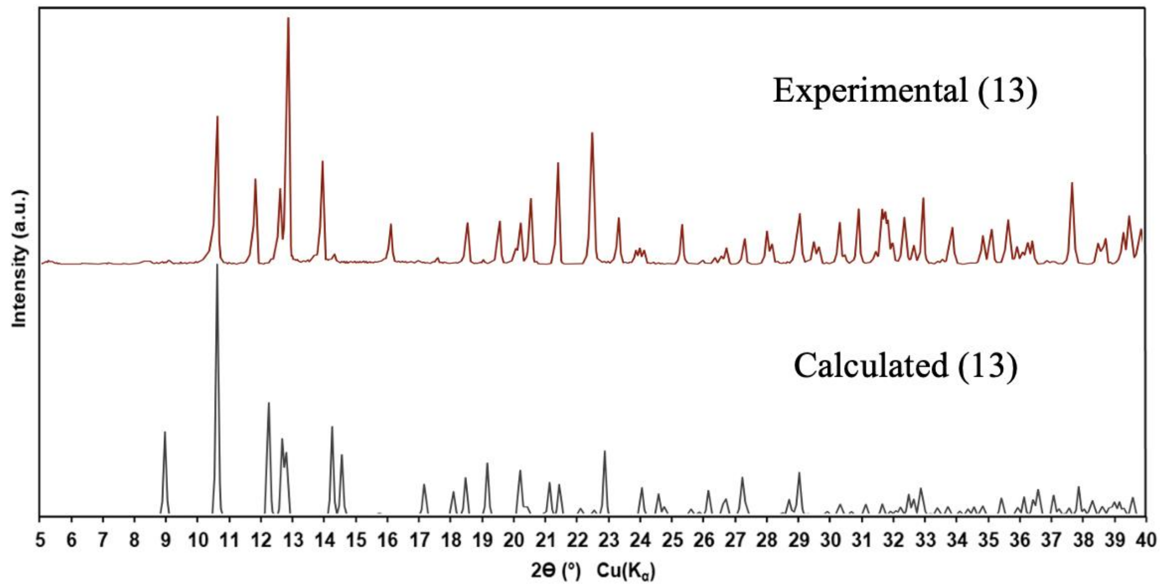

Figure S43. Powder X-ray diffraction pattern (collected with Cu Kα radiation) observed for 13 (brown) overlaid with the pattern calculated from the single crystal structure of 13 at 100 K (black).

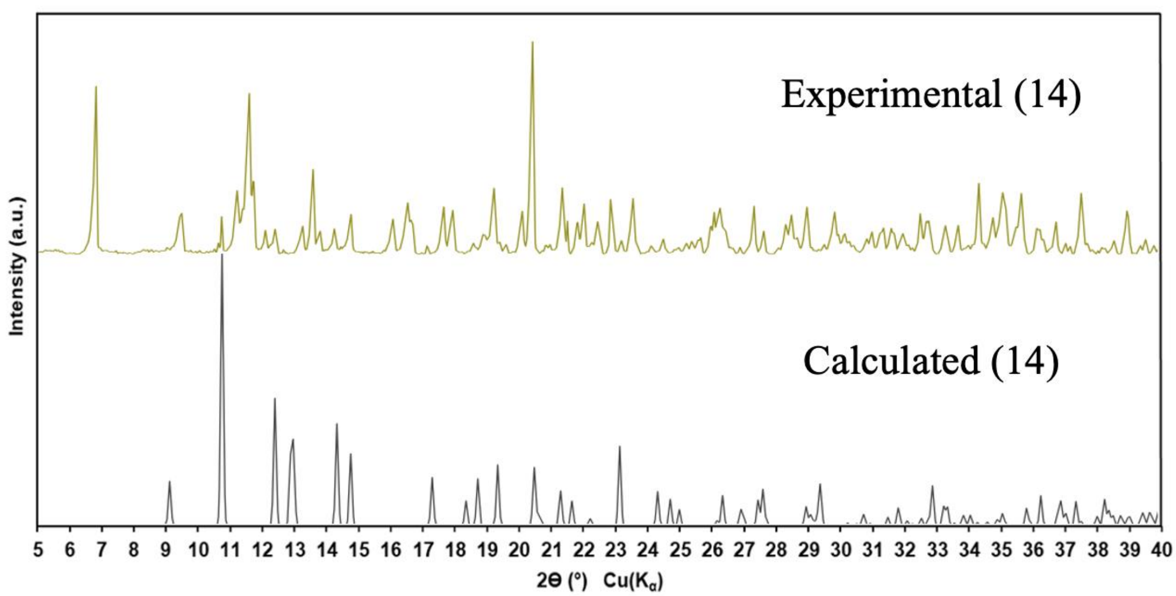

Figure S44. Powder X-ray diffraction pattern (collected with Cu Kα radiation) observed for 14 (yellow) overlaid with the pattern calculated from the single crystal structure of 14 at 100 K (black).

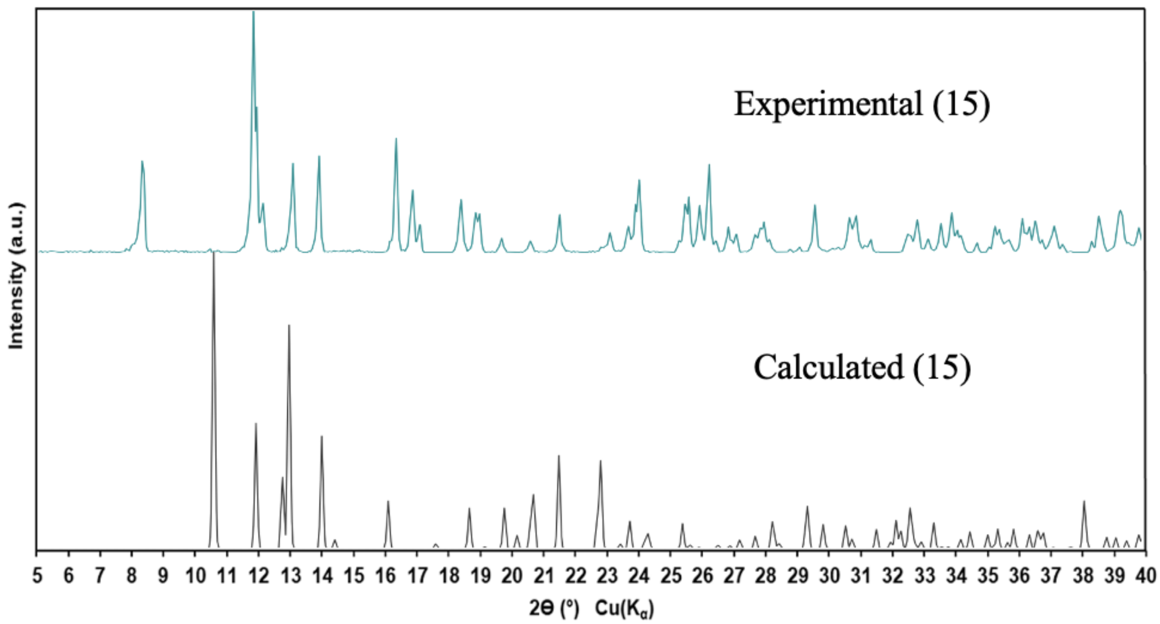

Figure S45. Powder X-ray diffraction pattern (collected with Cu Kα radiation) observed for 15 (teal) overlaid with the pattern calculated from the single crystal structure of 15 at 100 K (black).

6. RAMAN AND INFRARED PLOTS OF COMPOUNDS **1–15**.

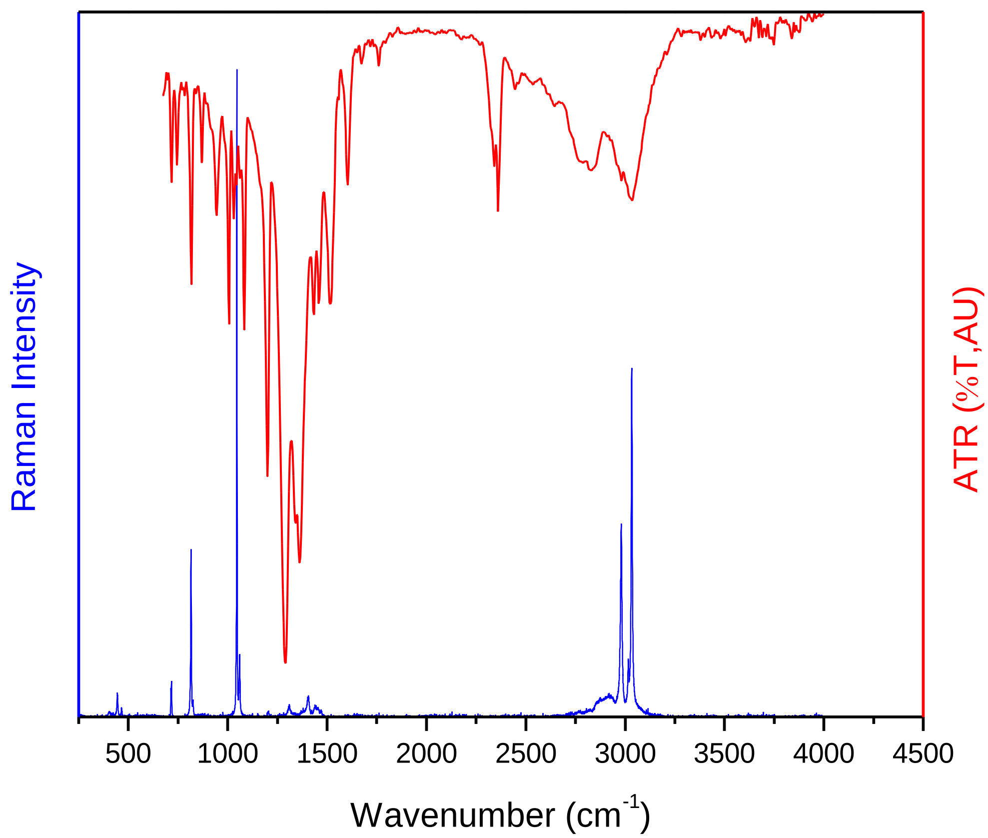

Figure S46. Infrared and Raman spectra of PiperH$_2$[Th(NO$_3$)$_5$(H$_2$O)$_2$]$_2$•[PiperH$_2$(NO$_3$)$_2$] (**1**) (Raman =blue, IR = red). IR (cm-1): 701, 749, 821, 869, 954, 997, 1089, 1203, 1294, 1361, 1427, 1456, 1523, 1590, 2360, 2829, 3029. Raman (cm-1): 210, 242, 410, 447, 458, 721, 749, 816, 926, 1036, 1211, 1317, 1418, 1469, 1527, 1563, 2769, 2818, 2924, 2980, 3021.

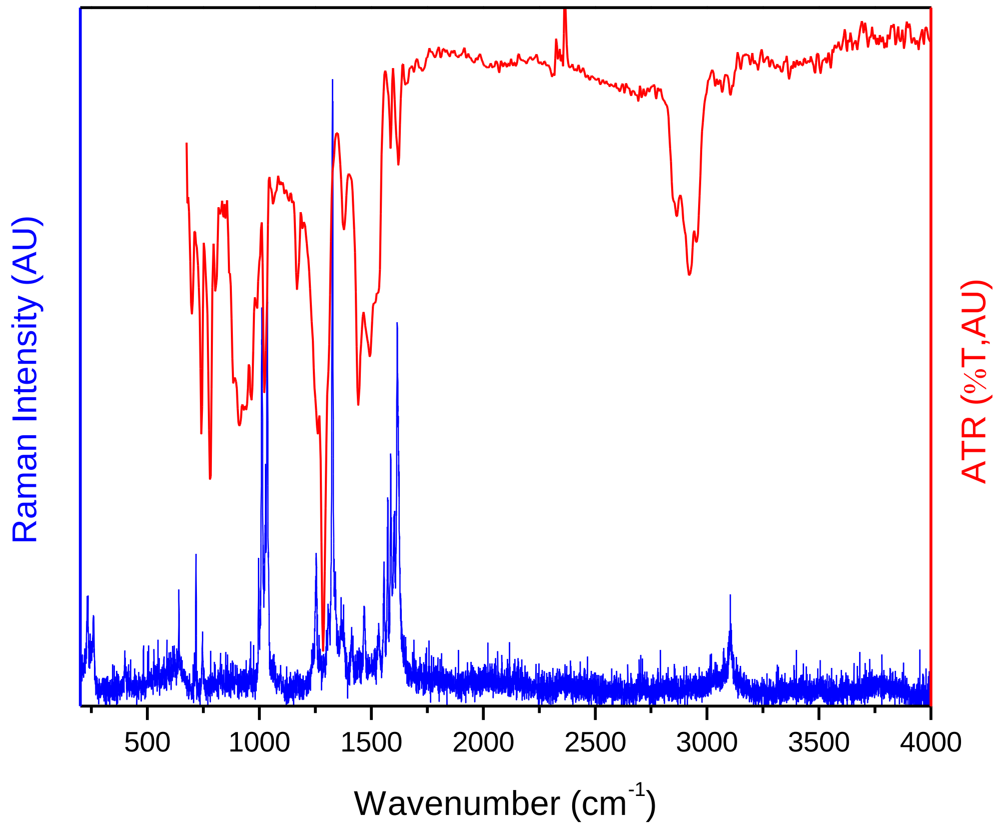

Figure S47. Infrared and Raman spectra of $(TerpyH_2)[Th(NO_3)_5(H_2O)_2]_2$•$[(TerpyH_2)_3(NO_3)_6]$•$4(H_2O)$ (**2**) (Raman =blue, IR = red). IR (cm^{-1}): 739, 800, 930, 1030, 1270, 1450, 1590, 3000. Raman: 240, 251, 749, 1017, 1253, 1357, 1465, 1675, 3150.

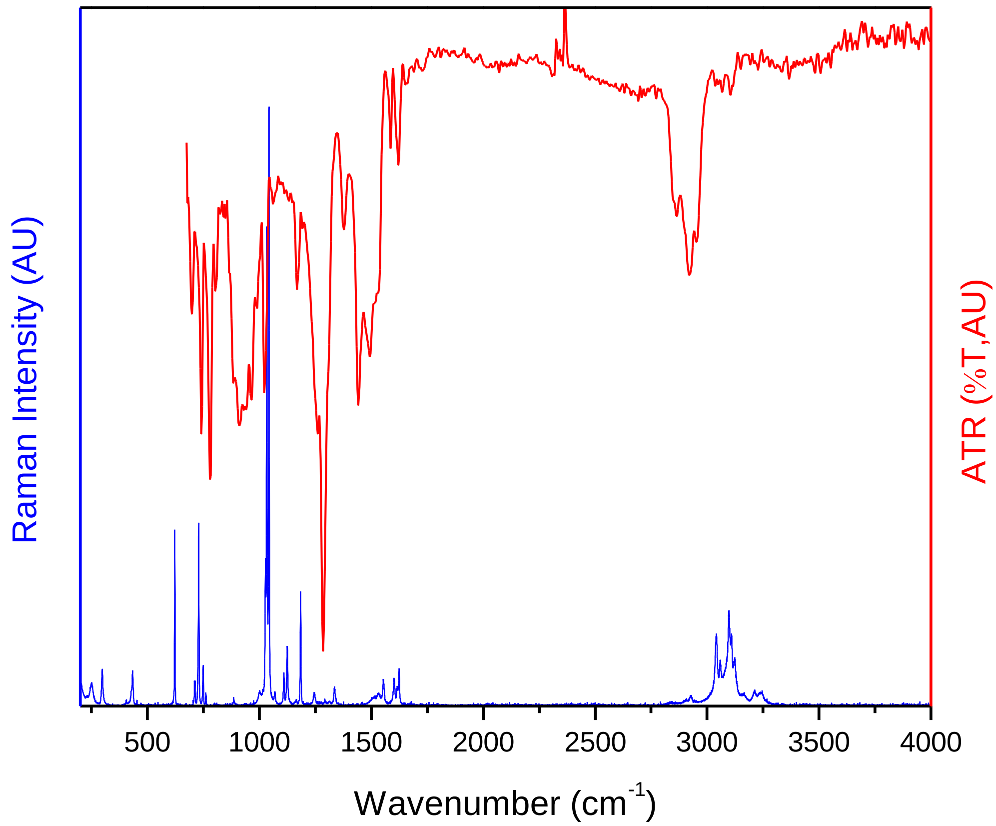

Figure S48. Infrared and Raman spectra $(PyH)_2[Th(NO_3)_6]$•$(PyH$•$NO_3)$, (**3**) (Raman =blue, IR = red). IR (cm^{-1}): 741, 810, 937, 1030, 1280, 1500, 1610, 3120. Raman (cm^{-1}): 253, 272, 472, 652, 749, 1017, 1275, 1578, 3180.

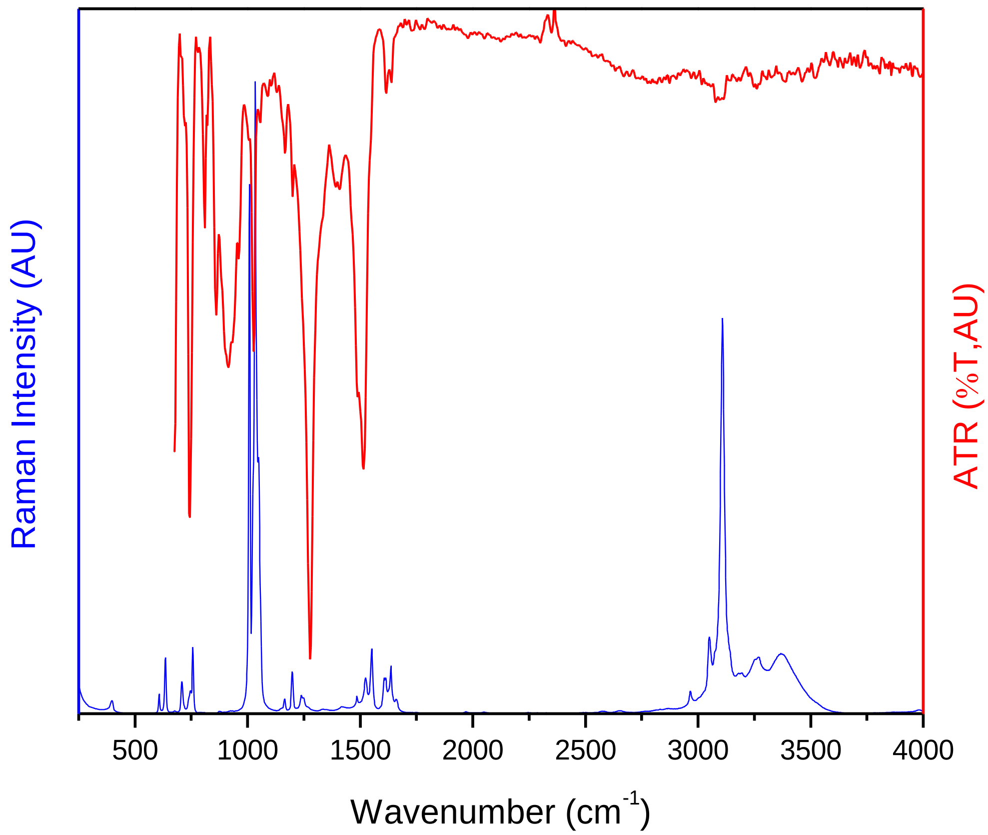

Figure S49. Infrared and Raman spectra of $(PyH)_2[Th(NO_3)_6]\bullet2(PyH\bullet NO_3)$ (**4**) (Raman =blue, IR = red). IR (cm^{-1}): 748, 806, 918, 1030, 1280, 1420, 1520, 1640, 3090. Raman (cm^{-1}): 473, 643, 753, 1039, 1198, 1575, 1635, 3120.

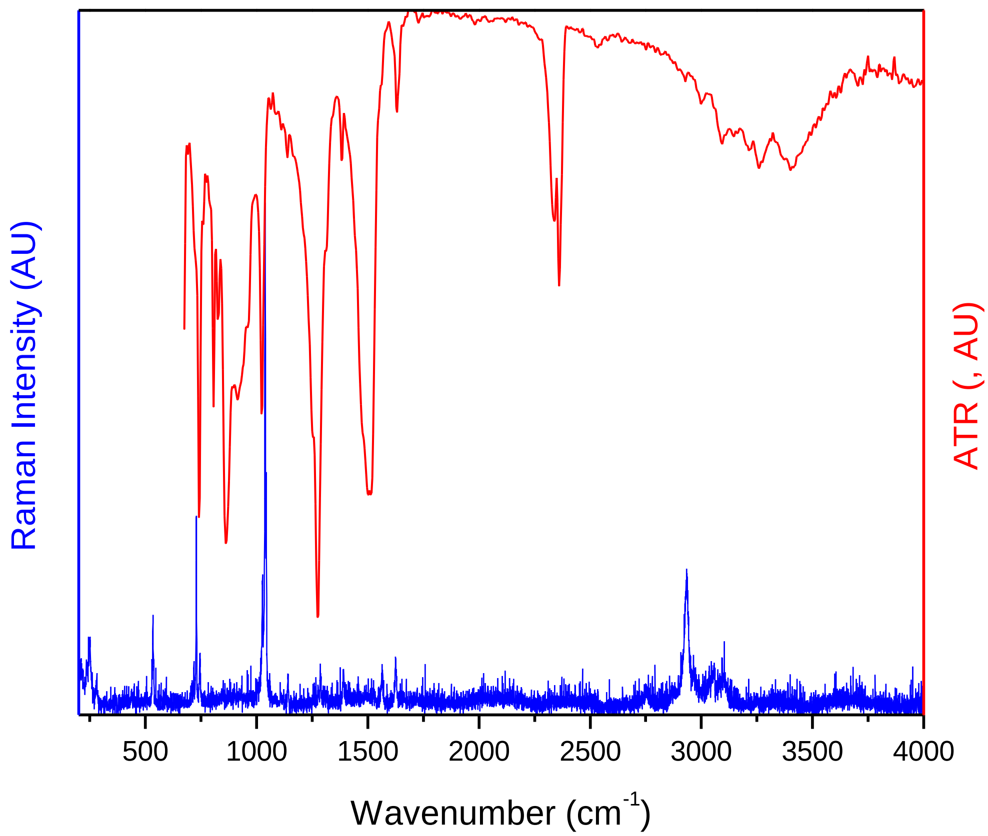

Figure S50. Infrared and Raman spectra of $(3,5\text{-DiMePyH})_2[Th(NO_3)_6]\cdot[(3,5\text{-DiMePyH})(NO_3)]$, (**5**) (Raman =blue, IR = red). IR (cm^{-1}): 741, 806, 860, 914, 964, 1270, 1520, 1620, 3490. Raman (cm^{-1}): 257, 510, 745, 1008, 2980, 3015.

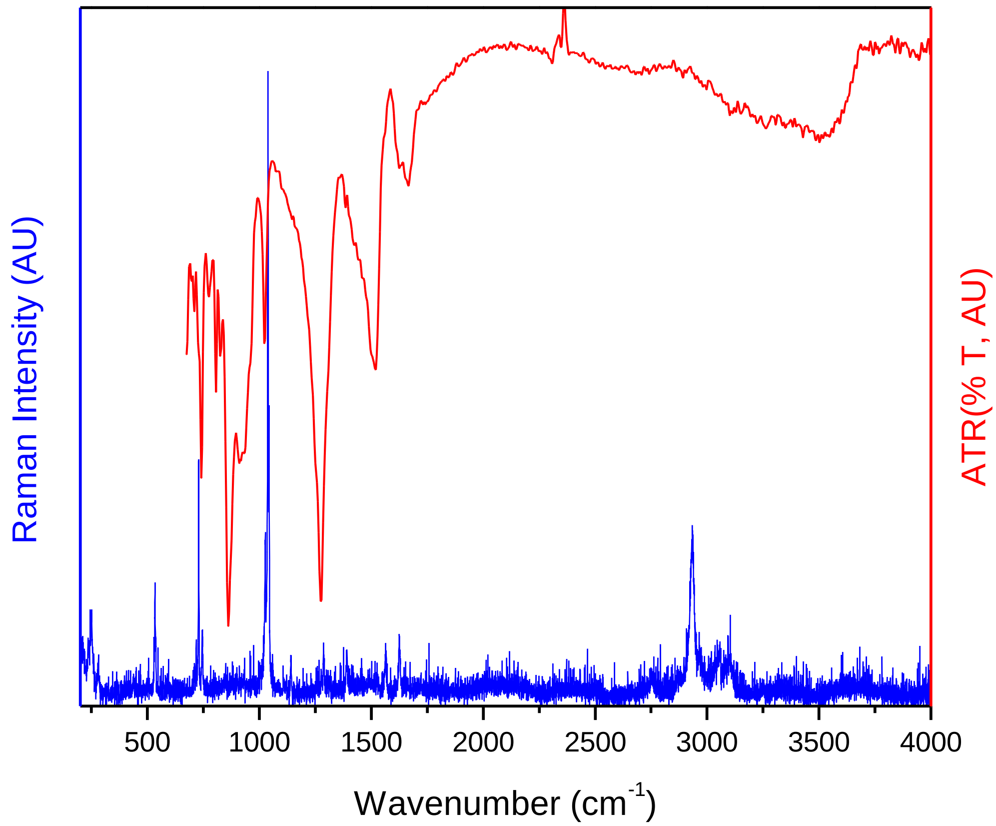

Figure S51. Infrared and Raman spectra of $(3,5\text{-DiMePyH})_2[Th(NO_3)_6]$ (**6**) (Raman =blue, IR = red). IR (cm^{-1}): 741, 806, 860, 933, 1030, 1280, 1520, 1670. Raman (cm^{-1}): 253, 515, 740, 1002, 2975, 3030.

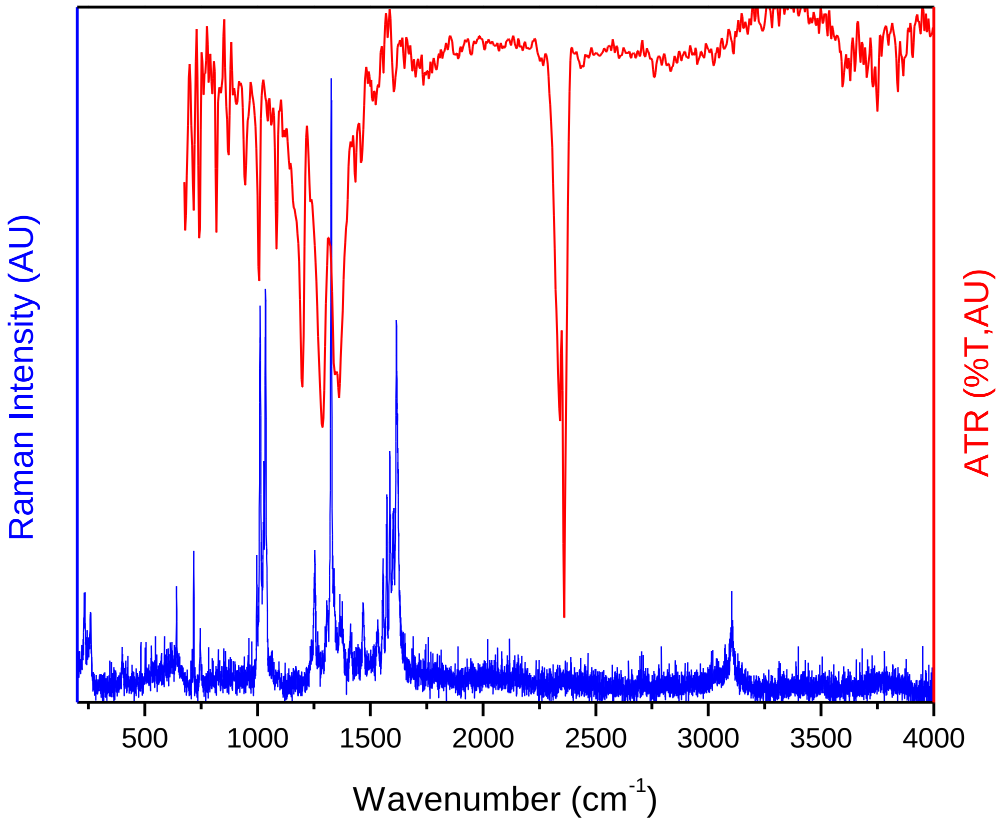

Figure S52. Infrared and Raman spectra of $(TerpyH_2)[Th(NO_3)_6]\bullet(TerpyH_2)(NO_3)_2$ (**7**) (Raman =blue, IR = red). IR (cm^{-1}): 790, 850, 1150, 1355, 1600, 2352. Raman (cm^{-1}): 237, 253, 753, 1027, 1249, 1363, 1470, 1670, 3230.

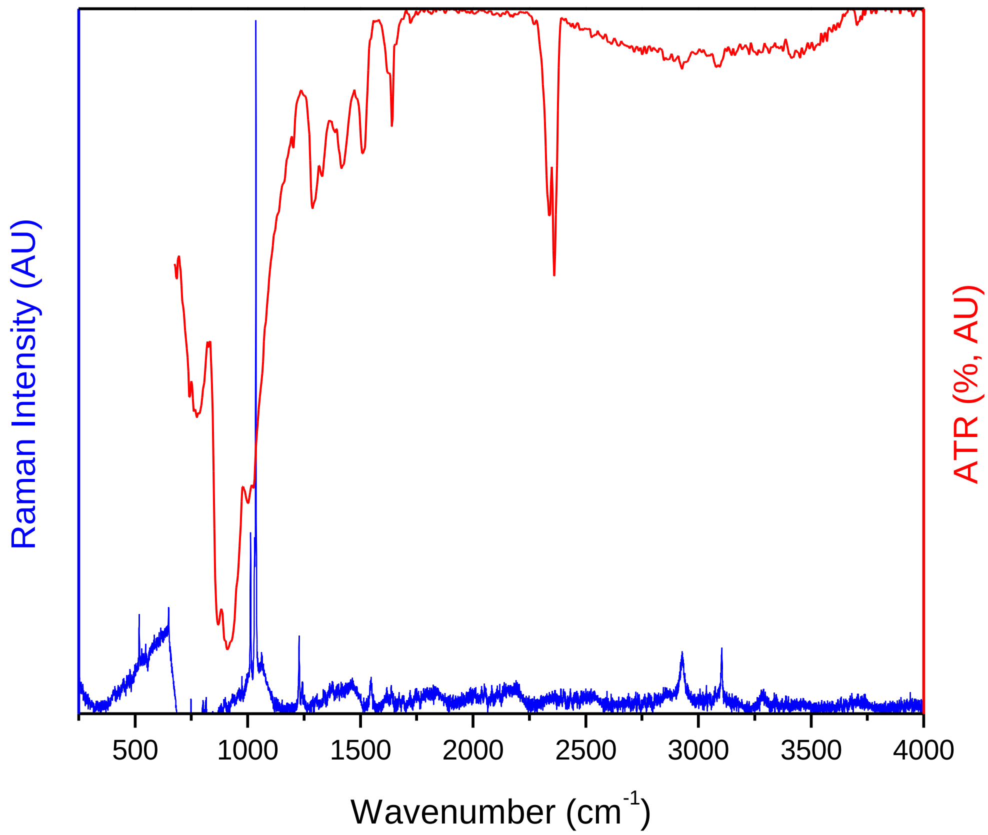

Figure S53. Infrared and Raman spectra of $(4\text{-MePyH})_2[Th(NO_3)_6]$, (**8**) (Raman =blue, IR = red). IR (cm^{-1}): 771, 918, 1030, 1300, 1430, 1510, 1640, 2360. Raman: 503, 1079, 1253, 1522, 2875, 3010.

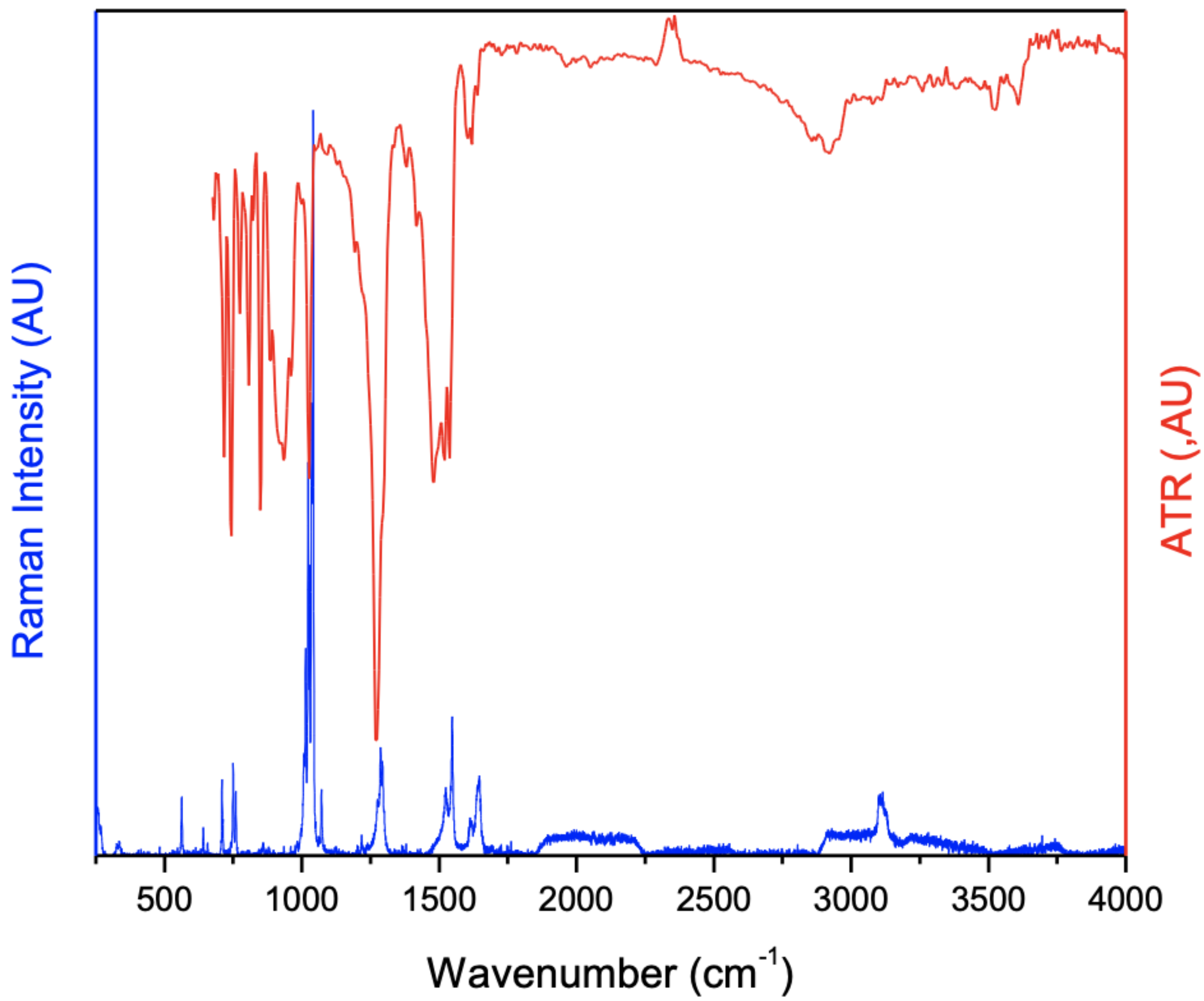

Figure S54. Infrared and Raman spectra of $[4,4\text{-BipyH}_2]_2[Th(NO_3)_6]_2$•$[4,4\text{-BipyH}_2$•$2NO_3]$ (**9**) (Raman =blue, IR = red). IR (cm^{-1}): 717, 748, 802, 849, 930, 1020, 1280, 1520, 1620, 2920. Raman: 252, 267, 589, 753, 1088, 1290, 1575, 2010, 3100.

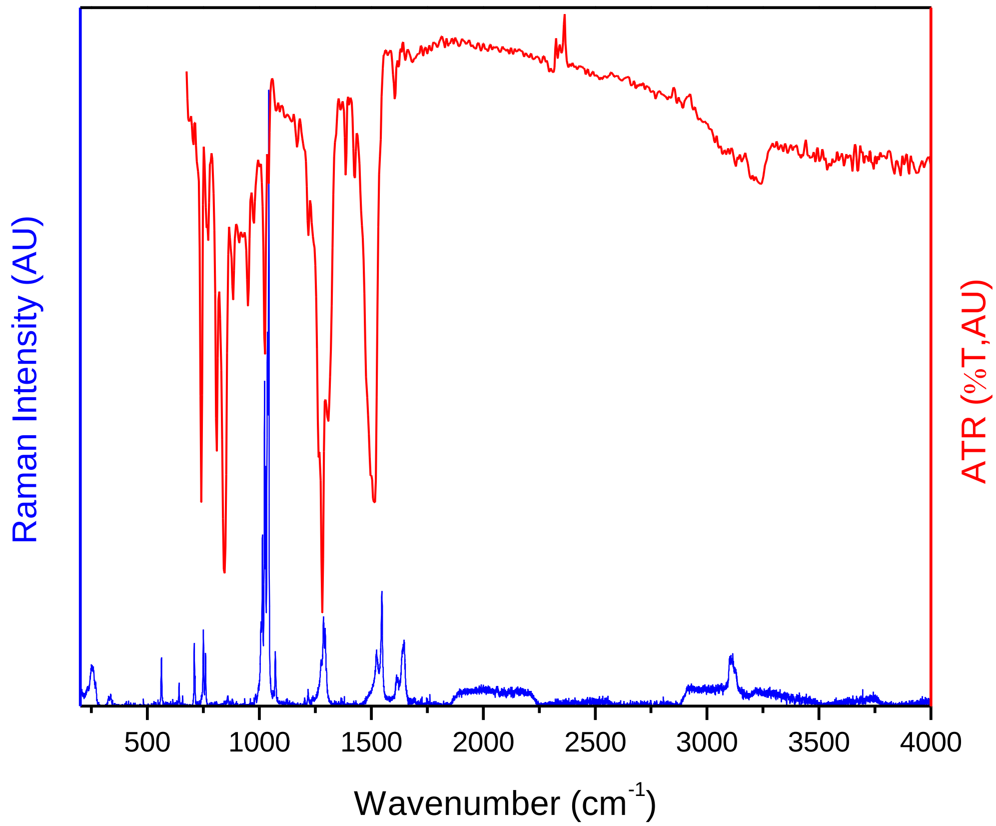

Figure S55. Infrared and Raman spectra of $(PhthalH)_2[Th(NO_3)_6]$ (**10**) (Raman =blue, IR = red). IR (cm^{-1}): 740, 810, 841, 949, 1020, 1280, 1380, 1430, 1510, 3220. Raman (cm^{-1}): 250, 271, 591, 749, 1091, 1292, 1578, 2015, 3101.

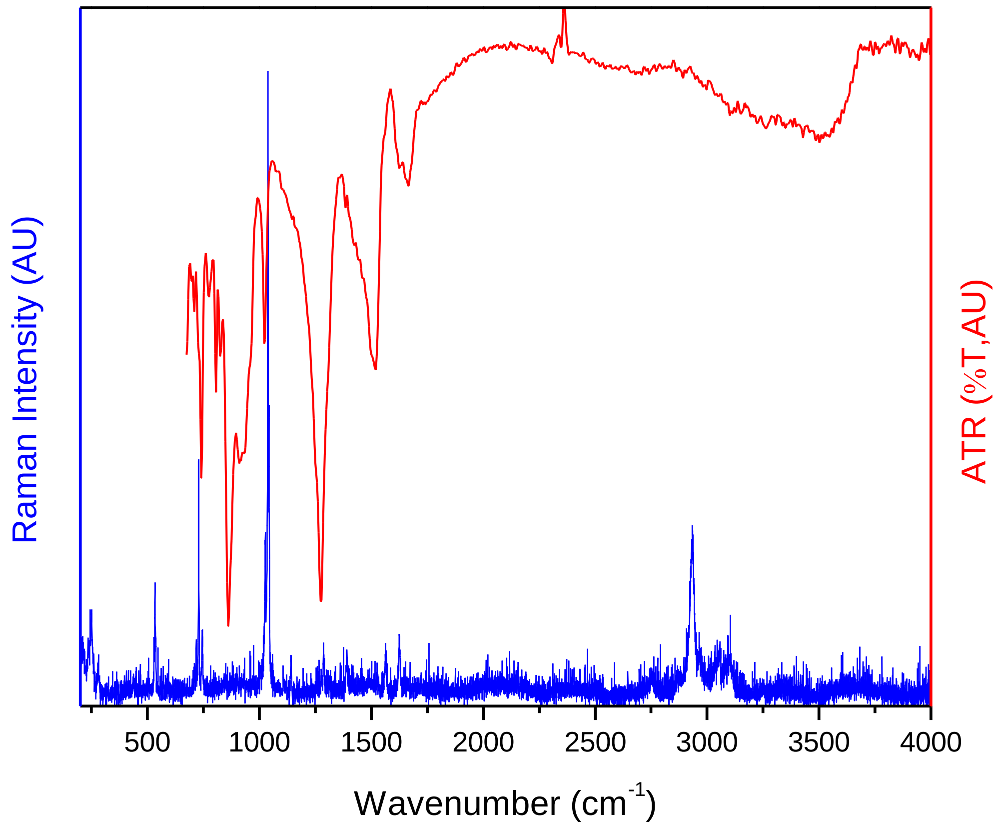

Figure S56. Infrared and Raman spectra of [TerpyH$_2$][Th(NO$_3$)$_6$]•H$_2$O (**11**) (Raman =blue, IR = red). IR (cm^{-1}): 751, 922, 1105, 1259, 1670, 1750, 3250. Raman (cm^{-1}): 235, 257, 753, 1025, 1257, 1362, 1469, 1678, 3160.

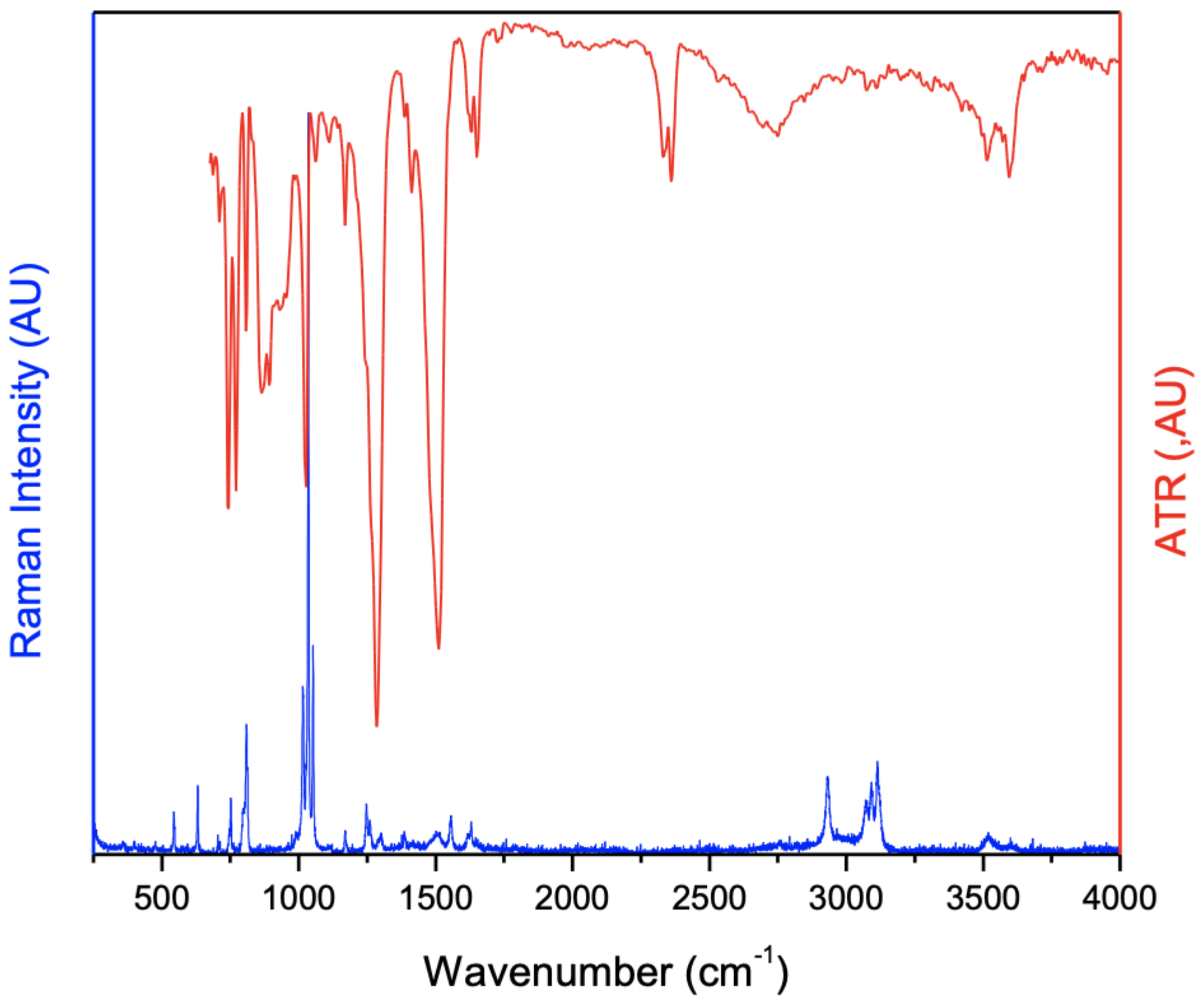

Figure S57. Infrared and Raman spectra of $(2\text{-MePyH})_2[Th(NO_3)_6]\cdot 2H_2O$, (**12**) (Raman =blue, IR = red). IR (cm^{-1}): 690, 741, 779, 801, 870, 947, 1029, 1068, 1102, 1266, 1519, 1657, 2328, 2367, 2741, 3503, 3593. Raman (cm^{-1}): 219, 240, 545, 633, 708, 755, 804, 1013, 1034, 1055, 1171, 1246, 1301, 1513, 1549, 1630, 2927, 3071, 3088, 3108, 3513.

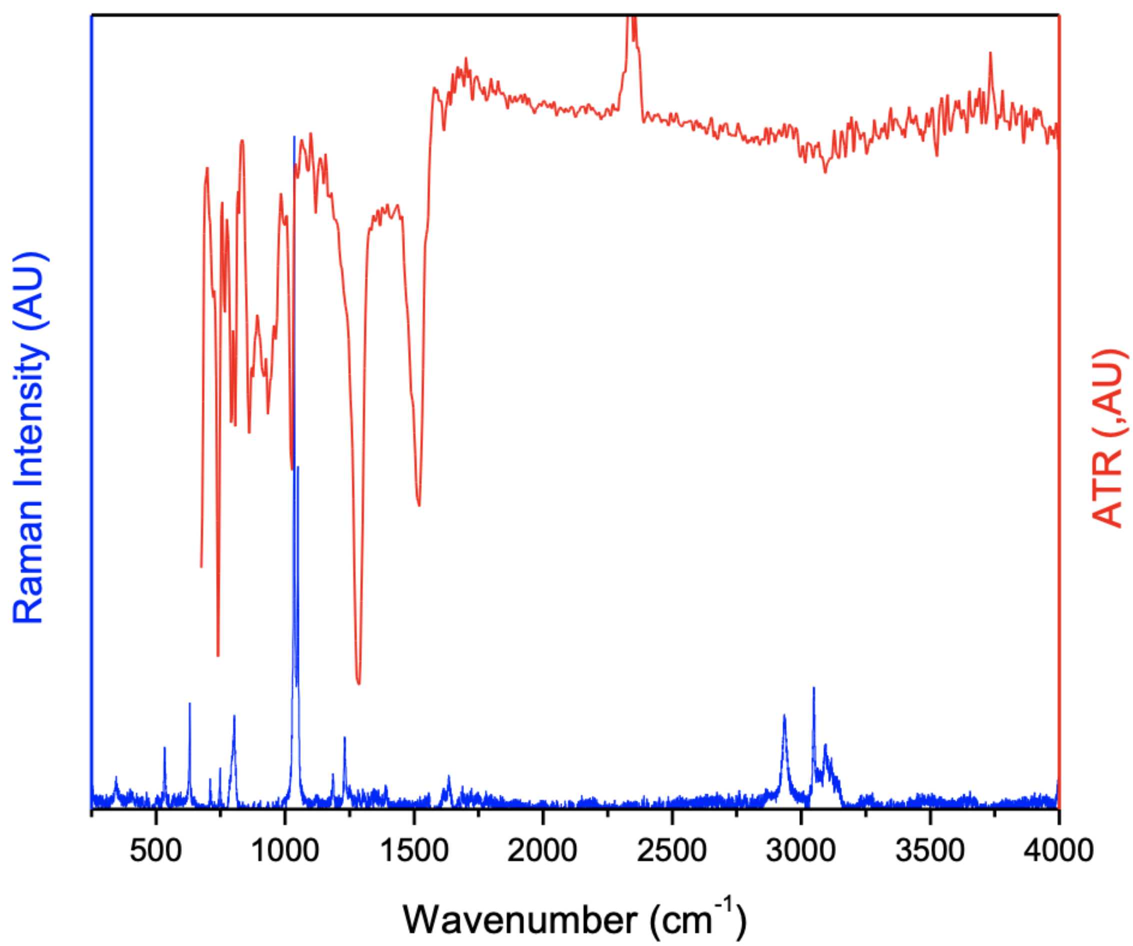

Figure S58. Infrared and Raman spectra of (3-MePyH)$_2$[Th(NO$_3$)$_6$] (**13**) (Raman =blue, IR = red). IR (cm^{-1}): 741, 802, 856, 941, 1030, 1270, 1530. Raman (cm^{-1}): 287, 514, 597, 752, 1056, 1247, 2875, 3015.

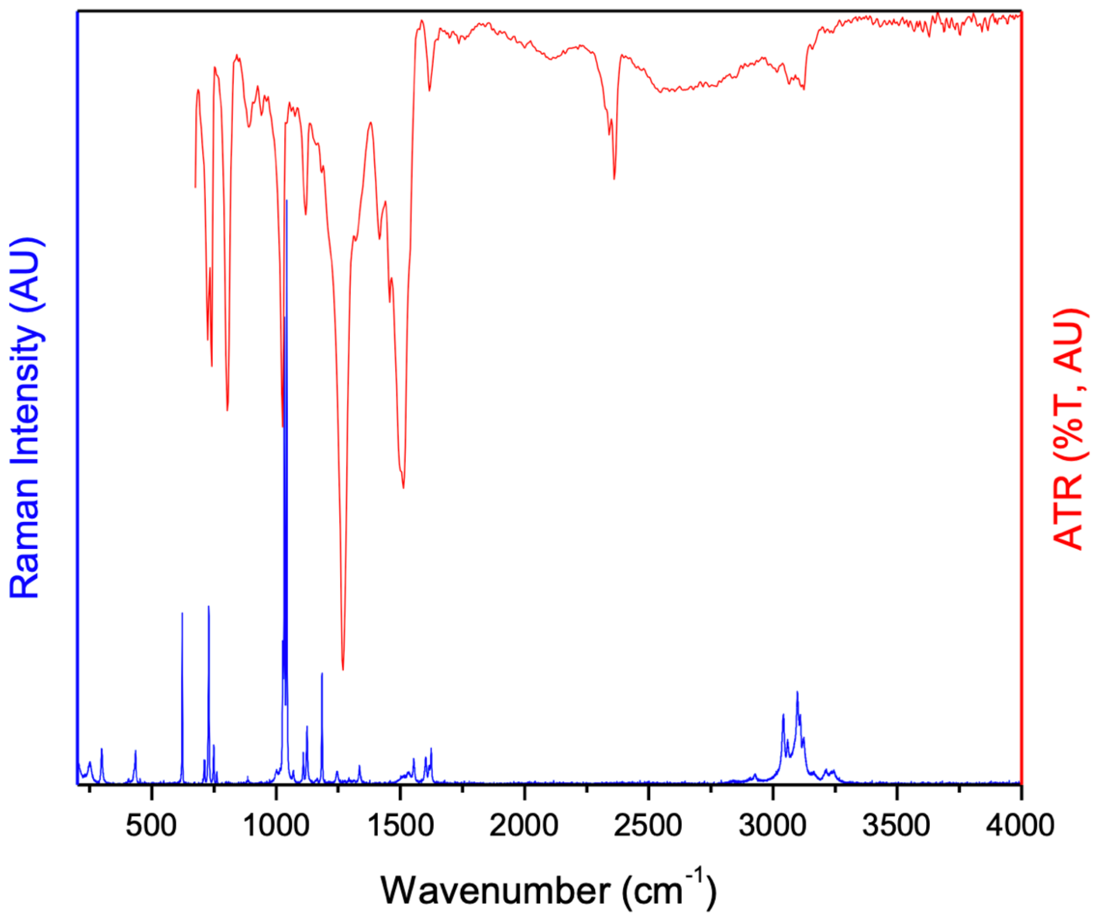

Figure S59. Infrared and Raman spectra of (3-ClPyH)$_2$[Th(NO$_3$)$_6$], (**14**) (Raman =blue, IR = red). IR (cm^{-1}): 729, 802, 895, 1030, 1120, 1270, 1520, 1620, 2360, 3120. Raman (cm^{-1}): 247, 256, 456, 612, 748, 1096, 1176, 1210, 1251, 1347, 1598, 1603, 3080.

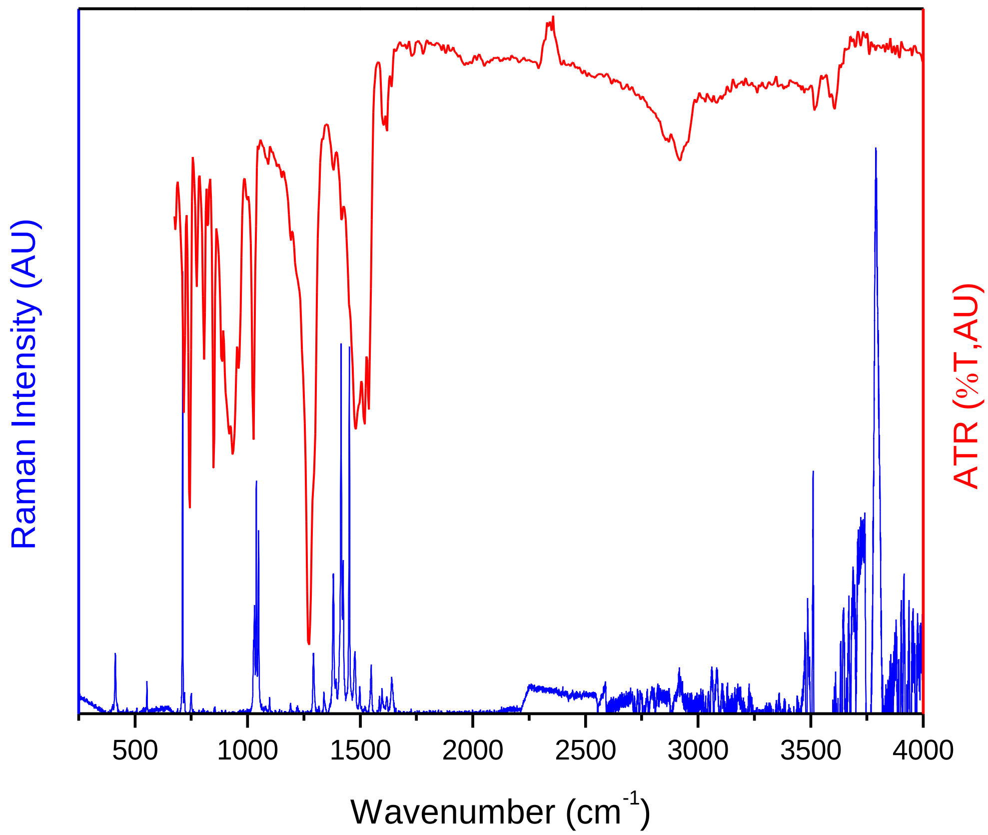

Figure S60. Infrared and Raman spectra of $(PhenH)_2[Th(NO_3)_6]•2[H_2O]$ (**15**) (Raman =blue, IR = red). IR (cm^{-1}): 717, 721, 771, 852, 941, 1020, 1540, 1610, 2920. Raman (cm^{-1}): 436, 687, 1144, 1354, 1443, 2365, 3501, 3754.

Table S1. Assignment of characteristic peaks for both Raman and IR peaks for compound **1** $PiperH_2[Th(NO_3)_5(H_2O)_2]_2$•$[PiperH_2(NO_3)_2]$**,** representative of the pentanitrato molecular unit.

IR (cm^{-1})	Raman(cm^{-1})	Assignment
3029	3021	
	2980	
	2924	
2829	2818	
	2769	
2360		
1590	1563	H_2O bend
1523	1527	NO nitrate/ H_2O bend
1456	1469	
1427	1418	
1361	1317	NO_2 group asymmetric
1294	1211	NO_2 group asymmetic
1203		
1089	1036	NO_2 symmetric stretch
997		
954	926	
869		
821	816	NO_3- group inversion
749	749	NO_2 bend
701	721	Find O-NO_2 bend.
	458	H_2O rock
	447	H_2O rock
	410	H_2O rock
	242	H_2O-Th
	210	NO_3- H_2O group-Th

Table S2. Assignment of characteristic peaks for both Raman and IR peaks for compound **12** (2-MePyH)$_2$[Th(NO$_3$)$_6$]•2H$_2$O**,** representative of the hexanitrato molecular unit.

IR (cm^{-1})	Raman(cm^{-1})	Assignment
3593		
3503	3513	
	3108	
	3088	
	3071	
	2927	
2741		
2367		
2328		
1657	1630	
	1549	N-O terminal stretch of NO_3^-
1519	1513	N-O terminal stretch of NO_3^-
	1301	Asymmetric NO_2
1266	1246	
1102	1171	
1068	1055	Symmetric NO_2
1029	1034	Symmetric NO_2
	1013	Symmetric NO_2
947		
870		
801	804	
779		
741	755	Symmetric ONO bends NO_2
	708	
690	633	Terminal NO_2 bend
	545	
	240	Th-NO_3 stretches
	219	Th NO_3 stretches

Table S3 Average Th–O_{H2O} and Th–O_{NO3} average bond distances for penta nitrato complexes **1-2** as well as the average Th-NO_3 distance for the 13 hexanitrato complexes.[a]

Compound	Th–OH_2 (Å)	Th–NO_3(Å)
1	2.4396(8)	2.59557(2)
2	2.4449(9)	2.567783(2)
3-15(average)	-	2.5616(1)

[a] Errors are the standard deviation of the mean.

Table S4 Average Th–O_{NO3} bond distances for **3–15**.[a]

Compound	Th–NO_3(Å)
3	2.5265(2)
4	2.5496(2)
5	2.5585(2)
6	2.5687(2)
7	2.5567(2)
8	2.5619(2)
9	2.5575(2)
10	2.5620(2)
11	2.5638(2)
12	2.5598(2)
13	2.5596(2)
14	2.5577(2)

15	2.5599(2)

[a] Errors are the standard deviation of the mean.

7. SUPRAMOLECULAR INTERACTIONS OBSERVED IN COMPOUNDS **1**–**15**.

Supramolecular interactions were calculated using the “Calc All” function within the PLATON software suite.[1] Significant noncovalent interactions for reported compounds – such as hydrogen bonding, and π–π stacking interactions – are tabulated below, guided by the classification of supramolecular interactions as reported previously.[2–4]

Noncovalent Interaction Notations:

- D = donor atom involved in supramolecular interaction.
- A = acceptor atom involved in supramolecular interaction.
- β = angle formed between C_g and the plane normal to C_g.
- C_g --- C_g = Distance between ring centroids.

Table S5. Selected noncovalent hydrogen bonding interactions– observed in (**1**).

Interaction	Distance (Å), D–H---A	Angle (º), ∠D–H---A
O(81)-H --- O(42)#1	2.829(2)	176(3)
O(81)-H --- O(43)	3.029(2)	125(2)
O(81)-H --- O(11)#2	2.854(2)	172(3)
O(91)-H --- O(41)	2.817(2)	164(3)
O(91)-H --- O(43)	2.902(2)	114(2)
O(91)-H --- O(21)#3	2.805(2)	175(3)
O(91)-H --- O(23)	3.189(2)	130(2)
N(61)-H --- (O33)	3.127(2)	159
N(61)-H --- (O3)	3.039(2)	114
N(61)-H --- (O51)	2.866(2)	169
N(61)-H --- (O52)	2.988(2)	116
N(71)-H --- (O52)	2.796(2)	167
N(71)-H --- (O51)#4	3.001(2)	160

Symmetry transformations used to generate equivalent atoms:
#1 x,1/2-y,-1/2+z #2 1+x,y,z #3 x,1/2-y,1/2+z #4 -1+x,y,z

Table S6. Selected noncovalent interactions – such as hydrogen bonding and $\pi-\pi$ stacking interactions – observed in (**2**). C_{g1} = centroid formed from ring containing atoms N_9, C_1, C_2, C_3, C_4, C_5; C_{g4} = centroid formed from ring containing atoms N_{12}, C_{16}, C_{17}, C_{18}, C_{19}, C_{20}; C_{g3} = centroid formed from ring containing atoms N_{11}, C_{11}, C_{12}, C_{13}, C_{14}, C_{15}; C_{g6} = centroid formed from ring containing atoms N_{14}, C_{26}, C_{27}, C_{28}, C_{29}, C_{30}.

Interaction	Distance (Å), D–H---A	Angle (º), ∠D–H---A	Distance (Å), C–H---C_g	β (º)
N(9)-H --- O(19)	2.725(4)	171(3)	-	-
N(11)-H --- O(19)	2.687(4)	168(4)	-	-
N(12)-H --- O(22)	2.681(4)	167(3)	-	-
N(14)-H --- O(22)	2.759(4)	168(3)	-	-
O(16)-H --- O(18)	2.713(3)	169(3)	-	-
O(16)-H --- O(23)	2.638(3)	176(3)	-	-
O(17)-H --- O(24)	2.689(3)	176(3)	-	-
O(17)-H --- O(27)	2.661(3)	172(3)	-	-
O(27)-H --- O(28)	2.765(3)	177(3)	-	-
O(27)-H --- O(26)	2.923(3)	171(3)	-	-
O(28)-H --- O(24)	2.845(3)	174(3)	-	-
O(28)-H --- O(3)	2.987(4)	165(3)	-	-
C_{g1} --- C_{g4}	-	-	3.5299(18)	13.1
C_{g3} --- C_{g6}	-	-	3.7674(18)	25.2

Table S7. Selected noncovalent interactions – such as hydrogen bonding, halogen–π, C–H–π, and π–π stacking interactions – observed in (**3**). C_{g1} = centroid formed from ring containing atoms N_{51}, C_{51}, C_{52}, C_{53}, C_{54}, C_{55}; C_{g2} = centroid formed from ring containing atoms N_{61}, C_{61}, C_{62}, C_{63}, C_{62_c}, C_{61_c}.

Interaction	Distance (Å), D–H---A	Angle (º), ∠D–H---A	Distance (Å), C_g---C_g	β (º)
N(51)-H --- O(41)	3.056(3)	151(6)	-	-
N(51)-H --- O(42)	2.928(2)	108(4)	-	-
N(61)-H --- O(41)#1	2.869(4)	148(9)	-	-
C_{g1} --- C_{g2}	-	-	3.5980(15)	22.3

Symmetry transformations used to generate equivalent atoms: #1 1-x,y,3/2-z

Table S8. Selected noncovalent interactions – such as hydrogen bonding, observed in (**4**).

Interaction	Distance (Å), D–H---A	Angle (º), ∠D–H---A
N(51)-H --- O(43)	2.849(2)	161(3)
N(61)-H --- O(42)	2.753(2)	177(3)
N(61)-H --- O(43)	3.112(2)	122(2)

Table S9. Selected noncovalent interactions – such as hydrogen bonding, and π–π stacking interactions – were observed in (**5**). C_{g2} = centroid formed from ring containing atoms N_{81}, C_{81}, C_{82}, C_{83}, C_{84}, C_{85}; C_{g3} = centroid formed from ring containing atoms N_{91}, C_{91}, C_{92}, C_{93}, C_{94}, C_{95}.

Interaction	Distance (Å), D–H---A	Angle (º), ∠D–H---A	Distance (Å), C_g---C_g	β (º)
N(71)-H --- O(61)	3.066(5)	173(2)	-	-
N(71)-H --- O(62)	3.421(2)	129(2)	-	-
N(81)-H --- O(63)	2.965(4)	143(5)	-	-
N(91)-H --- O(61)	3.129(2)	154(2)	-	-
N(91)-H --- O(63)	3.038(4)	174(3)	-	-
C_{g2} --- C_{g3}	-	-	3.7087(12)	23.6

Table S10. Selected noncovalent interactions – such as hydrogen bonding, and π–π stacking interactions – were observed in (**6**).

Interaction	Distance (Å), D–H---A	Angle (º), ∠D–H---A
N(41)-H --- O(12)	2.889(3)	154(4)

Table S11. Selected noncovalent interactions – such as hydrogen bonding interactions – were observed in (**7**).

Interaction	Distance (Å), D–H---A	Angle (º), ∠D–H---A
N(53)-H --- O(41)	2.6528(19)	166(2)
N(51)-H --- O(41)	2.685(2)	168(2)

Table S12. Selected noncovalent interactions – such as hydrogen bonding, and π–π stacking interactions – were observed in (**8**). C_{g1} = centroid formed from ring containing atoms N_{31}, C_{31}, C_{32}, C_{33}, C_{34}, C_{35}.

Interaction	Distance (Å), D–H---A	Angle (º), ∠D–H---A	Distance (Å), C_g---C_g	β (º)
N(31)-H --- O(23)#1	3.249(2)	159(2)	-	-
N(31)-H --- O(3)#2	3.124(2)	128(2)	-	-
N(31)-H --- O(12)#3	2.964(2)	109(2)	-	-
C_{g1} --- C_{g1}	-	-	3.7906(10)	17.2

Symmetry transformations used to generate equivalent atoms: #1 3/2-x,1/2+y,1/2-z; #2 1-x,-y,1-z; #3 2-x,-y,1-z

Table S13. Selected noncovalent interactions – such as hydrogen bonding interactions – were observed in (**9**).

Interaction	Distance (Å), D–H---A	Angle (º), ∠D–H---A
N(61)-H --- O(21)#1	2.932(3)	172(3)
N(71)-H --- O(81)#2	2.762(3)	179(3)
N(91)-H --- O(82)	2.767(4)	171(4)
N(91)-H --- O(82)	3.038(2)	127(3)

Symmetry transformations used to generate equivalent atoms: #1 1+x,y,z;   #2 -1+x,y,z

Table S14. Selected noncovalent interactions – such as hydrogen bonding, and π–π stacking interactions – were observed in (**10**). C_{g1} = centroid formed from ring containing atoms N_{31}, N_{32}, C_{31}, C_{32}, C_{37}, C_{38}; C_{g2} = centroid formed from ring containing atoms C_{32}, C_{33}, C_{34}, C_{35}, C_{36}, C_{37}.

Interaction	Distance (Å), D–H---A	Angle (º), ∠D–H---A	Distance (Å), C_g---C_g	β (º)
N(32)-H --- O(13)	2.968(5)	158(2)	-	-
C_{g1} --- C_{g2}	-	-	3.629(2)	21.5

Table S15. Selected noncovalent interactions – such as hydrogen bonding, and π–π stacking interactions – were observed in (**11**). C_{g2} = centroid formed from ring containing atoms N_{71}, C_{71}, C_{72}, C_{73}, C_{74}, C_{75}; C_{g3} = centroid formed from ring containing atoms N_{81}, C_{81}, C_{82}, C_{83}, C_{84}, C_{85}.

Interaction	Distance (Å), D–H---A	Angle (º), ∠D–H---A	Distance (Å), C_g---C_g	β (º)
N(61)-H --- O(91)#1	2.762(3)	160(3)	-	-
N(81)-H --- O(91)	2.745(3)	155(3)	-	-
O(91)-H --- O(2)	2.771(2)	177(2)	-	-
O(91)-H --- O(23)#2	2.829(2)	163(4)	-	-
C_{g2} --- C_{g3}	-	-	3.7773(12)	24.4

Symmetry transformations used to generate equivalent atoms: #1 1-x,1-y,1-z; #2 -1+x,y,z

Table S16. Selected noncovalent interactions – such as hydrogen bonding, and π–π stacking interactions – were observed in (**12**).

Interaction	Distance (Å), D–H---A	Angle (º), ∠D–H---A
O(41)-H --- O(21)	2.887(2)	168(3)
O(41)-H --- O(13)#1	2.941(2)	121(3)
O(41)-H --- O(2)#2	3.097(3)	146(3)
N(31)-H --- O(41)	2.711(3)	169(3)

Symmetry transformations used to generate equivalent atoms: #1 x,1+y,z; #2 x,1-y,1/2+z

Table S17. Selected noncovalent interactions – such as hydrogen bonding, and π–π stacking interactions – were observed in (**13**). C_{g1} = centroid formed from ring containing atoms N_{41}, C_{41}, C_{42}, C_{43}, C_{44}, C_{45}.

Interaction	Distance (Å), D–H---A	Angle (º), ∠D–H---A	Distance (Å), C_g---C_g	β (º)
N(41)-H --- O(21)	2.833(4)	143(4)	-	-
N(41)-H --- O(23)#1	3.093(4)	127(4)	-	-
C_{g1} --- C_{g1}	-	-	3.574(2)	7.0

Symmetry transformations used to generate equivalent atoms: #1 1/2-x,1/2-y,1-z

Table S18. Selected noncovalent interactions – such as hydrogen bonding, and π–π stacking interactions – were observed in (**14**). C_{g1} = centroid formed from ring containing atoms N_{31}, C_{31}, C_{32}, C_{33}, C_{34}, C_{35}.

Interaction	Distance (Å), D–H---A	Angle (º), ∠D–H---A	Distance (Å), C_g---C_g	β (º)
N(31)-H --- O(11)#1	2.790(3)	155(3)	-	-
N(31)-H --- O(13)	3.061(3)	119(2)	-	-
C_{g1} --- C_{g1}	-	-	3.5592(16)	8.1

Symmetry transformations used to generate equivalent atoms: #1 1-x,1-y,1-z

Table S19. Selected noncovalent interactions – such as hydrogen bonding, and π–π stacking interactions – were observed in (**15**). C_{g2} = centroid formed from ring containing atoms N_{41}, C_{41}, C_{42}, C_{43}, C_{45}, C_{46}; C_{g3} = centroid formed from ring containing atoms N_{51}, C_{51}, C_{52}, C_{53}, C_{54}, C_{55}.

Interaction	Distance (Å), D–H---A	Angle (º), ∠D–H---A	Distance (Å), C_g---C_g	β (º)
N(41)-H --- O(51)	2.735(3)	157(3)	-	-
O(51)-H --- O(21)	2.924(2)	165(3)	-	-
O(51)-H --- O(13)#1	2.986(3)	163(3)	-	-
C_{g2} --- C_{g3}	-	-	3.7087(12)	23.6

Symmetry transformations used to generate equivalent atoms: #1 1/2-x,-1/2+y,3/2-z

8. COMPUTATIONAL METHODS.

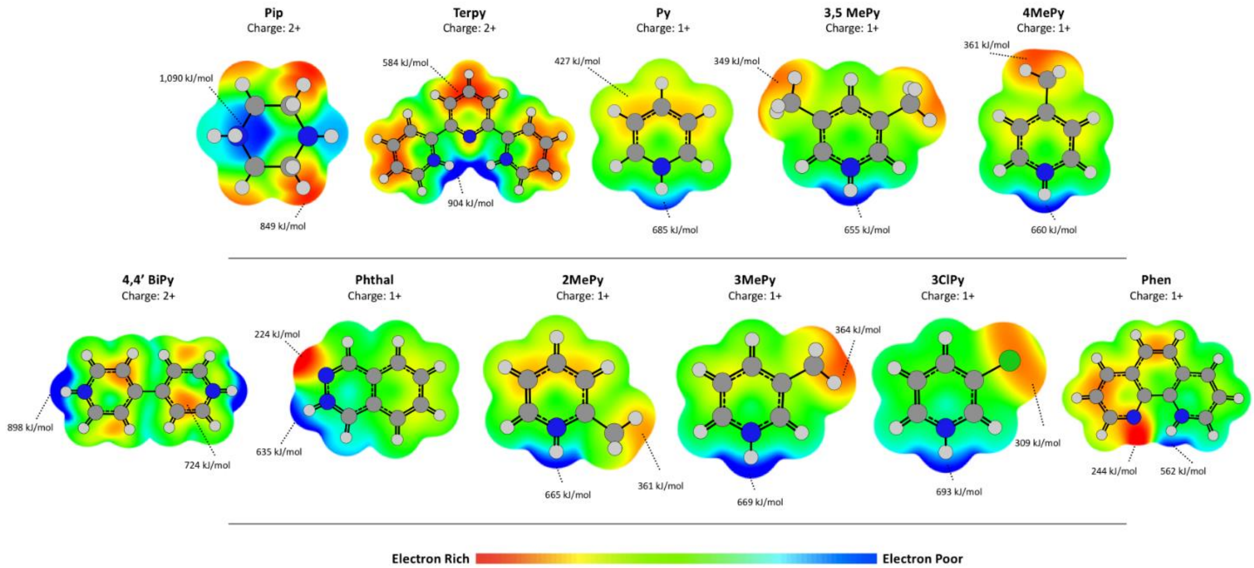

Figure S61. ESP surfaces of cationic organic units found in 1-15. Maximum and minimum potential values are highlighted.

Additional Details of Computational Methods

The geometries were optimized at the density functional theory (DFT) level[5] with the hybrid B3LYP exchange-correlation functional[6,7] in a self-consistent reaction field (SCRF)16[8] model for water. The DZVP2 basis set was used for the H, N, and O atoms,[7] and the cc-pVDZ-PP basis sets were used for Th.[9] This combination of basis sets is abbreviated as DZVP2. Vibrational frequencies were calculated to show that the structures were minima. These calculations were performed using the Gaussian16 program system.[10] The quasi-harmonic approximation from Truhlar and co-workers[11] was used to correct the entropy associated with low-frequency vibrational modes. Thus, all harmonic frequencies below 100 cm^{-1} were raised to 100 cm^{-1} before evaluation of the vibrational component to the entropy.

Single point calculations were performed at the CCSD(T) level[12–15] with the aug-cc-pVDZ basis sets for H, N and O and the cc-pVDZ-PP for Th using the optimized geometries in water. The single point MP2 energies[16] were extracted from the CCSD(T) calculations. All of the CCSD(T) calculations were performed with the MOLPRO 2020 program package.[17,18]

The solvation free energies in water at 298 K were calculated at the B3LYP/aD level using the with the COSMO (B3LYP/aD) parameters[19,20] as implemented in Gaussian 16. The aqueous Gibbs free energy (free energy in aqueous solution), ΔG_{aq}, was calculated from Equation 1.

$$\Delta G_{aq} = \Delta G_{gas} + \Delta\Delta G_{solv} \quad (1)$$

where ΔG_{gas} is the gas phase free energy and $\Delta\Delta G_{solv}$ is the aqueous solvation free energy. A dielectric constant of 78.39 corresponding to that of bulk water was used in the COSMO calculations. The reaction free energies in aqueous solution include a correction of +4.3 kcal/mol for each H_2O molecule produced in aqueous solution due to the definition of the standard state.

Table S20. Total energies at the B3LYP/DZVP2/Th(-PP) level in water (COSMO). Energies in Hartree. Free energies were calculated with quasi-harmonic treatment for the entropy with a frequency cut-off value of 100.0 cm^{-1}.

Cluster	ZPE	H0K	H 298 K	G 298 K
$Th(H_2O)_9^{4+}$	0.215786	-1094.575621	-1094.545580	-1094.629581
$Th(H_2O)_8NO_3^{3+}$	0.209910	-1298.682277	-1298.652285	-1298.736535
$Th(H_2O)_7NO_3^{3+}$	0.185287	-1222.220376	-1222.192499	-1222.273490
$Th(H_2O)_6NO_3^{3+}$	0.160368	-1145.761393	-1145.737099	-1145.810706
$Th(H_2O)_7(NO_3)_2^{2+}$	0.202434	-1502.790938	-1502.759548	-1502.847342
$Th(H_2O)_6(NO_3)_2^{2+}$	0.177282	-1426.333606	-1426.304778	-1426.388094
$Th(H_2O)_6(NO_3)_3^{1+}$	0.194663	-1706.891942	-1706.859978	-1706.950109
$Th(H_2O)_5(NO_3)_3^{1+}$	0.168560	-1630.439484	-1630.409832	-1630.495516
$Th(H_2O)_5(NO_3)_4$	0.186034	-1910.988584	-1910.956634	-1911.047446
$Th(H_2O)_4(NO_3)_4$	0.158848	-1834.536920	-1834.507687	-1834.594349
$Th(H_2O)_3(NO_3)_5^{1-}$	0.152361	-2038.643676	-2038.612228	-2038.702769
$Th(H_2O)_2(NO_3)_5^{1-}$	0.125795	-1962.190676	-1962.161189	-1962.249039
$Th(H_2O)_1(NO_3)_6^{2-}$	0.117209	-2166.283938	-2166.252351	-2166.343986

$Th(H_2O)_1(NO_3)_6^{2-}$ 5bi	0.119106	-2166.293908	-2166.263711	-2166.351609
$Th(NO_3)_6^{2-}$ 4bi	0.091686	-2089.834231	-2089.805036	-2089.892937
$Th(NO_3)_6^{2-}$ bi	0.093925	-2089.850666	-2089.822903	-2089.906159
$Th(H_2O)_2(NO_3)_5^{1-}$ bi	0.128035	-1962.198700	-1962.169673	-1962.254400
H_2O	0.021000	-76.447971	-76.444191	-76.465639
NO_3^{1-}	0.013523	-280.536069	-280.531936	-280.561603

Table S21. Total energies at the B3LYP /aD-pp aqueous single point level in water (COSMO)/gas phase. The ZPE, thermal, entropic corrections from B3LYPdDZVP2 level. Energies in Hartrees except for ΔG_{solv}(298 K) in kcal/mol.

Cluster	H 0K	H 298 K	G 298 K	E(COSMO) single point	E_{elec} gas	ΔG_{solv}(298 K) kcal/mol
$Th(H_2O)_9^{4+}$	-1093.365548	-1093.335507	-1093.419508	-1094.667699	-1093.581334	-681.704483
$Th(H_2O)_8NO_3^{3+}$	-1297.867651	-1297.837659	-1297.921909	-1298.748510	-1298.077561	-421.026307
$Th(H_2O)_7NO_3^{3+}$	-1221.409329	-1221.381452	-1221.462443	-1222.275961	-1221.594616	-427.550711
$Th(H_2O)_6NO_3^{3+}$	-1144.960464	-1144.936170	-1145.009777	-1145.807980	-1145.120832	-431.191772
$Th(H_2O)_7(NO_3)_2^{2+}$	-1502.280024	-1502.248634	-1502.336428	-1502.830300	-1502.482458	-218.274222
$Th(H_2O)_6(NO_3)_2^{2+}$	-1425.831439	-1425.802611	-1425.885927	-1426.363158	-1426.008721	-222.413087
$Th(H_2O)_6(NO_3)_3^{1+}$	-1706.548086	-1706.516122	-1706.606253	-1706.904595	-1706.742749	-101.559903
$Th(H_2O)_5(NO_3)_3^{1+}$	-1630.112065	-1630.082413	-1630.168097	-1630.441770	-1630.280625	-101.119893
$Th(H_2O)_5(NO_3)_4$	-1910.718971	-1910.687021	-1910.777833	-1910.975078	-1910.905005	-43.971599
$Th(H_2O)_4(NO_3)_4$	-1834.287883	-1834.258650	-1834.345312	-1834.510206	-1834.446731	-39.831354
$Th(H_2O)_3(NO_3)_5^{1-}$	-2038.337651	-2038.306203	-2038.396744	-2038.592268	-2038.490012	-64.166862
$Th(H_2O)_2(NO_3)_5^{1-}$	-1961.918706	-1961.889219	-1961.977069	-1962.128194	-1962.044501	-52.518655
$Th(H_2O)_1(NO_3)_6^{2-}$	-2165.835838	-2165.804251	-2165.895886	-2166.193675	-2165.953047	-150.995979
$Th(H_2O)_1(NO_3)_6^{2-}$ 5bi	-2165.856524	-2165.826327	-2165.914225	-2166.205711	-2165.975630	-144.377762
$Th(NO_3)_6^{2-}$ 4bi	-2089.421005	-2089.391810	-2089.479711	-2089.734487	-2089.512691	-139.178783
$Th(NO_3)_6^{2-}$ bi	-2089.435508	-2089.407745	-2089.491001	-2089.753046	-2089.529433	-140.319031
$Th(H_2O)_2(NO_3)_5^{1-}$ bi	-1961.912304	-1961.883277	-1961.968004	-1962.138358	-1962.040339	-61.507603
H_2O	-76.423598	-76.419818	-76.441266	-76.455020	-76.444598	-6.539779
NO_3^{1-}	-280.404126	-280.399993	-280.429660	-280.520295	-280.417649	-64.411528

Table S22. Total energies at the MP2 and CCSD(T)/aD(-PP) levesl with aqueous cluster geometry. Energies in Hartrees.

Cluster	CCSD(T)	MP2
$Th(H_2O)_9^{4+}$	-1090.846845	-1090.713591
$Th(H_2O)_8NO_3^{3+}$	-1294.889886	-1294.743260
$Th(H_2O)_7NO_3^{3+}$	-1218.566273	-1218.432839
$Th(H_2O)_6NO_3^{3+}$	-1142.261815	-1142.139976
$Th(H_2O)_7(NO_3)_2^{2+}$	-1498.849649	-1498.689773
$Th(H_2O)_6(NO_3)_2^{2+}$	-1422.535484	-1422.388534
$Th(H_2O)_6(NO_3)_3^{1+}$	-1702.655659	-1702.483377
$Th(H_2O)_5(NO_3)_3^{1+}$	-1626.352910	-1626.193805
$Th(H_2O)_5(NO_3)_4$	-1906.359221	-1906.174394
$Th(H_2O)_4(NO_3)_4$	-1830.055611	-1829.885136
$Th(H_2O)_3(NO_3)_5^{1-}$	-2033.660920	-2033.477589
$Th(H_2O)_2(NO_3)_5^{1-}$	-1957.373375	-1957.202906
$Th(H_2O)_1(NO_3)_6^{2-}$	-2160.847618	-2160.665881
$Th(H_2O)_1(NO_3)_6^{2-}$ 5bi	-2160.874759	-2160.693752
$Th(NO_3)_6^{2-}$ 4bi	-2084.564599	-2084.395650
$Th(NO_3)_6^{2-}$ bi	-2084.595116	-2084.427272
$Th(H_2O)_2(NO_3)_5^{1-}$ bi	-1957.396690	-1957.226615
H_2O	-76.273872	-76.260868
NO_3^{1-}	-279.786225	-279.761692

Table S23. Calculated Reaction Energies, ΔG_{aq}, for the Stepwise Addition of Nitrate to 9-Coordinate Thorium(IV)-Nitrate Complexes in kcal/mol.[a]

Reaction	B3LYP/DZVP2	B3LYP/aD	CCSD(T)/aD	MP2/aD
$Th(H_2O)_9^{4+} + NO_3^- \rightarrow Th(H_2O)_8NO_3^{3+} + H_2O$	-2.6	0.3	-1.8	-0.6
$Th(H_2O)_8NO_3^{3+} + NO_3^- \rightarrow Th(H_2O)_7(NO_3)_2^{2+} + H_2O$	-5.0	-2.5	-12.2	-11.2
$Th(H_2O)_7(NO_3)_2^{2+} + NO_3^- \rightarrow Th(H_2O)_6(NO_3)_3^{1+} + H_2O$	0.0	2.3	-1.7	-1.2
$Th(H_2O)_6(NO_3)_3^{1+} + NO_3^- \rightarrow Th(H_2O)_5(NO_3)_4 + H_2O$	3.4	4.8	3.6	4.2
$Th(H_2O)_5(NO_3)_4 + NO_3^- \rightarrow Th(H_2O)_2(NO_3)_5^{1-} + 3H_2O$	-13.6	-12.7	-26.2	-26.3
$Th(H_2O)_2(NO_3)_5^{1-} + NO_3^- \rightarrow ThH_2O(NO_3)_6^{2-} + H_2O$	3.5	5.8	3.6	3.2
$Th(H_2O)_2(NO_3)_5^{1-} + NO_3^- \rightarrow Th(NO_3)_6^{2-} + 2H_2O$	-4.9	-3.8	-3.3	-3.8

[a] Optimized at the B3LYP/aD/COSMO(aq) level.

Table S24. Calculated Reaction Energies, ΔG_{aq}, for 9-Coordinate Thorium(IV)-Nitrate Structures at 298 K in kcal/mol.[a]

Reaction	B3LYP/DZVP2	B3LYP/aD	CCSD(T)/aD	MP2/aD
$Th(H_2O)_8NO_3^{3+} \rightarrow Th(H_2O)_7NO_3^{3+} + H_2O$	2.7	2.7	9.8	9.7
$Th(H_2O)_7(NO_3)_2^{2+} \rightarrow Th(H_2O)_6(NO_3)_2^{2+} + H_2O$	0.3	-0.6	6.4	6.5
$Th(H_2O)_6(NO_3)_3^{1+} \rightarrow Th(H_2O)_5(NO_3)_3^{1+} + H_2O$	-2.6	-3.8	3.4	3.3
$Th(H_2O)_5(NO_3)_4 \rightarrow Th(H_2O)_4(NO_3)_4 + H_2O$	-3.6	-3.6	6.5	5.6
$Th(H_2O)_3(NO_3)_5^{1-} \rightarrow Th(H_2O)_2(NO_3)_5^{1-} + H_2O$	-6.5	-7.4	-16.7	-16.8
$Th(H_2O)_1(NO_3)_6^{2-} \rightarrow Th(NO_3)_6^{2-} + H_2O$	-8.4	-9.5	-6.9	-7.0

[a] Optimized at the B3LYP/aD/COSMO(aq) level.

Table S25. Relative Energies, in kcal/mol, for Selected Thorium(IV)-Nitrate Structures at 298 K in kcal/mol.[a]

Molecules	NO_3^- coordination	B3LYP/DZVP2	B3LYP/aD	CCSD(T)/aD	MP2/aD	Gas phase B3LYP/aD
$Th(H_2O)_2(NO_3)_5^{1-}$	5 bidentate	0	0	0	0	0
	3 monodentate, 2 bidentate	3.4	6.4	11.6	11.8	-2.6
$Th(NO_3)_6^{2-}$	6 bidentate	0	0	0	0	0
	2 monodentate, 4 bidentate	8.3	14.7	15.8	16.4	10.5
$Th(H_2O)_1(NO_3)_6^{2-}$	5 bidentate, 1 monodentate	0	0	0	0	0
	4 bidentate, 2 monodentate	4.8	7.6	14.4	14.8	14.2

Table S26. Frequencies (cm^{-1}), IR Intensities (km/mole) and Raman Activities ($Å^4$/amu) at B3LYP/DZVP2(H,O,N))/cc-pVDZ-PP(Th) level in water.

$Th(H_2O)_8NO_3^{3+}$			$Th(H_2O)_7NO_3^{3+}$			$Th(H_2O)_7(NO_3)_2^{2+}$			$Th(H_2O)_6(NO_3)_2^{2+}$			$Th(H_2O)_6(NO_3)_3^{1+}$		
Freq	IR	Ram	Freq	IR	Ram	Freq	IR	Ram	Freq	IR	Ram	Freq	IR	Ram
35.5	1.2	3.0	32.0	0.1	2.4	29.6	12.9	2.0	27.9	18.1	4.2	15.3	5.8	3.2
43.7	0.6	5.3	39.1	4.3	2.1	38.2	0.2	5.1	49.5	1.4	5.0	23.3	3.1	2.7
64.5	4.6	0.5	47.0	21.3	1.0	47.0	14.1	0.4	56.6	5.2	2.7	30.4	3.4	5.5
69.3	2.2	0.9	57.7	0.8	4.1	56.0	12.0	3.4	58.7	19.9	1.3	39.5	3.5	1.8
79.7	8.0	0.6	78.9	21.5	0.3	75.6	14.1	4.3	72.5	0.6	1.2	46.8	0.7	6.2
90.4	7.5	0.3	94.4	14.0	0.2	79.5	22.5	1.2	80.4	42.8	1.5	58.9	12.2	2.1
110.9	12.3	0.6	95.2	13.9	0.1	96.9	7.2	0.4	86.1	26.5	0.7	66.3	16.4	2.7
115.1	17.3	0.8	98.7	50.4	0.8	101.4	4.9	0.1	94.2	34.2	1.3	72.5	21.0	1.0
121.6	22.6	0.4	105.8	74.0	0.2	109.4	9.8	1.5	100.8	17.2	1.7	91.0	89.2	0.7
122.6	7.8	0.1	116.5	50.3	0.1	112.0	37.7	0.3	104.5	18.0	0.7	96.2	24.2	1.5
127.5	42.7	0.1	119.5	35.4	0.9	119.7	22.3	0.4	110.4	224.0	0.6	105.8	25.3	0.3
136.3	9.6	0.4	126.1	102.1	0.7	127.1	44.5	1.2	118.8	19.7	0.4	117.9	91.2	1.1
143.5	17.1	0.1	131.2	96.7	0.3	136.5	59.8	0.5	129.1	52.1	2.2	123.8	61.6	0.9
144.9	82.7	0.9	142.3	162.1	0.5	140.4	73.6	0.2	135.1	62.0	0.8	132.2	24.5	0.5
151.7	8.5	0.4	146.3	125.9	0.2	144.2	63.1	0.8	137.2	389.2	0.3	137.4	9.2	3.3
157.5	113.6	0.4	149.5	101.1	0.4	147.7	47.9	0.5	150.4	102.5	0.8	147.8	27.0	0.6
164.1	201.2	0.3	153.6	99.5	0.5	149.6	308.3	1.2	155.8	46.3	0.6	152.5	13.9	0.9
168.1	50.8	0.1	155.5	178.0	0.3	157.4	110.2	0.5	158.0	25.5	0.3	158.0	11.5	0.3
174.6	44.5	0.2	168.6	310.9	1.0	163.1	43.7	0.5	162.0	98.8	0.3	162.6	74.0	0.5
186.5	227.2	0.5	177.1	30.2	0.7	166.7	1.2	0.5	167.6	14.9	0.7	166.4	4.1	1.1
187.3	327.0	0.7	178.0	189.9	0.7	183.4	1.0	0.8	179.4	21.8	1.0	169.1	28.5	0.9
199.0	443.8	0.2	183.2	5.3	0.1	185.9	148.9	0.8	182.9	33.3	1.0	175.9	0.6	0.3
205.6	262.1	0.4	200.5	223.0	0.9	192.6	127.2	0.3	188.8	87.6	0.3	183.0	36.8	1.2
211.4	84.4	0.4	207.7	25.0	0.6	201.6	307.8	0.4	206.5	292.6	1.5	184.5	46.0	0.9

223.6	133.6	0.5	224.4	375.6	0.9	204.2	213.7	1.0	209.0	81.6	0.4	192.2	180.7	0.7
227.7	164.2	0.9	237.9	175.2	1.2	206.6	357.5	0.8	216.3	102.4	0.9	199.2	43.2	0.5
239.2	54.1	1.1	240.0	137.3	0.9	209.3	75.7	2.2	225.1	362.7	1.1	208.3	75.4	0.9
246.7	31.4	0.9	250.5	90.3	0.9	221.4	31.3	0.4	243.9	52.5	0.9	221.4	164.1	0.4
250.8	135.8	0.5	260.6	163.5	0.7	225.6	337.1	0.9	257.4	31.4	0.4	229.7	72.9	0.2
257.1	322.4	0.4	282.2	125.5	0.3	234.5	135.5	0.2	258.5	134.3	1.2	233.0	34.4	0.8
266.1	138.9	1.0	292.5	10.0	0.3	241.0	33.1	0.9	263.7	52.0	1.0	237.7	162.8	1.0
267.3	389.1	0.5	307.2	57.5	0.5	250.9	83.7	0.1	288.6	48.9	0.3	256.9	77.5	0.9
276.9	43.0	0.5	312.5	121.6	0.6	256.2	124.9	0.8	294.3	136.6	0.7	259.6	123.0	0.3
284.4	20.8	1.4	319.6	94.0	0.1	270.4	58.3	0.9	296.8	46.2	0.1	263.5	111.5	0.2
293.0	165.8	0.6	324.9	132.1	0.7	275.2	52.9	1.0	307.1	40.8	0.6	275.1	153.2	1.1
297.0	44.3	0.6	349.3	69.9	1.4	280.1	69.1	0.5	321.1	243.7	0.7	286.1	16.5	1.2
298.8	62.0	0.3	383.0	5.0	7.7	281.7	4.1	0.5	345.6	120.1	5.8	289.8	202.2	1.0
304.4	30.3	0.5	507.7	166.1	0.5	292.0	162.9	0.9	369.5	6.8	4.8	298.9	59.5	0.9
308.2	65.7	0.4	516.0	143.0	0.5	298.6	154.7	1.1	497.6	104.2	0.2	313.4	225.8	0.7
320.3	200.3	0.4	521.5	137.1	0.5	301.8	54.6	0.3	510.7	105.6	0.7	337.9	176.0	10.0
342.5	88.5	1.5	548.1	168.7	0.4	326.8	17.3	3.9	519.5	134.2	0.7	358.1	392.7	0.3
377.6	5.2	8.3	553.5	56.7	0.6	339.3	251.5	0.7	549.8	138.2	1.1	364.6	104.2	1.0
514.6	85.7	0.6	572.9	197.0	0.2	361.1	4.5	7.3	566.3	295.3	0.3	442.4	382.0	0.4
525.8	79.7	0.7	593.4	94.4	0.4	528.4	49.3	0.9	631.7	81.5	1.3	521.7	78.2	2.3
535.2	192.6	1.0	653.1	105.8	6.9	533.8	24.1	1.0	664.0	84.8	7.7	542.8	88.5	1.7
537.3	85.2	1.0	716.1	63.4	6.1	537.7	279.7	1.2	690.0	0.1	4.6	554.3	93.1	0.9
555.6	86.2	0.4	751.1	131.3	2.9	551.6	61.3	0.7	727.5	42.2	8.8	565.8	155.2	1.2
575.5	112.1	1.2	779.9	31.9	0.2	552.4	264.9	1.0	739.3	66.7	8.5	590.0	212.4	0.6
579.4	191.2	0.7	1013.3	725.2	46.8	564.4	98.5	1.3	781.6	27.3	0.1	638.5	124.5	2.0
606.8	154.1	0.3	1280.3	786.9	34.1	597.5	144.2	0.5	786.9	38.2	0.2	667.3	56.3	7.2
663.8	64.5	7.3	1512.7	1097.2	8.4	669.3	62.6	6.7	801.1	203.6	0.7	673.6	48.7	7.5
726.1	26.8	7.1	1607.3	236.5	0.8	692.3	0.2	5.2	1037.6	603.5	39.6	692.4	0.3	5.4
780.7	31.8	0.3	1608.1	90.8	2.0	725.2	10.4	6.9	1045.7	84.8	70.9	721.8	17.8	7.5
787.3	174.2	0.6	1611.0	173.2	0.9	737.8	69.1	6.9	1259.2	644.5	4.3	727.6	22.4	11.6

1047.1	437.9	63.1	1616.2	103.6	11.4	785.9	18.5	0.1	1281.2	902.5	25.9	739.0	54.4	9.2
1281.5	922.4	20.4	1617.0	139.8	1.6	788.7	29.7	0.1	1499.9	1074.0	10.7	785.4	22.1	0.1
1487.4	1111.0	8.8	1618.8	194.3	0.8	824.8	224.3	1.0	1560.3	1104.2	28.2	788.9	23.1	0.2
1598.1	161.5	1.6	1631.5	160.3	1.7	1054.3	140.6	35.7	1601.5	194.0	1.6	792.5	16.3	0.1
1603.4	132.8	2.3	3381.9	1086.0	182.4	1062.1	225.8	87.3	1607.2	151.0	1.7	839.1	298.9	1.1
1607.6	218.5	1.3	3748.4	95.7	56.2	1280.0	557.1	4.2	1609.0	159.8	1.2	843.0	153.6	0.8
1611.9	77.2	1.1	3749.5	319.9	33.8	1290.0	1099.4	13.4	1618.1	227.7	1.3	1052.8	406.4	27.1
1614.5	75.3	1.1	3751.0	486.3	15.8	1468.3	1134.6	9.5	1626.2	166.2	7.4	1057.6	287.7	27.1
1616.3	82.4	7.2	3752.1	74.6	227.3	1547.3	1087.6	26.3	1649.2	118.0	1.1	1065.6	95.4	170.2
1618.1	481.3	1.2	3755.2	215.7	54.4	1586.4	209.0	2.2	3312.8	1319.8	200.9	1280.9	1730.5	1.5
1621.3	71.9	2.8	3759.4	273.2	752.7	1600.8	222.2	1.0	3756.2	143.2	68.3	1293.1	1070.3	33.4
3263.1	1406.1	189.3	3809.3	382.6	149.4	1603.4	164.7	1.4	3758.0	171.1	91.3	1296.0	120.5	5.2
3756.1	118.1	61.5	3830.0	347.8	57.7	1607.7	201.5	1.4	3761.8	363.3	194.5	1471.5	955.1	10.4
3756.4	152.4	43.2	3830.9	354.3	60.6	1608.9	111.7	1.0	3764.4	198.0	91.0	1474.5	1024.1	10.5
3757.9	175.0	50.4	3833.6	586.6	44.3	1619.6	302.2	1.4	3767.6	224.2	511.7	1529.7	1157.2	20.9
3758.6	405.8	29.7	3833.6	142.6	75.1	1620.3	11.1	8.4	3803.6	316.8	136.8	1581.0	207.7	2.9
3759.4	151.1	88.5	3838.8	336.1	61.5	3234.7	1604.8	222.1	3837.2	317.6	64.8	1593.3	230.9	0.4
3761.3	333.2	41.9	3839.8	370.4	59.1	3762.8	43.5	38.3	3840.3	347.3	59.8	1604.2	194.8	2.0
3764.9	155.9	1012.0				3763.6	158.2	69.0	3843.6	323.4	62.1	1609.0	132.2	5.8
3814.4	351.6	153.0				3764.2	131.2	41.8	3850.0	338.0	59.1	1611.8	97.1	1.8
3838.8	330.3	60.1				3766.9	470.9	39.5	3851.2	331.1	58.4	1617.1	137.8	5.1
3839.8	305.2	54.0				3768.7	233.6	407.8				3289.9	1778.5	98.1
3841.1	346.5	69.2				3771.9	84.8	563.8				3297.7	923.7	298.7
3842.2	300.1	65.2				3815.7	308.5	136.0				3760.1	191.5	136.8
3842.6	339.1	67.7				3846.8	268.5	61.6				3765.7	174.0	139.0
3844.3	336.3	54.8				3848.9	319.8	65.3				3768.1	153.6	233.0
3844.7	362.9	51.8				3851.7	311.8	62.6				3773.3	156.0	224.3
						3853.5	380.9	62.1				3808.7	278.7	143.4
						3853.9	273.1	61.9				3814.0	275.8	117.0
						3857.6	315.6	53.8				3844.2	297.7	58.9

												3851.8	301.4	61.6
												3855.7	305.1	53.6
												3860.8	314.9	53.1

$Th(H_2O)_5(NO_3)_3^{1+}$			$Th(H_2O)_5(NO_3)_4$			$Th(H_2O)_4(NO_3)_4$			$Th(H_2O)_3(NO_3)_5^{-1}$			$Th(H_2O)_2(NO_3)_5^{-1}$		
Freq	IR	Ram	Freq	IR	Ram	Freq	IR	Ram	Freq	IR	Ram	Freq	IR	Ram
26.0	8.7	1.9	14.6	4.9	6.9	25.8	1.8	0.9	21.7	1.2	4.8	47.8	2.1	1.9
40.3	5.3	6.4	21.3	2.6	5.7	34.4	18.7	1.0	25.5	6.2	3.8	52.9	0.3	2.9
41.4	4.5	3.8	28.6	7.0	2.0	46.8	5.7	1.1	33.5	1.0	6.9	58.9	14.2	1.4
46.2	3.9	2.9	35.8	5.3	3.7	48.0	3.8	1.5	35.0	6.9	1.2	59.2	15.7	1.3
49.3	4.7	4.8	45.6	1.2	9.7	56.1	11.3	0.8	43.1	1.9	3.8	68.1	0.7	9.1
57.3	2.3	2.5	47.5	11.2	2.6	71.1	8.6	0.5	49.0	0.6	4.4	69.2	0.2	8.0
80.5	11.6	4.0	53.7	1.6	0.1	79.0	0.2	6.2	50.3	4.8	1.8	75.6	34.7	0.0
89.5	10.4	1.0	62.0	7.8	5.7	91.3	9.7	0.8	53.7	0.5	7.7	116.3	1.9	1.8
92.6	0.8	1.5	71.2	28.7	2.5	109.0	3.0	8.4	59.7	3.1	3.1	122.2	29.7	0.2
95.4	0.5	1.9	82.1	1.7	6.0	112.7	2.4	3.0	62.5	7.4	2.1	126.1	26.5	0.9
105.0	27.1	0.2	91.2	7.1	0.4	114.3	0.3	2.7	70.1	15.9	1.9	129.9	5.9	3.5
108.7	8.0	0.4	98.6	6.4	1.3	117.6	7.2	2.4	89.2	5.9	0.3	136.3	4.8	3.9
114.5	27.0	0.5	107.6	4.6	1.0	117.9	0.7	3.2	101.6	17.9	2.2	140.0	42.5	1.7
126.3	1.9	0.3	118.0	10.5	2.0	120.7	32.1	4.2	112.8	14.7	1.7	146.4	1.1	3.7
132.2	41.9	0.4	128.9	7.7	0.7	122.7	1.6	0.8	114.9	11.4	2.4	151.8	8.7	1.6
141.0	6.6	0.5	133.3	24.7	1.1	125.4	8.6	1.1	122.7	36.0	3.2	155.1	4.3	0.8
152.8	15.3	1.3	136.1	48.2	0.3	143.2	6.7	2.6	127.6	33.6	0.9	158.7	8.2	2.5
154.8	2.2	1.1	140.2	27.3	0.4	153.1	11.5	0.3	138.3	1.3	1.9	161.1	18.6	1.7
163.7	48.4	0.6	142.3	7.3	0.8	157.6	70.9	0.6	148.1	50.7	0.5	164.3	6.7	0.9
170.9	31.2	1.4	147.8	4.6	2.0	160.3	65.0	0.5	152.0	8.4	0.4	165.2	17.4	0.9
177.8	112.4	1.1	150.9	9.7	1.6	164.2	8.3	1.8	158.9	42.3	1.3	170.0	8.6	2.6
182.7	148.8	2.0	151.6	22.8	0.5	175.6	15.2	1.2	164.2	61.9	1.5	177.8	5.4	0.0
185.3	394.7	0.7	161.1	31.8	0.3	180.6	5.1	1.6	169.3	14.6	3.3	189.0	66.2	1.7

197.9	66.1	0.9	164.8	43.0	1.2	184.4	8.3	0.8	171.8	16.8	0.8	190.8	86.1	1.5
203.6	21.0	1.7	166.1	0.2	0.5	188.4	5.7	1.5	181.7	14.8	2.3	193.0	13.2	0.2
207.6	184.8	0.2	182.3	50.6	0.4	220.2	146.3	0.4	185.6	20.1	1.1	194.3	15.9	0.4
213.7	169.5	1.2	193.8	17.5	0.2	224.5	170.4	0.9	193.5	66.7	0.7	196.9	49.6	0.8
219.6	52.9	0.5	203.6	40.4	1.7	227.7	106.0	0.9	202.4	20.3	2.7	198.6	144.1	0.3
231.3	50.2	0.9	207.1	162.9	0.5	237.8	11.0	3.4	213.4	47.1	1.7	203.1	7.7	4.2
246.4	262.4	1.4	236.7	90.6	1.0	279.3	149.0	0.1	216.8	67.2	2.2	204.6	113.5	0.5
248.0	105.7	0.3	247.7	18.9	0.5	283.3	221.5	0.1	229.0	57.1	1.2	205.2	80.4	0.2
256.6	261.0	1.6	250.3	32.3	0.6	297.6	419.8	0.5	237.0	132.0	0.6	224.7	0.5	6.8
276.1	356.2	0.7	271.1	43.9	0.1	318.7	2.1	11.6	254.5	50.5	3.3	227.0	4.3	7.6
294.6	102.5	0.3	285.9	373.6	0.7	353.5	178.0	0.8	272.9	404.3	0.4	256.7	215.4	0.1
304.9	18.9	0.2	286.9	46.9	0.5	360.7	203.1	0.8	290.9	49.2	1.0	284.6	0.6	12.4
318.1	74.2	3.6	305.1	54.4	0.3	361.8	169.9	1.1	307.9	152.5	7.7	338.4	504.2	0.2
334.3	85.7	0.9	319.5	125.5	12.8	371.7	49.2	3.7	348.2	141.2	0.2	341.4	302.6	0.2
360.1	10.4	6.6	333.6	164.7	1.2	554.1	204.0	0.4	364.2	23.4	2.2	555.4	70.4	1.3
527.5	131.7	1.0	362.4	90.5	1.4	571.9	123.4	0.7	385.5	157.7	1.1	567.9	126.4	0.7
530.6	165.5	0.5	404.4	227.5	0.2	574.0	295.3	0.2	573.4	396.5	0.6	691.4	0.1	3.2
560.8	109.4	0.9	472.5	67.7	0.9	581.3	199.5	0.3	592.5	288.7	1.2	691.7	0.1	3.1
566.7	413.8	0.6	492.4	945.0	2.2	664.0	198.2	2.0	601.3	93.1	0.6	694.2	1.0	1.2
600.4	86.1	0.2	514.0	124.4	0.9	664.3	12.9	5.9	672.6	48.1	6.2	694.5	0.3	8.8
666.9	58.0	6.2	548.6	21.2	0.8	666.1	14.4	5.6	673.4	45.5	8.4	695.2	0.3	9.4
668.6	54.9	7.4	576.0	720.5	3.2	666.5	31.7	9.3	678.3	22.4	6.7	731.7	115.1	3.0
690.5	0.3	4.2	589.3	250.5	0.8	717.3	19.4	16.5	691.0	1.1	1.9	732.4	43.4	5.9
719.0	14.3	3.6	613.8	229.1	4.1	722.4	143.1	6.2	693.7	1.4	10.2	733.5	42.8	6.2
721.1	86.7	13.7	645.4	181.4	8.6	723.1	2.9	3.4	720.0	28.9	6.2	733.9	96.0	3.6
737.8	43.5	8.7	652.1	79.9	11.2	726.6	2.2	6.8	721.7	3.3	14.1	747.3	0.0	13.0
756.8	116.1	1.9	666.6	58.3	5.9	767.9	177.7	0.7	724.1	25.9	7.3	787.0	7.5	0.0
760.3	134.8	1.4	669.5	69.6	6.7	773.2	181.9	0.6	733.8	77.9	15.1	788.2	36.7	0.1
785.6	31.4	0.1	688.6	14.0	5.7	776.5	179.1	0.3	740.6	26.6	4.5	789.3	35.7	0.1
788.6	39.8	0.1	700.9	15.9	2.9	778.4	225.0	0.4	786.9	25.6	0.1	790.8	2.2	0.3

790.4	18.7	0.2	713.2	33.1	7.4	809.4	26.5	0.0	787.6	53.2	0.9	791.0	4.9	0.3
1043.4	871.4	16.5	721.9	19.1	10.7	809.9	15.6	0.1	788.0	17.1	0.1	1056.7	32.4	18.6
1043.7	147.1	27.4	723.1	76.1	2.8	810.4	52.9	0.0	789.2	39.9	0.4	1057.3	11.5	16.2
1054.7	47.9	151.8	726.1	19.1	10.3	810.5	4.2	0.1	790.0	39.8	0.1	1059.3	162.3	9.9
1264.3	702.9	5.9	734.4	91.8	0.7	1001.4	826.8	23.0	791.9	16.9	0.3	1060.7	164.2	11.1
1278.9	1338.2	4.2	784.6	22.9	0.1	1003.0	861.6	26.7	816.7	183.8	1.0	1063.3	1.0	213.4
1286.2	658.3	39.0	792.9	177.7	0.3	1005.9	611.5	42.0	819.6	263.1	1.6	1286.2	83.3	1.6
1478.7	911.8	9.8	794.6	21.0	0.2	1025.6	2.1	187.8	1053.1	99.0	26.9	1287.4	12.9	1.7
1480.7	1172.6	6.4	795.8	45.2	0.1	1223.8	2281.0	6.2	1053.3	60.3	23.5	1300.9	375.1	6.3
1551.2	1212.1	28.4	799.4	5.5	0.3	1225.6	1018.4	22.2	1055.3	487.8	32.7	1304.6	393.7	6.4
1602.0	65.9	11.1	1047.7	245.6	70.6	1229.7	53.0	1.0	1058.2	474.8	20.2	1308.7	2412.3	0.0
1606.8	54.4	9.8	1048.4	676.8	9.6	1243.9	0.6	109.3	1067.7	14.6	261.0	1505.2	81.6	15.3
1616.0	257.9	1.7	1051.5	517.3	14.7	1422.9	338.7	3.4	1276.8	1334.4	2.6	1505.9	85.0	15.4
1617.5	287.4	1.4	1063.7	55.2	205.4	1424.3	3493.0	4.2	1284.1	887.4	15.0	1519.4	2847.0	1.5
1618.1	45.5	1.3	1269.7	699.8	3.7	1424.8	201.1	9.4	1294.2	425.9	3.1	1524.4	2901.8	1.0
3327.8	1602.2	124.1	1272.8	1408.4	2.3	1426.9	208.2	47.9	1296.1	584.1	10.0	1550.7	0.0	95.3
3339.8	841.9	266.5	1278.8	1961.7	8.3	1578.2	61.3	6.7	1300.9	1449.5	29.0	1621.1	196.5	3.0
3759.9	273.6	109.9	1296.5	30.3	50.1	1584.7	69.6	7.9	1461.3	751.1	9.8	1630.1	164.8	4.1
3762.1	165.1	69.3	1476.0	1577.9	9.8	1588.7	60.0	4.3	1466.4	1057.7	10.0	3768.3	249.6	119.0
3764.1	159.1	385.2	1479.4	728.5	12.2	1590.4	129.7	6.1	1469.0	1237.2	7.9	3771.6	103.8	284.8
3815.5	333.2	145.8	1484.6	1172.1	16.2	3329.9	710.0	39.5	1521.5	1613.2	16.2	3850.1	298.3	60.0
3822.3	352.7	156.6	1487.2	419.1	13.0	3331.3	2016.9	277.0	1532.1	930.8	29.6	3852.6	277.3	65.2
3843.5	317.8	63.1	1571.5	139.1	14.1	3336.2	573.2	147.1	1611.0	39.5	3.4			
3846.3	332.0	63.5	1605.9	177.3	8.1	3338.2	1066.6	386.2	1617.6	130.4	13.8			
3847.1	311.2	58.6	1614.3	83.1	7.7	3749.1	363.7	48.7	1638.8	113.5	5.3			
			1614.9	297.3	6.3	3749.3	324.0	93.0	3310.3	1296.7	180.4			
			1662.4	102.2	3.9	3749.9	216.0	194.4	3331.7	1408.3	217.4			
			3340.7	1281.8	221.9	3751.8	222.9	177.3	3374.4	1015.9	229.5			
			3585.9	507.3	166.4				3811.9	291.0	120.5			
			3614.9	177.7	49.8				3821.5	278.8	116.8			

			3621.0	264.0	270.0				3826.3	266.4	138.2			
			3638.1	625.0	351.8									
			3716.5	608.3	86.8									
			3734.4	582.3	90.7									
			3802.4	314.8	81.2									
			3811.0	353.2	111.7									
			3820.2	281.9	128.3									

$ThH_2O(NO_3)_6^{2-}$			$Th(NO_3)_6^{2-}$ (all bidentate)			$Th(NO_3)_6^{2-}$ (mixed mono/bidentat)		
Freq	IR	Ram	Freq	IR	Ram	Freq	IR	Ram
31.1	3.9	3.7	50.2	4.0	0.0	10.6	4.2	0.2
49.8	1.4	3.3	52.5	3.8	0.0	22.0	4.4	1.0
53.4	6.8	0.1	53.9	3.3	0.0	29.1	1.4	7.2
57	4.5	1.8	60.3	0.0	11.1	33.8	0.8	6.8
59.7	4.9	9.3	61.6	0.0	10.6	37.1	0.8	3.4
62.5	3.9	6.7	64.2	0.0	10.9	43.8	11.2	0.8
64.1	7.9	8.3	71.7	15.8	0.0	45.4	0.3	3.6
66.9	14.4	0.8	73.0	15.6	0.0	49.1	1.8	0.1
70.9	15.7	0.7	73.4	14.9	0.0	55.9	1.4	2.4
78.1	10.1	6.1	110.8	0.0	0.0	57.8	9.7	2.9
92.9	14.3	1.1	111.7	0.0	0.0	59.2	5.9	5.9
97.2	31.3	0.2	120.5	0.0	15.6	60.0	4.7	4.9
112.6	0.1	6.2	121.1	0.0	15.2	82.9	6.0	2.0
118.7	12.6	9.3	121.6	0.0	15.4	93.2	1.2	2.9
122	0.2	6.4	164.9	0.6	0.0	95.6	0.8	7.8
140.6	7.7	6.5	168.9	66.1	0.0	124.4	4.0	5.6
157.3	3.2	1.5	169.7	70.5	0.0	128.2	11.6	1.6
160.3	56.5	0.7	170.3	0.0	0.2	134.7	3.9	3.5
160.7	16.4	2	170.4	71.2	0.0	136.0	15.0	9.3

165.9	13.9	0.8	170.6	0.0	0.2	143.3	14.3	0.4
167.8	21.2	2.3	173.2	0.7	0.0	156.9	5.9	1.0
173.6	37.8	0.8	173.9	1.1	0.0	162.5	6.4	0.2
175.4	62.8	1.1	174.1	2.1	0.0	169.0	8.5	1.0
181.2	60.1	3.2	176.3	0.0	1.7	176.9	9.9	5.3
187.3	25	0.4	177.5	0.0	1.6	185.1	7.0	0.4
188.7	2.7	1	178.0	0.0	1.8	185.8	59.0	2.6
192	21.3	0.8	194.0	0.0	2.7	194.4	124.1	0.8
193.1	18.7	2.9	195.2	0.0	2.7	198.0	8.9	1.0
196.4	63.8	0.6	195.3	0.0	2.8	202.5	68.3	0.2
199.7	37.4	0.9	205.1	184.6	0.0	206.1	119.5	0.4
205.4	19.3	0.9	205.7	186.9	0.0	207.0	246.2	0.2
208.5	86.6	0.8	206.0	185.0	0.0	211.0	188.7	0.9
213.5	103.4	2.1	227.8	0.0	11.4	235.9	2.0	11.2
215.4	23.9	4.4	692.8	0.0	0.0	668.2	26.1	4.7
259.5	38.9	6.5	692.9	0.0	0.0	669.7	8.4	12.9
307.4	170.6	1.5	693.1	0.0	0.0	689.9	0.0	2.1
350.9	79	0.6	695.1	0.0	12.4	690.3	0.1	5.2
614.6	184	1.3	695.2	0.0	12.3	692.2	0.4	5.8
682.9	50	6.5	695.4	0.0	12.5	694.7	0.2	10.3
691.5	0.2	2.7	733.0	126.2	0.0	716.8	78.9	1.5
693.4	0	0.7	733.2	126.3	0.0	719.7	4.8	19.6
695.3	0.3	9.8	733.4	126.6	0.0	731.8	116.6	3.1
695.6	0.4	8.6	737.4	0.0	29.9	734.9	116.5	8.1
695.8	0.1	10.7	737.7	0.0	30.1	736.7	34.3	21.0
719.6	11.9	8.2	748.1	0.0	1.4	748.2	0.1	8.0
732	100.7	0.8	788.1	0.0	0.0	786.4	41.8	0.2
733.4	133.3	0.1	788.1	50.1	0.0	786.5	5.4	0.2
736.7	2.2	26.5	789.0	0.0	0.0	788.5	22.9	0.1
738.5	43.6	18.6	789.1	50.0	0.0	789.2	20.1	0.1

745.7	14.2	2.6	789.7	0.0	0.0	789.6	15.2	0.1
787.2	28.1	0.1	789.7	49.7	0.0	790.8	20.9	0.1
789.4	21.8	0	1059.0	0.0	41.3	1017.1	1068.0	9.5
789.7	26.9	0	1059.2	0.0	41.5	1027.9	94.0	85.1
790	23	0	1059.7	162.2	0.0	1049.6	62.8	21.1
790.4	25.2	0	1059.7	164.1	0.0	1052.4	131.0	50.6
792	23.1	0.2	1059.8	162.1	0.0	1053.3	139.1	4.5
920.6	303.1	1	1063.9	0.0	318.8	1058.7	25.0	201.7
1056.5	107.9	32.9	1293.4	1558.1	0.0	1274.5	236.4	3.8
1058.4	63.8	40.6	1293.5	1561.9	0.0	1275.6	657.9	1.5
1062.1	112	34.7	1293.6	1559.8	0.0	1283.2	2105.9	3.2
1063.7	25.2	91.8	1296.5	0.0	4.4	1286.4	889.7	2.6
1070.8	97.3	61.2	1296.7	0.0	4.4	1294.2	772.5	1.2
1074.8	88.6	165.8	1296.9	0.0	4.4	1300.4	40.0	52.5
1289.3	2160.9	2.8	1513.2	0.0	29.0	1491.2	967.4	15.3
1294.1	53.9	4.2	1513.4	0.0	29.1	1492.9	1182.3	13.0
1303.2	1561	2	1518.1	2408.7	0.0	1520.7	299.7	21.3
1305.3	159.3	4.5	1518.3	2409.6	0.0	1528.7	2168.3	4.8
1308.4	386.6	8.7	1518.5	2414.5	0.0	1530.7	2093.9	7.8
1313.4	728.3	2.7	1551.3	0.0	60.5	1551.2	60.9	68.7
1443.5	949.1	7.5						
1505.5	600.9	20.0						
1510.1	2025.0	7.5						
1511.8	903.9	18.4						
1520.6	2384.0	0.0						
1543.7	151.8	54.9						
1644.2	134.7	2.7						
3209.1	1726.1	253.2						
3821.6	221.8	123.3						

Table S27. Cartesian coordinates in Å for aqueous optimized geometries of Th complexes at the B3LYP/DZVP2(H,O,N)/cc-pVDZ-PP(Th) level.

$Th(H_2O)_9^{4+}$

TH	-0.000837	0.000058	0.001153
O	0.103924	-2.108597	-1.327959
H	-0.406381	-2.316765	-2.129774
O	-0.089336	2.181276	-1.200258
H	-0.639318	2.947633	-0.959508
O	-0.001697	-0.085565	2.486442
H	-0.529174	-0.688975	3.039410
H	0.476377	0.515995	3.084108
H	0.662439	-2.879962	-1.125967
H	0.437770	2.436108	-1.977086
O	-1.839453	1.405932	0.897185
H	-2.628449	1.710812	0.414957
O	-1.698791	-1.610550	0.814310
H	-1.771596	-2.533639	0.515780
O	-1.790760	-0.026167	-1.719658
H	-2.536830	-0.648716	-1.775943
H	-1.962000	1.633460	1.834941
H	-1.937841	0.669473	-2.384122
H	-2.491198	-1.405693	1.342241
O	1.688844	1.556891	0.929618
H	2.472931	1.321237	1.456394
O	1.798329	0.142155	-1.708120
H	2.556160	0.752594	-1.706527
O	1.835183	-1.461331	0.815547
H	2.631622	-1.730534	0.324452
H	1.964255	-1.717882	1.745327
H	1.962030	-0.522527	-2.399975
H	1.764618	2.499807	0.700642

$Th(H_2O)_8NO_3^{3+}$

O	2.048168	-1.111413	-1.545205
O	0.029627	-2.474740	-0.115590
O	1.877261	1.668241	-1.137366
O	2.304988	-1.047542	1.259991
O	-0.414758	0.096665	-2.358206
O	1.420359	1.625770	1.614820
O	-0.448388	-0.443085	2.306019
TH	0.408945	-0.004085	0.000364
H	2.342292	-1.238216	2.213470
H	3.012287	-1.561581	0.833358
H	0.009978	-0.236049	3.138626
H	-1.113552	-1.125020	2.504747
H	2.193199	1.468337	2.184648

H	0.924737	2.371484	1.996130
H	2.272055	2.418852	-0.660281
H	1.870656	1.896538	-2.083527
H	0.648138	-3.169843	0.168785
H	-0.859493	-2.869054	-0.143828
H	0.143632	0.076456	-3.154694
H	-1.260747	0.505112	-2.611681
H	1.904693	-1.970356	-1.979253
H	2.770670	-0.663499	-2.018435
O	-4.086138	-0.917645	-0.031454
O	-3.329096	1.137542	0.030737
N	-3.154410	-0.109374	-0.017464
O	-1.929370	-0.574568	-0.055857
O	-0.859834	2.085382	0.043029
H	-1.847219	1.951371	0.013626
H	-0.638060	2.921849	-0.399513

$Th(H_2O)_7NO_3^{3+}$

O	2.749911	-0.819566	-0.148650
O	0.610004	-2.136477	1.284505
O	1.394469	0.839542	-2.091730
O	0.109360	-1.736661	-1.707200
O	1.843403	1.798795	0.889914
O	-0.272929	0.424907	2.353155
Th	0.414764	-0.012997	0.024436
H	0.269707	0.863446	3.032092
H	-1.065777	0.072623	2.794932
H	2.804107	1.747933	1.040251
H	1.558731	2.699940	1.124877
H	1.857857	1.693525	-2.161364
H	1.037506	0.634866	-2.974344
H	0.556387	-2.237830	2.250885
H	0.749978	-3.021312	0.903708
H	0.818675	-2.194561	-2.192799
H	-0.719753	-2.217428	-1.878361
H	3.189936	-1.414472	0.483941
H	3.423911	-0.516163	-0.782162
O	-3.995758	-0.937899	-0.059540
O	-3.295903	1.121090	-0.339490
N	-3.100273	-0.098781	-0.133954
O	-1.850343	-0.513544	0.015257
O	-0.773829	2.077466	-0.386274
H	-1.759278	1.982548	-0.442274
H	-0.495930	2.826832	-0.940519

$Th(H_2O)_7(NO_3)_2^{2+}$

H	-1.004576	1.466714	-2.740941
H	-2.258614	1.673970	-1.832236
H	0.606560	3.110115	-1.061136
H	1.952870	2.299415	-0.989322
H	-0.700373	3.015020	1.319622
H	-2.121994	2.526995	0.885819
H	0.266364	-2.862506	0.582372
H	1.676134	-2.105888	0.691686
H	0.974864	1.156625	2.801226
H	2.104957	1.575588	1.795890
H	-1.804514	-0.136500	2.730630
H	-0.748069	-1.294742	2.733784
H	-0.279869	-1.312601	-2.772743
H	1.231442	-1.337289	-2.362055
O	-1.458422	1.133454	-1.947739
O	0.983902	2.219726	-0.964147
O	-1.202870	2.238694	1.018941
O	0.686051	-2.006793	0.771085
O	1.305236	1.031559	1.895478
O	-0.972470	-0.439444	2.329678
O	0.381052	-0.898281	-2.191922
Th	-0.146739	0.189249	0.015673
O	2.304800	0.007476	-0.499701
O	3.286204	-1.731393	0.456072
N	3.386738	-0.633433	-0.163152
O	4.483240	-0.149272	-0.472260
O	-4.006803	-1.560903	-0.250792
O	-2.733525	0.174395	0.232079
N	-2.905038	-1.036443	-0.170626
O	-1.813970	-1.658988	-0.483857

$Th(H_2O)_6(NO_3)_2^{2+}$

H	0.512722	-0.869850	-2.840262
H	-1.044795	-0.727445	-2.864335
H	0.523958	2.478796	-2.188737
H	1.846576	1.671334	-1.983097
H	-1.463328	3.133307	-0.406483
H	-2.543939	2.153619	-0.980213
H	0.308599	-1.397748	2.584297
H	1.704015	-1.067672	1.890678
H	1.005267	2.237873	2.201440
H	1.545978	2.797253	0.834893

H	-2.433494	1.236891	1.959940
H	-1.438052	0.496907	2.916422
O	-0.271638	-0.762154	-2.274312
O	0.999850	1.904557	-1.563900
O	-1.669148	2.193760	-0.556026
O	0.768912	-0.753955	2.018652
O	0.963270	2.129732	1.235728
O	-1.595750	0.743110	1.989153
Th	-0.162784	0.291415	-0.003709
O	2.007530	-0.517951	-0.535080
O	3.215775	-1.345625	1.119893
N	3.137241	-1.025928	-0.093288
O	4.064979	-1.165847	-0.892425
O	-3.334447	-2.460631	-0.193108
O	-2.508597	-0.454158	-0.600008
N	-2.412591	-1.664114	-0.146760
O	-1.258924	-1.953374	0.362635

$Th(H_2O)_6(NO_3)_3^{1+}$

H	-2.094261	1.206258	2.289429
H	-0.698163	1.667762	2.816940
H	0.905421	-2.614568	1.683155
H	2.194217	-1.950526	1.020194
H	-0.799345	0.769847	-2.714142
H	0.756690	0.587777	-2.736634
H	-1.530173	-1.579213	2.483850
H	2.134654	0.234936	2.580530
H	-2.231131	-1.892614	1.097265
H	2.121707	1.662145	1.930150
O	-1.149514	0.973067	2.306762
O	-1.353750	-1.738687	1.541055
O	1.601305	0.849657	2.048949
O	1.325381	-1.764862	1.468583
O	-0.052719	0.353000	-2.251316
Th	-0.006169	-0.013874	0.266474
O	-0.198301	-2.149842	-1.058913
H	-0.054326	-3.055059	-0.736355
H	-0.112775	-2.163461	-2.027066
O	2.193453	-0.208530	-0.801674
O	4.043889	-0.697672	-1.853079
N	3.270097	-0.931516	-0.914983
O	3.496090	-1.836802	-0.063854
O	1.073755	2.287070	-0.163284

N	-0.003139	2.974101	-0.362958
O	-1.093494	2.299788	-0.285512
O	0.022336	4.175190	-0.612778
O	-4.076268	-0.619241	-1.758615
O	-2.314925	-0.053987	-0.594732
N	-3.313476	-0.862482	-0.814067
O	-3.481191	-1.853823	-0.049830

$Th(H_2O)_5(NO_3)_3^{1+}$

H	-2.542022	0.742142	1.957107
H	-1.522224	1.922764	2.084440
H	0.519133	-3.247192	0.098696
H	1.890665	-2.447372	-0.140128
H	-0.541610	-0.477527	-2.878040
H	1.002252	-0.699199	-2.741164
H	-1.635555	-2.289172	1.897026
H	1.566364	-1.134606	2.706017
H	-2.583242	-1.718681	0.738796
H	0.656367	0.010588	3.269400
O	-1.618924	1.000238	1.792228
O	-1.642716	-1.857978	1.025819
O	0.800123	-0.570798	2.502801
O	0.971613	-2.398334	0.234236
O	0.166114	-0.687391	-2.244175
Th	-0.058385	-0.165754	0.196131
O	2.289380	0.011046	-0.333887
O	4.360098	0.087730	-1.028866
N	3.386071	-0.598955	-0.703790
O	3.405278	-1.859016	-0.707814
O	0.841776	2.045716	1.088299
N	0.664507	2.739173	0.010095
O	0.112412	2.090794	-0.963251
O	0.995286	3.911509	-0.080830
O	-4.149573	0.491532	-1.735269
O	-2.135394	0.038092	-1.016960
N	-3.429399	-0.157765	-0.970426
O	-3.883438	-1.005768	-0.156716

$Th(H_2O)_5(NO_3)_4$

H	2.159607	0.836626	-2.195479
H	1.105672	1.987340	-2.306873
H	-1.238294	-2.825656	-0.948224
H	-2.399220	-1.806169	-1.283255

H	0.536362	0.050509	2.833551
H	0.128621	1.516701	2.360556
H	1.216877	-2.616876	-1.228635
H	-1.242204	0.738257	-3.028778
H	2.282864	-1.500295	-1.567352
H	-2.468052	0.546639	-2.056222
O	1.198994	1.028564	-2.165804
O	1.322311	-1.685024	-1.515053
O	-1.523923	0.810098	-2.100555
O	-1.430132	-1.905822	-1.215531
O	-0.008479	0.546496	2.200097
Th	-0.061058	-0.022915	-0.228172
O	2.270724	0.300935	0.506280
N	3.475460	0.249443	0.013387
O	3.622324	-0.082322	-1.200938
O	4.431307	0.524481	0.747716
O	0.209359	-1.964683	1.250114
N	0.342589	-3.260572	1.166636
O	0.287632	-3.803331	0.024863
O	0.513859	-3.906482	2.205954
O	-2.349098	0.252191	0.603484
N	-3.587385	0.074907	0.232976
O	-3.817250	-0.288205	-0.957570
O	-4.486670	0.264917	1.058822
O	-0.159476	2.386232	0.024917
N	0.067518	3.410408	0.804362
O	0.229491	3.210524	2.038354
O	0.104737	4.538433	0.299185

$Th(H_2O)_4(NO_3)_4$

H	-1.551039	1.611547	-2.215586
H	0.011006	1.629979	-2.534121
H	1.759827	-1.869368	-1.804523
H	0.235849	-1.971647	-2.249196
H	-1.857477	-1.476502	2.051206
H	-0.342810	-1.581736	2.520365
H	0.100954	1.959636	2.272458
H	1.648969	1.848435	1.922814
O	-0.722546	1.113777	-2.113336
O	0.921333	-1.379518	-1.847267
O	-0.997895	-1.023107	2.030353
O	0.807311	1.362502	1.917453
Th	-0.002836	0.008716	-0.004481

O	1.684550	-1.395758	0.941581
N	2.087005	-2.006466	2.030621
O	1.243808	-2.250215	2.931915
O	3.276611	-2.329092	2.115389
O	-1.782680	-1.392840	-0.760346
N	-2.207997	-2.176854	-1.722121
O	-1.378032	-2.600425	-2.566950
O	-3.406999	-2.472981	-1.748428
O	1.863664	1.287041	-0.777344
N	2.403615	1.881376	-1.814579
O	1.670654	2.168017	-2.795995
O	3.610588	2.142585	-1.775480
O	-1.773736	1.515569	0.562886
N	-2.276135	2.252817	1.525382
O	-1.520423	2.619112	2.461741
O	-3.470635	2.561466	1.461925

$Th(H_2O)_3(NO_3)_5^{1-}$

Th	-0.043652	0.078886	-0.018929
O	-1.161002	1.972103	1.212254
H	-0.775721	2.863249	1.236249
O	1.437057	-0.020480	-2.048987
H	1.056986	-0.115149	-2.937958
O	-0.888189	1.615890	-1.796196
H	-1.807844	1.931573	-1.801928
H	-2.121170	2.053840	0.980386
H	-0.294839	2.411863	-1.845513
H	2.144598	-0.712273	-1.948035
O	0.995380	0.556870	2.333704
O	-0.475933	-1.042467	2.231938
N	0.336139	-0.346846	2.961926
O	0.459301	-0.543843	4.167880
O	1.102478	3.408031	-1.633418
O	1.488998	2.003660	0.033429
N	1.856933	3.013916	-0.699982
O	2.938295	3.565495	-0.448342
O	-1.142350	-1.233921	-2.008161
O	-1.517574	-3.407457	-1.989168
N	-1.082494	-2.390941	-1.455616
O	-0.529396	-2.412155	-0.285251
O	3.135795	-1.931835	-1.280731
O	2.015340	-1.189998	0.473109
N	2.851673	-2.037055	-0.054071

O	3.358515	-2.904419	0.670831
O	-3.690721	1.547477	0.415012
O	-4.626697	-0.360796	-0.124429
N	-3.626835	0.307873	0.176549
O	-2.476953	-0.292343	0.266368

$Th(H_2O)_2(NO_3)_5^{1-}$ 5 bidentate

H	-0.273118	-0.786364	3.041936
H	-0.341467	0.767936	3.031236
H	0.251109	-0.792517	-3.046161
H	0.343502	0.759053	-3.043480
N	2.150759	2.173375	0.017299
N	2.739556	-1.377228	0.011286
N	-0.462963	-3.010059	-0.000964
N	-3.028936	-0.495177	-0.013111
N	-1.400025	2.711593	-0.012208
O	1.988587	1.369213	-0.975646
O	1.340878	1.997874	1.001855
O	3.017376	3.045342	0.024039
O	1.923481	-1.473689	-0.979444
O	2.320458	-0.666764	0.998511
O	3.840993	-1.925644	0.013094
O	0.075271	-2.395454	0.995385
O	-0.787547	-2.260606	-0.997182
O	-0.652669	-4.223484	-0.000738
O	-2.279075	-0.832587	0.976707
O	-2.417516	0.062355	-0.997843
O	-4.243918	-0.692323	-0.016712
O	-1.484251	1.894077	0.979965
O	-0.682746	2.302324	-0.999829
O	-1.964624	3.802898	-0.015712
O	0.002821	0.000883	2.542394
O	-0.002595	0.000253	-2.543541
TH	0.000798	-0.000033	-0.000467

$Th(H_2O)_2(NO_3)_5^{1-}$ 2 bidentate 3 monodentate

TH	-0.046601	0.017871	0.149013
O	-1.601708	1.811418	-0.445419
H	-2.539471	1.537729	-0.579828
H	-1.300875	2.422394	-1.158667
O	0.213766	-1.824809	1.796669
H	1.081776	-2.293499	1.685030
H	-0.468879	-2.488054	1.994045

O	-0.329707	-2.169934	-1.159895
N	-0.485547	-1.630589	-2.320944
O	-0.429782	-0.335723	-2.331895
O	-0.671900	-2.286748	-3.336514
O	-0.716847	1.078527	2.372534
N	0.475985	1.337336	2.796027
O	1.424758	0.991621	1.988418
O	0.692003	1.867172	3.877903
O	-2.270198	-0.753039	0.619439
N	-3.538756	-0.627853	0.315897
O	-3.913054	0.389039	-0.321349
O	-4.316358	-1.519165	0.679330
O	0.013387	3.193849	-2.136154
O	1.195654	1.791496	-0.901620
N	1.138678	2.747394	-1.796646
O	2.201702	3.175979	-2.262853
O	2.189405	-0.878164	-0.178965
O	2.677261	-2.632686	1.076253
N	2.997604	-1.854148	0.137377
O	4.054846	-1.972826	-0.495094

$Th(H_2O)_1(NO_3)_6^{2-}$ 5 bidentate, 1 monodentate

N	-3.46687200	0.35368600	-1.00023200
N	2.47691400	-0.74166400	1.79595100
N	0.68271800	-2.46177000	-1.72535700
N	-0.41641800	2.47865600	1.63086800
N	2.20788700	1.59412800	-1.65184300
N	-1.59673900	-1.65858000	1.83710800
O	2.61390900	-0.00244700	0.75285300
O	-2.45066300	-0.25756700	-0.50431500
O	-3.28754300	1.30341700	-1.82829000
O	1.28032400	-1.14662900	2.02017400
O	-4.61395300	-0.00241600	-0.66969900
O	3.42516600	-1.03676300	2.52428300
O	-0.27499700	-1.63294100	-1.97892300
O	0.53181000	1.66285100	1.92317500
N	-3.46687200	0.35368600	-1.00023201
N	2.47691400	-0.74166400	1.79595101
N	0.68271800	-2.46177000	-1.72535701
N	-0.41641800	2.47865600	1.63086801
N	2.20788700	1.59412800	-1.65184301
N	-1.59673900	-1.65858000	1.83710801
O	2.61390900	-0.00244700	0.75285301

O	-2.45066300	-0.25756700	-0.50431501
O	-3.28754300	1.30341700	-1.82829001
O	1.28032400	-1.14662900	2.02017401
O	-4.61395300	-0.00241600	-0.66969901
O	3.42516600	-1.03676300	2.52428301
O	-0.27499700	-1.63294100	-1.97892301
O	0.53181000	1.66285100	1.92317501

$Th(H_2O)_1(NO_3)_6^{2-}$ 4 bidentate, 2 monodentate

Th	0.069608	0.205975	0.093204
O	-2.026933	-2.714030	-2.220690
O	-0.762449	-2.228156	-0.480307
N	-1.411881	-1.899951	-1.535136
O	-1.372043	-0.642991	-1.836227
O	-1.901742	-0.506634	1.453724
N	-3.142300	-0.893061	1.336483
O	-3.623883	-1.087539	0.200174
O	-3.798579	-1.055128	2.388403
O	0.779301	-1.564774	1.783923
O	2.689566	-1.631332	2.884761
N	1.944760	-1.091164	2.072304
O	2.265643	-0.014415	1.445887
O	0.924446	2.609772	0.588022
N	1.925760	2.637539	-0.227382
O	2.107418	1.560854	-0.898095
O	2.645860	3.627908	-0.344899
O	-1.900142	1.850430	-0.098629
O	-0.521629	1.931492	-1.778830
N	-1.596839	2.381214	-1.235694
O	-2.286955	3.253525	-1.757674
O	1.579193	-0.981541	-1.385262
N	2.155229	-2.150010	-1.528490
O	2.608130	-2.727798	-0.519619
O	2.241558	-2.616264	-2.682104
O	-0.194578	1.134537	2.484685
H	-1.049220	0.938983	2.905690
H	0.043921	2.047964	2.713434

$Th(NO_3)_6^{2-}$ 6 bidentate

N	1.864434	1.257391	-2.050932
N	-1.864434	-1.257391	2.050931
N	2.117959	0.377120	2.153304

N	-2.117960	-0.377119	-2.153303
N	-1.145089	2.745141	0.643489
N	1.145087	-2.745142	-0.643488
O	-1.848430	0.008597	1.815903
O	1.848430	-0.008597	-1.815903
O	1.032571	1.952421	-1.355966
O	-1.032571	-1.952421	1.355966
O	2.618137	1.764997	-2.877952
O	-2.618137	-1.764997	2.877952
O	2.301545	0.741014	0.931801
O	-2.301545	-0.741014	-0.931800
O	0.972338	-0.157338	2.397619
O	-0.972338	0.157338	-2.397619
O	2.973432	0.529106	3.022110
O	-2.973432	-0.529107	-3.022109
O	-0.129281	2.257109	1.266346
O	0.129281	-2.257109	-1.266346
O	-1.640676	1.986826	-0.271595
O	1.640676	-1.986826	0.271595
O	-1.607663	3.853424	0.903279
O	1.607663	-3.853424	-0.903280
Th	0.000000	0.000000	0.000000

$Th(NO_3)_6^{2-}$ 4 bidentate 2 monodentate

Th	-0.001615	0.049956	0.008421
O	1.779473	-2.314309	3.059012
O	0.838817	-2.126571	1.071806
N	1.266366	-1.628900	2.182366
O	1.109354	-0.353787	2.300553
O	1.709981	-0.548232	-1.553086
N	2.972763	-0.928530	-1.512339
O	3.502974	-1.132579	-0.403644
O	3.563395	-1.064932	-2.597948
O	-0.864337	-2.153008	-0.981541
O	-1.862663	-2.387278	-2.935597
N	-1.329886	-1.680343	-2.087804
O	-1.189002	-0.406742	-2.234312
O	-0.128873	2.109850	-1.511804
N	-1.348105	2.445210	-1.245257
O	-1.949304	1.685143	-0.395686
O	-1.889523	3.416275	-1.762467
O	2.044220	1.575211	0.355950

O	0.247670	2.173356	1.430587
N	1.488767	2.412307	1.163512
O	2.090940	3.367889	1.641439
O	-1.766072	-0.448047	1.546439
N	-3.044707	-0.768511	1.474661
O	-3.554666	-0.952875	0.352827
O	-3.668767	-0.871205	2.544493

9. REFERENCES.

(1) Spek, A. L. Single-Crystal Structure Validation with the Program PLATON. *J. Appl. Crystallogr.* **2003**, *36* (1), 7–13. https://doi.org/10.1107/S0021889802022112.
(2) Janiak, C. A Critical Account on N-n Stacking in Metal Complexes with Aromatic Nitrogen-Containing Ligands. *J. Chem. Soc. Dalt. Trans.* **2000**, No. 21, 3885–3896. https://doi.org/10.1039/b003010o.
(3) Steiner, T. *C-H - O Hydrogen Bonding in Crystals*; 1996; Vol. 6. https://doi.org/10.1080/08893119608035394.
(4) Thomas, S. The Hydrogen Bond in the Solid State. *Angew. Chemie Int. Ed.* **2002**, *41*, 48–76.
(5) A Parr, R. G.; Yang, W. *Density Functional Theory of Atoms and Molecules.*; 1989.
(6) Becke, A. D. Density-Functional Thermochemistry. III. The Role of Exact Exchange. *J. Chem. Phys.* **1993**, *98* (7), 5648–5652. https://doi.org/10.1063/1.464913.
(7) Godbout, N.; Salahub, D. R.; Andzelm, J.; Wimmer, E. Optimization of Gaussian-Type Basis Sets for Local Spin Density Functional Calculations. Part I. Boron through Neon, Optimization Technique and Validation. *Can. J. Chem.* **1992**, *70* (2), 560–571. https://doi.org/10.1139/v92-079.
(8) B. Tomasi, J.; Mennucci, B.; Cammi, R. Quantum Mechanical Continuum Solvation Models. *Chem. Rev.* **2005**.
(9) Peterson, K. A. Correlation Consistent Basis Sets for Actinides. I. the Th and U Atoms. *J. Chem. Phys.* **2015**, *142* (7). https://doi.org/10.1063/1.4907596.
(10) Frisch, M. J.; Trucks, G. W.; Schlegel, H. B.; Scuseria, G. E.; Robb, M. A.; Cheeseman, J. R.; Scalmani, G.; Barone, V.; Petersson, G. A.; Nakatsuji, H.; Li, X.; Caricato, M.; Marenich, A. V.; Bloino, J.; Janesko, B. G.; Gomperts, R.; Mennucci, B.; Hratch, D. J. Gaussian 16, Revision A.03. Gaussian Inc.: Wallingford, CT, USA. 2016.
(11) Ribeiro, R. F.; Marenich, A. V.; Cramer, C. J.; Truhlar, D. G. Use of Solution-Phase Vibrational Frequencies in Continuum Models for the Free Energy of Solvation. *J. Phys. Chem. B* **2011**, *115* (49), 14556–14562. https://doi.org/10.1021/jp205508z.
(12) Purvis, G. D.; Bartlett, R. J. A Full Coupled-Cluster Singles and Doubles Model: The Inclusion of Disconnected Triples. *J. Chem. Phys.* **1982**, *76* (4), 1910–1918. https://doi.org/10.1063/1.443164.
(13) Raghavachari, K.; Trucks, G. W.; Pople, J. A.; Head-gordon, M. Krishnan RAGHAVACHARI, Gary W. TRUCKS. *Chem. Phys. Lett.* **1989**, *157* (6), 479–483.
(14) Watts, J. D.; Gauss, J.; Bartlett, R. J. Coupled-Cluster Methods with Noniterative Triple Excitations for Restricted Open-Shell Hartree-Fock and Other General Single Determinant Reference Functions. Energies and Analytical Gradients. *J. Chem. Phys.* **1993**, *98* (11), 8718–8733. https://doi.org/10.1063/1.464480.
(15) Bartlett, R. J.; Musiał, M. Coupled-Cluster Theory in Quantum Chemistry. *Rev. Mod. Phys.* **2007**, *79* (1), 291–352. https://doi.org/10.1103/RevModPhys.79.291.
(16) Pople, J. A.; Binkley, J. S.; Seeger, R. Theoretical Models Incorporating Electron Correlation. *Int. J. Quantum Chem.* **1976**, *10* (10 S), 1–19. https://doi.org/10.1002/qua.560100802.
(17) Werner, H.-J.; Knowles, P. J.; Knizia, G.; Manby, F. R.; Schütz, M.; Celani, P.; Györffy, W.; Kats, D.; Korona, T.; Lindh, R. . et al. MOLPRO, version 2020.1, a package of ab initio

programs.
(18) Werner, H. J.; Knowles, P. J.; Manby, F. R.; Black, J. A.; Doll, K.; Heßelmann, A.; Kats, D.; Köhn, A.; Korona, T.; Kreplin, D. A.; et al. The Molpro Quantum Chemistry Package. *J. Chem. Phys.* **2020**, *152* (14). https://doi.org/10.1063/5.0005081.
(19) Klamt, A. COSMO-RS: From Quantum Chemistry to Fluid Phase Thermodynamics and Drug Design. **2005**.
(20) Klamt, A.; Schüürmann, G. COSMO: A New Approach to Dielectric Screening in Solvents with Explicit Expressions for the Screening Energy and Its Gradient. *J. Chem. Soc. Perkin Trans. 2* **1993**, No. 5, 799–805. https://doi.org/10.1039/P29930000799.